Title
Cytosolic detection of the vacuolar pathogen, Mycobacterium tuberculosis

Permalink
https://escholarship.org/uc/item/3wz3w3wz

Author
Bell, Samantha Lynn

Publication Date
2015

Peer reviewed|Thesis/dissertation

Cytosolic detection of the vacuolar pathogen, *Mycobacterium tuberculosis*

by

Samantha L. Bell

DISSERTATION

Submitted in partial satisfaction of the requirements for the degree of

DOCTOR OF PHILOSOPHY

in

Biomedical Sciences

in the

GRADUATE DIVISION

of the

UNIVERSITY OF CALIFORNIA, SAN FRANCISCO

Acknowledgements

First and foremost, I would like to thank my entire loving family for their support. My best friend and sister, Maryann Bell, has been a constant source of emotional support, strategic advice, and financial bankrolling of my frequent visits to NYC for trips to Veselka. My parents, Gene Bell, Susan Carothers, Jannice Hobart, and Mark Carothers, have given their endless encouragement and unconditional love throughout my graduate career. My grandfather, Eugene Bell, and my departed grandparents, Raymond McAnallen, Helen McAnallen, and Barbara Bell, have been a lasting inspiration, and their overflowing pride and high expectations have motivated me to do my best. Finally, my brother from another mother and father, Raj Chovatiya, has been an irreplaceable supporter whom I can relate to like no other person on this planet. I love them all and appreciate everything they have done for me.

I also have immense gratitude for the many fantastic mentors I have had during my graduate career. Most importantly, I am grateful to my thesis advisor, Jeff Cox, who allowed me to join his lab and become a part of the Cox lab family. Jeff has taught me so much during my time in his lab, but most notably I have learned to think big and take chances, because that is how exciting science happens. As a result, it has been beyond thrilling to do science in the Cox lab. I am also deeply grateful for my unofficial postdoc mentor, Robbie Watson, who not only taught me how to do nearly everything I know but also to not be lazy. Doing experiments and talking through ideas with him was always entertaining, and I do not think I would have finished graduate school without him. Finally, I deeply appreciate my undergraduate research advisor, Jeff Brodsky, and the rest of the Brodsky lab at the University of Pittsburgh for giving me the foundation in research that has allowed me to be successful at UCSF.

Thank you to the incredible friends I've made while at UCSF, especially my classmates (BMS and Tetrad) and my labmates. I was never without a happy hour drinking buddy, whether we needed to celebrate victories, lament setbacks, overanalyze the juiciest new gossip, or just beautify it. Being surrounded by such amazing, intelligent, super fun, and loving people made graduate school fun, and I will miss everyone immensely.

Finally, I'd like to thank my Thesis Committee, Anita Sil and Scott Oakes, for their invaluable guidance and support, and my numerous collaborators at UCSF and elsewhere for their important contributions.

Chapter 2 contains material previously submitted for publication:

Bell SL*, Watson RO*, MacDuff DA, Kimmey JM, Diner EJ, Olivas J, Vance RE, Stallings CL, Virgin HW, Cox JS. The cytosolic sensor cGAS detects *Mycobacterium tuberculosis* DNA to induce type I interferons and activate autophagy. *Cell Host Microbe*, 2015 Jun 1. pii: S1931-3128(15)00208-5.

*Authors contributed equally to this work.

Abstract

Type I interferons (IFNs) are critical mediators of antiviral defense, but their elicitation by bacterial pathogens can be detrimental to hosts. Many intracellular bacterial pathogens, including *Mycobacterium tuberculosis*, induce type I IFNs following phagosomal membrane perturbations. Cytosolic *M. tuberculosis* DNA has been implicated as a trigger for IFN production, but the mechanisms remain obscure. We report that the cytosolic DNA sensor, cyclic GMP-AMP synthase (cGAS), is required for activating IFN production via the STING/TBK1/IRF3 pathway during *M. tuberculosis* and *L. pneumophila* infection of macrophages, whereas *L. monocytogenes* short-circuits this pathway by producing the STING agonist, c-di-AMP. Upon sensing cytosolic DNA, cGAS also activates cell-intrinsic antibacterial defenses, promoting autophagic targeting of *M. tuberculosis*. Importantly, cGAS binds *M. tuberculosis* DNA during infection, providing direct evidence that this unique host-pathogen interaction occurs *in vivo*. These data uncover a mechanism by which IFN is likely elicited during active human infections.

Table of Contents

List of Tables

List of Figures

Chapter 2

Chapter 3

Chapter 1: Background

Mycobacterium tuberculosis is the bacterium that causes tuberculosis, the second most deadly infectious disease worldwide, second only to HIV/AIDS. In 2013, there were 9 million new tuberculosis cases, and 1.5 million people died from tuberculosis (World Health Organization, 2014). As such, tuberculosis is a massive public health concern worldwide. *M. tuberculosis* is transmitted via aerosolized droplets produced most frequently when an infected person coughs (Kaufmann, 2001). With an infectious dose of 1-10 bacteria (Riley et al., 1995), *M. tuberculosis* is extremely contagious, but in healthy people, only 10% develop an active disease after exposure (Alimuddin et al., 2013; World Health Organization, 2014). In the remaining 90% of people, the immune system is able to control the infection, and they maintain a latent infection and remain disease-free (Kaufmann, 2001). However, in immune compromised individuals, there is a greatly increased risk of developing active disease in one's lifetime. As such, HIV-positive patients, who accounted for 13% of new cases in 2013, are especially vulnerable to developing serious disease (World Health Organization, 2014).

Despite our historic ability to treat tuberculosis with antibiotics, drug resistance has made it an increasingly difficult disease to treat. Multi-drug resistance tuberculosis (MDR-TB) is on the rise and is caused by strains resistant to either isoniazid or rifampicin, two of the most effective antibiotics for *M. tuberculosis* and two ingredients in the four-drug cocktail used for first-line treatment (also includes ethambutol and pryazinamide) (World Health Organization, 2014). According to recent estimates, approximately 3.5% of new tuberculosis cases are caused by multi-drug resistant isolates (MDR-TB), and an astonishing 20% of previously treated cases are multi-drug resistant (World Health Organization, 2014). Two important reasons for the prevalence of drug resistance are the long course of treatment (minimum of six months for

uncomplicated cases; minimum of twenty months for MDR-TB) and the unpleasant, sometimes very toxic, side effects of these antibiotics (Alimuddin et al., 2013). Together, this results in poor patient adherence to treatment regimens, accelerating the development of resistant infections. Directly observed treatment (DOT) has sought to increase patient adherence, but nonetheless, resistance is on the rise. Among MDR-TB patients, treatment is successful in only 50% of cases, and it is estimated that 9% of cases have extensively-drug resistant tuberculosis (XDR-TB) for which there are very limited treatment options and an even lower treatment success rate of 20% (World Health Organization, 2012; 2014). Without intervention, 70% of tuberculosis patients die within ten years (World Health Organization, 2014), so severe drug resistance renders XDR-TB a nearly untreatable infectious disease. Because of its highly contagious nature, the increasing prevalence of drug resistance, and the poor outcomes without treatment, it is critical we research *M. tuberculosis* pathogenesis in order to develop new, more effective treatments.

Early during infection, *M. tuberculosis* is phagocytosed by alveolar macrophages, resident lung macrophages typically very efficient at killing pathogens (Kaufmann, 2001). However, rather than being destroyed, *M. tuberculosis* overcomes and modulates this hostile environment to survive and replicate (Pieters, 2008; Russell, 2001; Welin and Lerm, 2012). *M. tuberculosis* utilizes many strategies to avoid this killing, but in general they are only partially understood. First, *M. tuberculosis* is able to inhibit phagosome maturation and fusion with destructive lysosomes (Russell, 2001). *M. tuberculosis*-containing phagosomes accumulate the early endosome marker Rab5 but fail to retain the late endosome marker Rab7 (Clemens et al., 2000), which blocks trafficking to lysosomes. Additionally, *M. tuberculosis*-containing phagosomes do not fully acidify and remain at a pH of around 6.4 (Sturgill-Koszycki et al., 1994). How this block in maturation is achieved is relatively unclear, but it is thought that *M.*

tuberculosis-derived lipids and phosphatases may play a key role (Vergne et al., 2003; 2005). Even in a mature phagolysosome, *M. tuberculosis* is exquisitely resistant to killing. *M. tuberculosis* makes a catalase peroxidase, KatG, which destroys reactive oxygen species, rendering them an ineffective killing mechanism (Ng et al., 2004). Reactive nitrogen species are crucial for host defenses, but they too can be counteracted by the bacterium through various mechanisms (Darwin et al., 2003; MacMicking et al., 1997; Ouellet et al., 2002).

Another key strategy used by *M. tuberculosis* to modulate macrophages involves its ESX-1 secretion system, which is a type VII secretion system required for virulence (Stanley et al., 2003; Xu et al., 2007). An important secreted effector of the this system, ESAT-6, is thought to have membrane lysing activity (de Jonge et al., 2007), and early reports suggested that *M. tuberculosis* could escape the phagosome to prevent destruction by lysosomes and to replicate in the nutrient-rich host cytosol (van der Wel et al., 2007; Welin and Lerm, 2012). While subsequent work has demonstrated that this complete phagosomal escape is either extremely uncommon or an experimental artifact, it has become clear that *M. tuberculosis* does utilize its ESX-1 secretion system to permeabilize the phagosomal membrane (Clemens et al., 2002; Manzanillo et al., 2012; McDonald et al., 2008). This allows for nutrient acquisition and, importantly, communication with and modulation of host signaling molecules. Additionally, cytosolic host sensors can then access and detect the bacterium, and the Cox lab has demonstrated that the cytosolic surveillance pathway (CSP) involving STING/TBK1/IRF3 is activated in an ESX-1-dependent manner (Manzanillo et al., 2012; O'Riordan et al., 2002). This pathway is typically triggered during viral infections and elicits an antiviral response, but during intracellular bacterial infections, it is pro-bacterial and results in an immune response that promotes bacterial pathogenesis (Auerbuch et al., 2004; Manzanillo et al., 2012). Of course, this cytosolic exposure also comes at a cost to *M. tuberculosis*, as additional host sensors can

detect the presence of a dangerous invading microbe in the cytosol. Recent work in the Cox lab

has shown that a portion of *M. tuberculosis* bacilli (~30%) is targeted to the selective autophagy

pathway in an ESX-1-dependent manner (Watson et al., 2012). This results in fusion of *M.*

tuberculosis-containing autophagosomes with lysosomes, which efficiently destroys bacteria

and restricts intracellular replication (Watson et al., 2012).

Chapter 2: The cytosolic sensor cGAS detects *Mycobacterium tuberculosis* DNA to induce type I interferons and activate autophagy

Abstract

Type I interferons (IFNs) are critical mediators of antiviral defense, but their elicitation by bacterial pathogens can be detrimental to hosts. Many intracellular bacterial pathogens, including *Mycobacterium tuberculosis*, induce type I IFNs following phagosomal membrane perturbations. Cytosolic *M. tuberculosis* DNA has been implicated as a trigger for IFN production, but the mechanisms remain obscure. We report that the cytosolic DNA sensor, cyclic GMP-AMP synthase (cGAS), is required for activating IFN production via the STING/TBK1/IRF3 pathway during *M. tuberculosis* and *Legionella pneumophila* infection of macrophages, whereas *Listeria monocytogenes* short-circuits this pathway by producing the STING agonist, c-di-AMP. Upon sensing cytosolic DNA, cGAS also activates cell-intrinsic antibacterial defenses, promoting autophagic targeting of *M. tuberculosis*. Importantly, cGAS binds *M. tuberculosis* DNA during infection, providing direct evidence that this unique host-pathogen interaction occurs *in vivo*. These data uncover a mechanism by which IFN is likely elicited during active human infections.

Introduction

Innate immune cells discriminate pathogens from non-pathogens at the earliest stages of infection and tailor their responses to match the level of the threat (Vance et al., 2009). Using a wide array of pattern recognition receptors to recognize various microbial components in different cellular compartments, cells can distinguish the specific type of threat and

subsequently initiate an appropriately tailored antimicrobial response (Kawai and Akira, 2010). Innate immune cells can also detect pathogens by sensing membrane perturbations mediated by bacterial virulence factors, either by directly sensing membrane damage or by recognizing specific bacterial molecules in the cytosol (Manzanillo et al., 2012; Thurston et al., 2012; Vance et al., 2009). Cytosolic detection leads to activation of three potent antimicrobial effector pathways – the inflammasome (Lamkanfi and Dixit, 2011), autophagy (Watson et al., 2012), and the cytosolic surveillance pathway (CSP) characterized by elicitation of type I interferons (IFNs) (Monroe et al., 2009; O'Riordan et al., 2002). While type I IFNs (IFN-α, IFN-β) are potent antiviral signaling molecules, they counteract antibacterial signaling pathways (Mayer-Barber et al., 2011; Teles et al., 2013) and promote infection of many intracellular bacteria including *Mycobacterium tuberculosis* (Manca et al., 2001; Manzanillo et al., 2012; Stanley et al., 2007) and *Listeria monocytogenes* (Auerbuch et al., 2004; Carrero et al., 2004; O'Connell et al., 2004). While we do not fully understand the mechanisms of this inhibition, it suggests that bacterial pathogens have evolved mechanisms to activate this antiviral pathway for their own benefit. Likewise, clinical studies have shown that elevated levels of type I IFNs are a biomarker of active TB disease in humans (Berry et al., 2010), indicating that this pathway is engaged during bacterial replication *in vivo*.

Elicitation of IFN-β requires the pore-forming toxin listeriolysin O during *L. monocytogenes* infection (O'Riordan et al., 2002), and the membrane-disrupting activity of the ESX-1 secretion system during *M. tuberculosis* infection (Manzanillo et al., 2012). *L. monocytogenes* actively secretes the bacterial second messenger cyclic diadenylate monophosphate (c-di-AMP) that binds to the host protein STING and activates the STING/TBK1/IRF3 signaling axis to promote a signature transcriptional response that includes IFN-β (Burdette et al., 2011; Sauer et al., 2011; Woodward et al., 2010). In contrast to *L.*

monocytogenes, *M. tuberculosis* and another intracellular bacterial pathogen, *Legionella pneumophila*, appear to activate this same STING-dependent pathway (Lippmann et al., 2008; Manzanillo et al., 2012; Monroe et al., 2009) via recognition of pathogen-derived nucleic acids, although the evidence for this is indirect.

Surprisingly, the STING pathway also potently activates autophagy, a degradative pathway implicated in resistance to intracellular pathogens (Birmingham et al., 2006; Deretic and Levine, 2009; Zhao et al., 2008). Activation of STING and the kinase TBK1 leads to targeting of bacteria and cytosolic DNA to the ubiquitin-mediated selective autophagy pathway in macrophages, and ATG5, a core autophagy protein, is crucial for limiting *M. tuberculosis* growth during infection (Watson et al., 2012). Despite our growing understanding of the links between the CSP and selective autophagy, the nature of the nucleic acid ligand and the host receptor proteins involved remain major unanswered questions.

Recent studies have identified a novel DNA sensor, cyclic GMP-AMP synthase (cGAS), as the central cytoplasmic DNA sensor upstream of STING during viral infection (Gao et al., 2013; Schoggins et al., 2014; Sun et al., 2013). Upon binding dsDNA, cGAS synthesizes the secondary messenger cGAMP, which in turn binds to and activates STING, leading to the production of IFN-β through IRF3. Despite some controversy over the involvement of a variety of other DNA receptors (Burdette and Vance, 2013; Unterholzner, 2013), cGAS is absolutely required for IFN induction upon both DNA transfection and viral infection, and is likely the major cytosolic DNA receptor (Li et al., 2013). cGAS is required for IFN-β induction during *Chlamydia trachomatis* and *Francisella novicida* infection, but its functional role during bacterial infections is largely unknown (Storek et al., 2015; Zhang et al., 2014).

Here, we report two different mechanisms by which bacterial pathogens activate the CSP: *M. tuberculosis* and *L. pneumophila* activate cGAS during infection, while *L.*

monocytogenes bypasses cGAS and directly activates STING via c-di-AMP. Furthermore, we show that recognition of *M. tuberculosis* by cGAS is a critical host-pathogen interaction as it promotes the delivery of bacilli to the ubiquitin-mediated selective autophagy pathway during macrophage infection and has an unexpected role in cell-autonomous bacterial control. Importantly, we also show that cGAS binds *M. tuberculosis* genomic DNA during macrophage infection, providing evidence of direct interactions between an *M. tuberculosis* ligand and a host sensor *in vivo*.

Results

cGAS is required to induce the CSP during intracellular bacterial infection

Previous studies have demonstrated that induction of the CSP during *M. tuberculosis* infection requires the STING/TBK1/IRF3 signaling axis. However, the mechanism of STING activation was unknown. To test the role of cGAS during *M. tuberculosis* infection, primary murine bone marrow-derived macrophages (BMDMs) were isolated from $cGas^{-/-}$ and $Sting^{-/-}$ mice. These cells were unresponsive to transfection with interferon-stimulatory DNA (ISD), a 45 bp dsDNA sequence sufficient for activating cGAS (Stetson and Medzhitov, 2006), as measured by quantitative PCR of IRF3 targets (IFN-β and IFIT1 mRNAs, Figure 2.1A), and by monitoring IRF3 phosphorylation (Figure 2.1C). Delivery of the STING ligand cGAMP via transfection bypassed the cGAS requirement (Figure 2.1B), in agreement with previous reports in other cell types establishing that cGAS functions upstream of STING (Sun et al., 2013).

Importantly, infection with the Erdman strain of *M. tuberculosis* led to robust CSP activation in wild-type BMDMs as measured by both protein and transcript levels. This response was completely blocked in $cGas^{-/-}$ and $Sting^{-/-}$ macrophages (Figure 2.2, A and B), similar to

infection of wild-type macrophages with an ESX-1 mutant, which fails to induce the CSP (Manzanillo et al., 2012). We observed similar results using a clinical isolate of *M. tuberculosis* (CDC1551) which, unlike the Erdman strain, has the capacity to produce the STING agonist c-di-GMP (Figure 2.2C) (Manzanillo et al., 2012). This response is specific to the STING/TBK1/IRF3 pathway as the mRNA level of TNFα, which is not regulated by IRF3, was generally unaffected by these mutations (Figure 2.2D). Independent shRNA knockdown of cGAS in the RAW 264.7 murine macrophage cell line (Figure 2.3A), and in the U937 human macrophage cell line (Figure 2.4A) confirmed the key role of this receptor in responding to cytosolic DNA (Figures 2.3B and 2.4B) and *M. tuberculosis* infection (Figures 2.3C and 2.4C). Taken together, these data demonstrate that cGAS is the major sensor that activates the CSP during *M. tuberculosis* infection of macrophages. These results also provide the strongest evidence to date that CSP activation by wild-type *M. tuberculosis* is due to exposure of DNA in the cytosol, and support previous findings that endogenous levels of bacterial-produced cyclic dinucleotides are not a major contributor in triggering this response during macrophage infection (Dey et al., 2015; Manzanillo et al., 2012).

We next tested the role of cGAS during infection with another intracellular bacterial pathogen, *L. pneumophila*, which elicits type I IFNs by accessing the cytosol through its type IV secretion system (T4SS) (Stetson and Medzhitov, 2006). *L. pneumophila* infection failed to induce the CSP in *cGas*^{-/-} BMDMs (Figure 2.5A). In addition, *sdhA* mutant *L. pneumophila* cells, which enter into the cytoplasm more readily than wild-type bacteria (Creasey and Isberg, 2012), induced significantly higher levels of IFN-β mRNA, and this too was dependent on cGAS (Figure 2.5A). Although previous studies had implicated the RNA-sensing MAVS pathway in detection of *L. pneumophila* (Lamkanfi and Dixit, 2011; Monroe et al., 2009; Opitz et al., 2006), our results are consistent with a previous report implicating the STING pathway (Lippmann et al., 2011).

The absolute requirement for cGAS is consistent with the notion that DNA is exposed to the cytosol during *L. pneumophila* infection via vacuolar perforations from its T4SS (Monroe et al., 2009; Stetson and Medzhitov, 2006).

While *L. monocytogenes* can activate STING directly by exposing bacterial-derived c-di-AMP to the cytosol (Sauer et al., 2011; Woodward et al., 2010), the contribution of DNA sensing has not been directly tested. In contrast with *M. tuberculosis*, CSP activation by *L. monocytogenes* infection was mostly independent of cGAS (Figure 2.5B). In *cGas*^{-/-} BMDMs there was only a slight reduction in IFN-β and no decrease in IFIT1 mRNA levels compared to infected wild-type BMDMs, whereas the response was completely blocked in *Sting*^{-/-} BMDMs (Sauer et al., 2011). The absolute requirement of STING but not cGAS indicates that *L. monocytogenes* successfully short-circuits the CSP pathway by providing its own second messenger, whereas *M. tuberculosis* and *L. pneumophila* generate the signal via DNA binding to cGAS.

Finally, infection with *Salmonella enterica* serovar Typhimurium led to normal levels of IFN-β and IFIT1 mRNAs in both *cGas*^{-/-} and *Sting*^{-/-} BMDMs, indicating that this pathogen predominantly activates type I IFNs via a CSP-independent mechanism, likely via the TLR4/TRIF pathway (Figure 2.5C) (Kawai and Akira, 2010; Zughaier et al., 2005). Taken together, these data suggest that intracellular bacterial pathogens have evolved the ability to activate type I IFNs via different mechanisms.

cGAS targets cytosolic DNA and *M. tuberculosis* to the selective autophagy pathway

Although type I IFNs are generally thought to promote bacterial infection, newly-recognized connections between DNA sensing and autophagy, a powerful antimicrobial

pathway with broad roles in immune defense, suggests that cGAS activation may also promote bacterial clearance (Gutierrez et al., 2004; Liang et al., 2014; Watson et al., 2012). Indeed, STING/TBK1 are required for both removal of cytoplasmic DNA via the autophagy pathway and for full targeting of *M. tuberculosis* to the ubiquitin-mediated autophagy pathway in macrophages (Liang et al., 2014; Watson et al., 2012). To test the role of cGAS in autophagic targeting, we transfected murine embryonic fibroblasts (MEFs) with Cy3-labeled dsDNA and observed that a similar percentage of DNA puncta colocalized with cGAS as with the selective autophagy markers LC3, ubiquitin, NDP52, and activated phospho-TBK1 (pTBK1) (Figure 2.6, A and B). Multicolor fluorescence microscopy revealed that the large majority of cGAS+ dsDNA structures contained all of these selective autophagy markers in both transfected MEFs and RAW 264.7 cells (Figure 2.7, A-C). Importantly, in *cGas*^{-/-} macrophages, colocalization of the autophagy targeting components, ubiquitin and LC3, with transfected DNA was reduced by approximately 50% (Figure 2.8A). Curiously, we consistently observed a stronger reduction in selective autophagy marker colocalization with DNA in *Sting*^{-/-} macrophages compared to *cGas*^{-/-} cells, suggesting that other factors, perhaps additional DNA sensors including IFI204 (Manzanillo et al., 2012; Unterholzner, 2013), work upstream of STING to target cytosolic DNA to autophagy. The requirement for STING in selective autophagic targeting is consistent with our previous finding that TBK1 is also required for this effect, whereas IRF3 is only required for the transcriptional output of this pathway (Watson et al., 2012). ShRNA-mediated knockdown of cGAS or STING in murine or human macrophage cell lines also led to decreased recruitment of selective autophagy markers to dsDNA 4 h post-transfection (Figure 2.8, B and C), though we did not observe the cGAS-independent contribution to this effect. We suspect that this difference between the genetic knockouts versus knockdowns is due to variable knockdown efficiency or other experimental artifacts resulting from the lentiviral expression of shRNAs. As an additional method of testing the role of cGAS in targeting dsDNA to the selective autophagy pathway, we

measured the levels of LC3-II, the lipidated form of LC3 generated during activation of autophagy, in wild-type, *cGas*^{-/-}, and *Sting*^{-/-} BMDMs after transfection with dsDNA. Western blot analysis revealed that while wild-type BMDMs had increased LC3-II levels after dsDNA transfection, *cGas*^{-/-} and *Sting*^{-/-} BMDMs failed to induce LC3-II conversion (Figure 2.9A). Importantly, the effect of cGAS on autophagy is not due to general defects in bulk autophagy as starvation of macrophages led to LC3-II conversion and degradation regardless of genotype (Figure 2.9B).

To begin to test the role of cGAS in autophagic targeting of *M. tuberculosis*, we infected RAW 264.7 cells expressing epitope-tagged cGAS with mCherry-expressing *M. tuberculosis* and monitored cGAS localization. Early in infection, cGAS colocalized with approximately 20% of wild-type *M. tuberculosis*, and this colocalization decreased at later time points (Figure 2.10, A and B). Importantly, we observed significantly decreased colocalization of cGAS with ESX-1 mutant bacteria at all time points, confirming that recognition requires ESX-1-mediated cytosolic access. As observed with transfected DNA, the majority of cGAS+ bacilli also colocalized with pTBK1 and LC3, suggesting that cGAS is important for recruiting these selective autophagy markers to intracellular *M. tuberculosis* (Figure 2.11, A and B). Time course studies showed that the appearance of cGAS on bacilli coincided with pTBK1 recruitment but preceded the recruitment of the terminal autophagy marker LC3 (Figure 2.11C), which is consistent with the notion that cGAS is a proximal sensor of bacteria that leads to subsequent targeting.

We next determined the requirement of cGAS for targeting *M. tuberculosis* to the selective autophagy pathway. Consistent with our previous observations, *Sting*^{-/-} BMDMs were defective in recruiting ubiquitin, LC3, NDP52, pTBK1, and Atg12, giving rise to an approximately 75-80% decrease in colocalization of any of these markers with bacteria compared with wild-type (Figures 2.12 and 2.13) (Watson et al., 2012). Importantly, *cGas*^{-/-} BMDMs were also

defective for autophagic targeting of *M. tuberculosis*, with a reduction in colocalization of ~50%, which mirrors our observations with transfected cytosolic dsDNA. Stable shRNA knockdowns of cGAS or STING in mouse and human macrophage cell lines led to similar results (Figures 2.14, A and B). Consistent with the recruitment of selective autophagy markers to *M. tuberculosis*, wild-type BMDMs had increased levels of LC3-II conversion, while *cGas*^{-/-} and *Sting*^{-/-} BMDMs were partially defective for LC3-II conversion after infection (Figure 2.13F). Together, these data indicate that DNA sensing by cGAS is required for full targeting of *M. tuberculosis* to the ubiquitin-mediated selective autophagy pathway, and indicate that a cGAS-independent pathway is also at play.

Previous work demonstrated that the autophagy protein ATG5 is important for controlling intracellular *M. tuberculosis* replication during *in vivo* mouse infections and *ex vivo* macrophage infections (Gutierrez et al., 2004; Watson et al., 2012). In contrast, IRF3-driven type I IFNs appear to work in a cell extrinsic fashion as they only promote infection *in vivo* (Manca et al., 2001; Manzanillo et al., 2012; Stanley et al., 2007). Given the potential positive and negative roles of these two outputs of STING/TBK1 activation during infection, we sought to determine the overall role of cGAS in *M. tuberculosis* pathogenesis. Infection of *cGas*^{-/-} mice (Schoggins et al., 2014) led to partially decreased type I IFN levels when compared with wild-type mice (Figure 2.15, A and B), indicating that while this pathway is activated by *M. tuberculosis* during infection, other pathways can stimulate IFN *in vivo*. Moreover, these animals had no overt defect in overall resistance to *M. tuberculosis* as we observed similar bacterial burdens in the tissues of these mice at both early and late time points after infection (Figure 2.15, C and D), and none of the *cGas*^{-/-} succumbed to infection during the 100-day experiment (Figure 2.15E). Consistent with these observations, a parallel study using the same *M. tuberculosis* strain but different *cGas*^{-/-} mice (Collins et al., 2015; Li et al., 2013), also found that *M. tuberculosis*-infected *cGas*^{-/-} mice

have similar bacterial loads and cytokine levels compared to wild-type mice through an extended time-course of infection. In these studies, Collins et al. report a small increase in susceptibility of *cGas*$^{-/-}$ mice to *M. tuberculosis* manifest after the 100-day time point, a phenotype that was not observed in *Sting*$^{-/-}$ mice. Although we do not understand the basis for these small discrepancies, both studies support the overall conclusion that removing cGAS from the context of an intact immune system is insufficient to dramatically alter host resistance to *M. tuberculosis*. This is in stark contrast to both *Irf3*$^{-/-}$ and myeloid-specific *Atg5*$^{-/-}$ mice (Manzanillo et al., 2012; Watson et al., 2012), which have phenotypes manifest at much earlier times post-infection. Since we observed a significant reduction in autophagic targeting in *cGas*$^{-/-}$ macrophages, we sought to determine the cell-intrinsic contribution of cGAS in controlling *M. tuberculosis* replication in macrophages. Consistent with cGAS targeting *M. tuberculosis* to the selective autophagy pathway for destruction by lysosomes, *cGas*$^{-/-}$ and *Sting*$^{-/-}$ BMDMs were permissive for *M. tuberculosis* growth, resulting in three-fold higher bacterial numbers compared to wild-type macrophages five days post-infection (Figure 2.16, A and B). Thus, while cGAS appears to be dispensable for overt bacterial resistance in a mouse model, this receptor is required for cell-intrinsic bacterial killing in macrophages. While we do not understand why the susceptibility of *cGas*$^{-/-}$ macrophages does not translate to a similar phenotype during infection of the entire mouse, we suspect that compensatory factors manifest only *in vivo*, such as the involvement of additional host DNA sensors or functionally redundant autophagic targeting pathways, may be at play (Manzanillo et al., 2012; Storek et al., 2015; Thurston et al., 2012; Unterholzner, 2013; Zhao et al., 2008). Alternatively, the decrease of pro-bacterial type I IFNs in *cGas*$^{-/-}$ mice during *M. tuberculosis* infection may be balanced by the reduced antibacterial capacity of selective autophagy in the macrophages of *cGas*$^{-/-}$ mice. Finally, while cGAS activation leads to both interferon and autophagic targeting in macrophages, specific functions of IRF3 (Di Paolo et al., 2013) and ATG5 (Choi et al., 2014; Liu et al., 2014; Zhao et al., 2008)

independent of their roles in interferon production and autophagic targeting, respectively, may still be active in $cGas^{-/-}$ mice.

cGAS binds *M. tuberculosis* genomic DNA in vivo in an ESX-1 dependent manner

Our finding that cGAS is activated by *M. tuberculosis* in macrophages and in mice supports the notion that a novel interaction occurs between a bacterial-derived molecule (DNA) and a host cytosolic sensor *in vivo*. However, the evidence suggesting that bacterial DNA is the actual bacterial ligand responsible for triggering the CSP is only circumstantial (Manzanillo et al., 2012; Watson et al., 2012). Moreover, surprisingly few bona fide physical interactions have been identified between *M. tuberculosis* and macrophages in the context of infection. This prompted us to explore the molecular mechanism by which *M. tuberculosis* activates cGAS by detecting a physical association of cGAS and DNA within macrophages. Consistent with previous findings, we were able to efficiently co-precipitate cGAS following transfection with biotin-labeled ISD in macrophages (Figure 2.17A) (Liang et al., 2014; Sun et al., 2013). To perform the reciprocal experiment using unlabeled DNA, we adapted a chromatin-immunoprecipitation (ChIP) protocol to capture DNA bound by cGAS in live cells. We first transfected macrophages with ISD, and after formaldehyde crosslinking and immunoprecipitating with α-FLAG beads (Figure 2.17B), we measured the abundance of ISD by qPCR. Importantly, we identified an enrichment of ISD only in immunoprecipitates from FLAG-cGAS-expressing cells transfected with ISD, but not in untransfected cells or cells expressing cGAS with a different epitope tag (Strep-cGAS, Figure 2.17C).

We next utilized this ChIP-like methodology to determine if cGAS binds directly to *M. tuberculosis* genomic DNA during infection. We infected cGAS-expressing macrophages with *M. tuberculosis*, crosslinked and immunoprecipitated cGAS (Figure 2.18A), and measured the

15

abundance of several *M. tuberculosis* DNA sequences, including the IS6110 transposon and the CRISPR repeat, two repetitive elements in the *M. tuberculosis* genome (Figure 2.18B). These *M. tuberculosis*-derived sequences were significantly enriched in FLAG-cGAS immunoprecipitates as compared to controls (FLAG-GFP and Strep-cGAS). Importantly, we observed an enrichment of mycobacterial DNA bound by cGAS in cells infected with wild-type *M. tuberculosis* compared to cells infected with ESX-1 mutant bacteria, which cannot actively access the cytosol (Figure 2.18B). The *M. tuberculosis* DNA sequences that were detected in the ESX-1 mutant-infected cells likely arise from nonspecific phagosomal rupture that can occur when macrophages undergo necrotic cell death during infections with high bacterial burdens (Lee et al., 2006). Furthermore, we did not observe any change in the abundance of host-derived DNA sequences in the immunoprecipitates after *M. tuberculosis* infection (Figure 2.18C), although the low levels of host sequences that were detected may be due to low levels of nonspecific binding of cGAS to nuclear DNA during normal cell processes (Schoggins et al., 2014). Together, these data show that bacterial-derived DNA exposed to the cytosol is bound by cGAS during infection.

Discussion

Our data support a model in which *M. tuberculosis* triggers the STING/TBK1 pathway using the ESX-1 secretion system to disrupt phagosomal membranes, allowing bacterial DNA access to cGAS in the cytosol. Subsequent activation of TBK1 likely couples a number of cellular events, including the IRF3-dependent IFN response and antibacterial autophagic targeting (Figure 2.19). Although indirect evidence had implicated the role of cytosolic bacterial DNA in triggering these pathways (Manzanillo et al., 2012; Watson et al., 2012), here we

provide the most definitive evidence to date that bacterial DNA is a bona fide "pathogen-associated molecular pattern" sensed by *M. tuberculosis*-infected cells.

This work provides a detailed view of one of the molecular interactions that occurs during *M. tuberculosis* infection of macrophages, but the modest decreases in type I IFNs and similar CFU counts during *cGas*⁻/⁻ mouse infection were strikingly negligible considering the strong cGAS dependence we observed in macrophages. Indeed, the situation *in vivo* is certainly much more complicated. It is possible that cGAS appears to be dispensable for host defenses because the antibacterial effects of autophagy are perfectly counterbalanced by the pro-bacterial effects of type I IFNs *in vivo*. However, a more likely explanation involves considering the complexities of an intact immune system in which additional cell types may utilize alternative DNA sensors like IFI204 or DAI to trigger type I IFNs (Bhat and Fitzgerald, 2014; Unterholzner, 2013). In fact, the partial defect in autophagic targeting in *cGas*⁻/⁻ macrophages compared to *Sting*⁻/⁻ macrophages may indicate that other sensors are indeed involved in other immune responses *in vivo*.

However, the true *in vivo* contributions of both the selective autophagy pathway and type I IFNs may be less than once thought. When *Atg5*⁻/⁻ mice are infected with *M. tuberculosis*, they succumb much more rapidly than would be expected from a failure to target 30% of bacilli to selective autophagy; inflammation is much more severe in these mice, and bacterial burdens are extremely high (Watson et al., 2012). Because ATG5 is crucial for many cellular processes including bulk autophagy, antigen presentation, cytokine secretion, and inflammasome inactivation, this extreme phenotype is likely a large overestimate of the true *in vivo* contribution of selective autophagy (Deretic et al., 2013). Infecting mice deficient in a specific selective autophagy gene like *Ndp52* would provide better insight into how this specific pathway contributes to pathogenesis *in vivo*.

Additionally, very recent work in our lab has suggested that *Irf3$^{-/-}$* mice may not be significantly more resistant to *M. tuberculosis* compared to wild-type mice (unpublished results, T. Parry). Other groups have studied the pro-bacterial effects of type I IFNs by administering IFN-α/β before *M. tuberculosis* infection; they observed increased bacterial burdens and susceptibility in these mice, but this artificial administration of type I IFNs is very different from the elicitation of endogenous type I IFNs during *M. tuberculosis* infection (Manca et al., 2001). However, type I IFNs are known to be induced during *M. tuberculosis* infection in humans as high type I IFN levels are a strong biomarker of active disease (Berry et al., 2010). Therefore, it is possible that studying the contribution of type I IFNs is simply not as relevant in our mouse model of infection. In such a case, utilizing one of the new humanized mouse models to study immune responses during *M. tuberculosis* infection might be enlightening (Brehm et al., 2014).

The mechanism by which DNA is liberated from *M. tuberculosis* has remained a major unanswered question. We currently do not know if it is a regulated process in which *M. tuberculosis* actively secretes its genomic DNA or if it is a by-product of infrequent bacterial lysis. The former case would require that the bacterium maintain more than one copy of its genome, which is not unprecedented for *M. tuberculosis* (Parrish et al., 1998). Furthermore, in *M. smegmatis*, the ESX-1 secretion system has been implicated in DNA transfer (Nguyen et al., 2010). Interestingly, *M. tuberculosis* is capable of forming biofilms *in vitro*, so DNA secretion may be related to this uncommon form of a community-oriented living (Ojha et al., 2008). Thus far, experiments divorcing the membrane permeabilization and DNA secretion activities of the ESX-1 secretion system have been challenging. Interestingly, *M. tuberculosis* strains lacking the ESX-1 secretion system but expressing the pore-forming listeriolysin O toxin to mediate phagosome permeabilization are only partially targeted to the selective autophagy pathway

(Watson et al., 2012). This observation supports the notion that there are additional functions for the ESX-1 secretion system beyond cytosolic access, one of which may be DNA secretion.

Another possible source of cytosolic DNA for triggering cGAS activation is damaged mitochondria, as recent work has demonstrated that mitochondrial DNA (mtDNA) can activate cGAS (Rongvaux et al., 2014; West et al., 2015; White et al., 2014). Interestingly, in addition to observing *M. tuberculosis* DNA bound to cGAS, in some preliminary experiments we also observed mtDNA bound to cGAS in an infection-dependent and ESX-1-dependent manner. Whether this mtDNA is liberated when bacterial pore-forming effectors also inadvertently permeabilize mitochondrial membranes or whether the host actively damages mitochondria in order to amplify proinflammatory responses and trigger cell death remains an interesting question of investigation. Regardless of how and what DNA is exposed to the cytosol, we suspect that the nucleic acid may be sensed by cGAS at the bacterial cell surface, providing important spatial cues for the selective recruitment of autophagic vesicles. However, it is possible that this spatial cue is short-lived or highly dynamic as cGAS remains colocalized with bacteria only briefly early during infection, and we only detect cGAS bound to *M. tuberculosis* DNA soon after infection.

It is tempting to speculate that *M. tuberculosis* has evolved specifically to use its own chromosomal DNA to elicit type I IFNs, as these cytokines are produced throughout *in vivo* mouse infections as well as in active human disease (Berry et al., 2010; Stanley et al., 2007). However, we have very little information to provide insight into how these IRF3 targets provide a pro-bacterial environment for *M. tuberculosis* and other intracellular pathogens. Over 100 genes are induced in response to activation of the CSP, but it is likely that many of these have redundant functions, rendering an shRNA screen of limited value in dissecting this question (Leber et al., 2008; Manzanillo et al., 2012). Because the IRF3 transcriptional response is

19

traditionally an antiviral defense, one possibility is that in creating an tailored antiviral immune response, these cells become exceptionally specialized in combating a viral infection, leaving them especially vulnerable to an intracellular bacterial pathogen. Because different bacteria have all evolved diverse mechanisms to elicit this response, it may be an easy target for bacterial pathogens as the potential for evolution of bacteria to elicit this response would, in theory, be relatively straightforward as it simply requires exposure of existing metabolites such as nucleic acids or cyclic dinucleotides to the inside of infected cells.

However, activation of the CSP also comes at a cost to bacterial replication as cGAS/STING/TBK1 activation simultaneously induces autophagic targeting. This cost is likely evident in our consistent observation that only 30% of *M. tuberculosis* bacilli are targeted to the selective autophagy pathway (Watson et al., 2012). This percentage may reflect a balance that has been achieved through evolution in which sufficient bacteria are exposed to the cytosol to elicit type I IFNs, but not so many are targeted for destruction by autophagy to inhibit a productive infection. However, we do not currently have a good mechanistic explanation for this phenomenon. One possibility is that the targeted one-third is the highest ESX-1-expressing population and so the most readily exposed to the cytosol. Consistent with this model, when we infect macrophages with increasing ratios of bacteria, 30% targeting is maintained, suggesting it may indeed stem from bacterium-intrinsic processes (Watson et al., 2012). This model would be further supported by a mutant with an overactive ESX-1 secretion system, which should be targeted to selective autophagy at a higher frequency than wild-type during infection. Another possible model is that during cytosolic exposure, the selective autophagy machinery is recruited into a cohesive signaling platform, sequestering a vast majority of the markers and adaptors to a signal site within an infected cell. Supporting this model is the observation that, like *M. tuberculosis*, only one-third of cytosolic DNA puncta are targeted to the selective autophagy

after transfection, suggesting this phenomenon is independent of bacterial physiology. Alternatively, it is possible that, on average, a majority of bacteria are in fact targeted but our quantification of selective autophagy markers captures only a brief snapshot of a highly dynamic process. Live cell imaging of the targeting and delivery of cytosolic DNA or *M. tuberculosis* to autophagosomes might better quantify the true rate of targeting to this degradation pathway.

Although possible, we have no evidence that *M. tuberculosis* actively blocks autophagic targeting. However, the ability of other pathogens, like *L. pneumophila* (Choy et al., 2012) and *L. monocytogenes* (Tattoli et al., 2013), to inhibit autophagy may be a more common mechanism by which pathogens shift the balance of cytosolic detection toward promoting infection. Understanding how to shift this balance instead toward autophagic targeting to control infection represents an attractive host-directed therapeutic strategy to combat infection in humans.
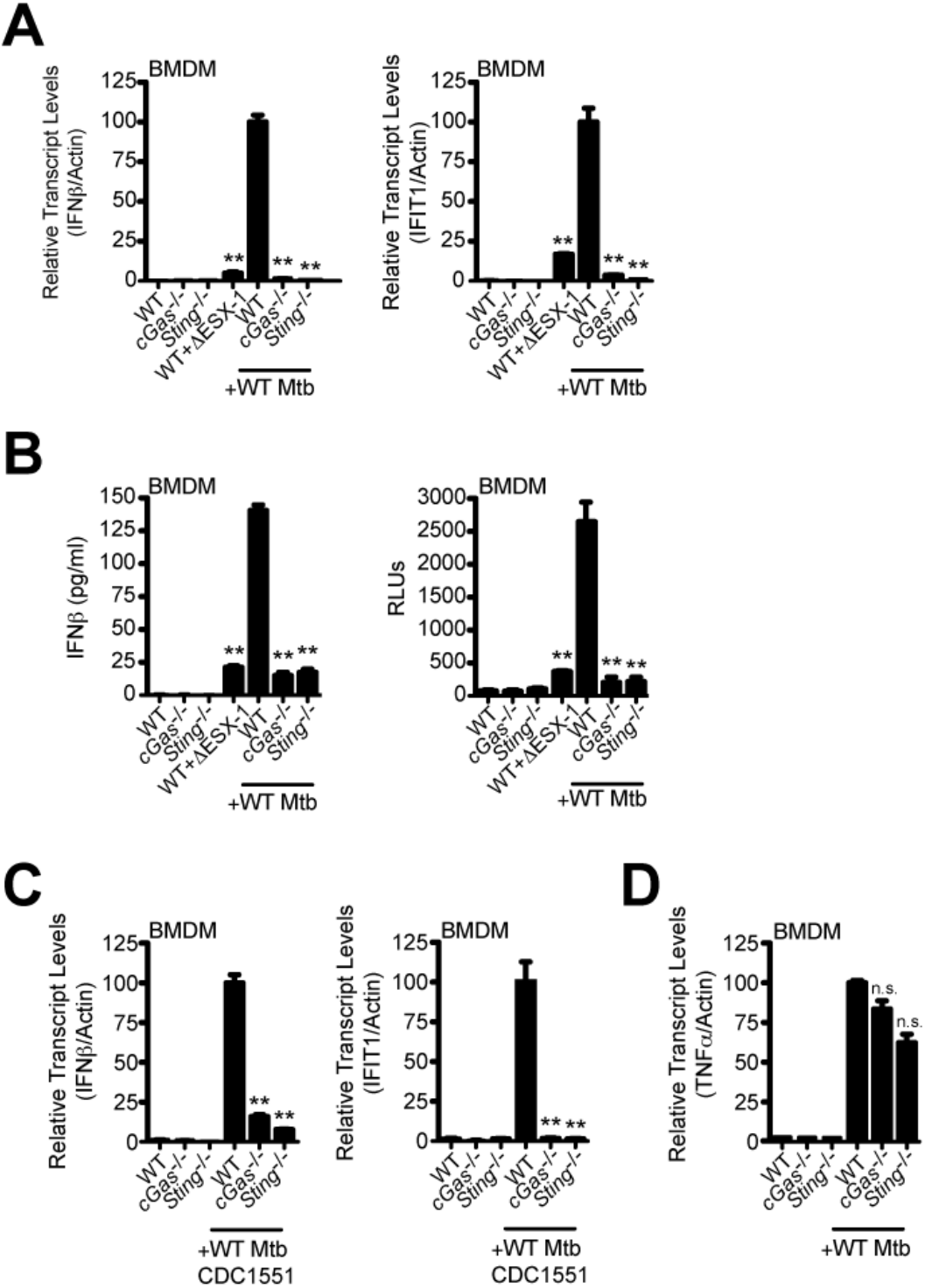
Figure 2.1
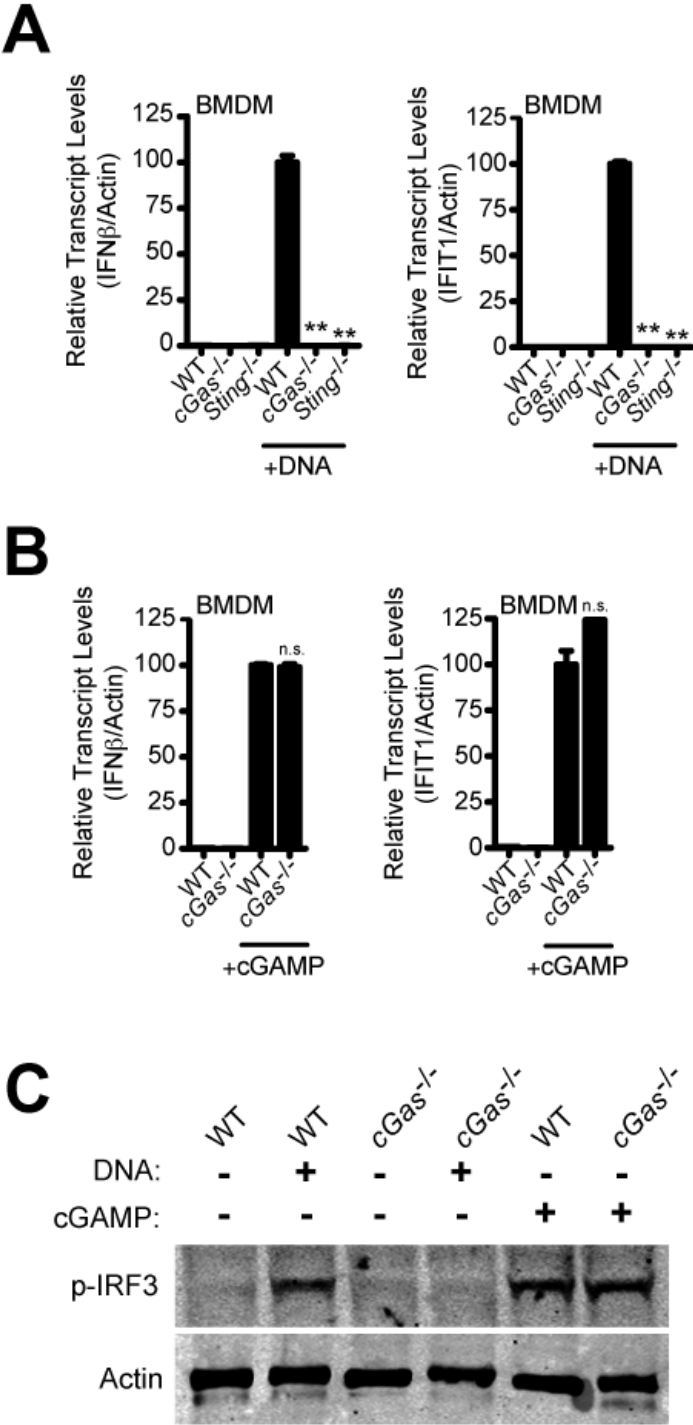
Figure 2.1. cGAS is essential in primary mouse macrophages for inducing the cytosolic surveillance pathway in response to cytosolic DNA.

(A) WT, *cGas*-/-, and *Sting*-/- murine bone marrow derived macrophages were transfected with interferon-stimulatory DNA (ISD) for 4 h, and IFN-β and IFIT1 transcript levels were measured. mRNA levels are expressed as percentages relative to transfected WT cells.

(B) WT and *cGas*-/- BMDMs were transfected with 2'-3'-cGAMP for 4 h, and IFN-β and IFIT1 transcript levels were measured.

(C) Western blot analysis of IRF3 phosphorylation in WT and *cGas*-/- BMDMs transfected with DNA or 2'-3'-cGAMP. n.s., not significant, $**p < 0.005$ by two-tailed t-test.

Figure 2.2

Figure 2.2. cGAS is essential for induction of the cytosolic surveillance pathway during

***M. tuberculosis* infection.**

(A) WT, *cGas*$^{-/-}$, and *Sting*$^{-/-}$ BMDMs were infected with wild-type (WT) or ΔESX-1 *M. tuberculosis* (Erdman strain) for 4 h, and IFN-β and IFIT1 transcript levels were measured by RT-qPCR. mRNA levels are expressed as percentages relative to infected WT cells.

(B) BMDMs infected as in (A) but IFN-β was measured by ELISA (left) or with ISRE-luciferase reporter cells (right) 24 h post-infection.

(C) Same as (A) but BMDMs were infected with *M. tuberculosis* strain CDC1551.

(D) Same as (A) but TNFα transcript levels were measured. n.s., not significant, **$p < 0.005$ by two-tailed t-test.

Figure 2.3

Figure 2.3. cGAS is essential for induction of the cytosolic surveillance pathway in a mouse macrophage-like cell line.
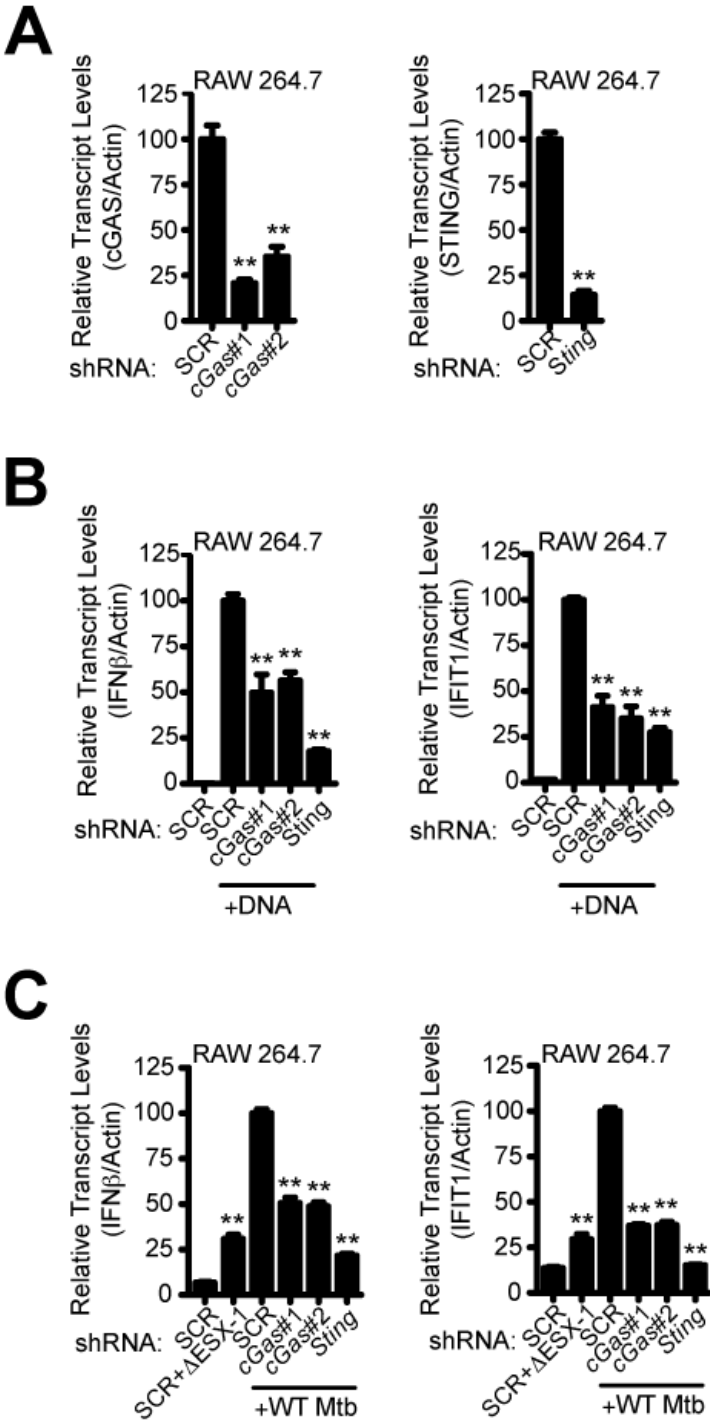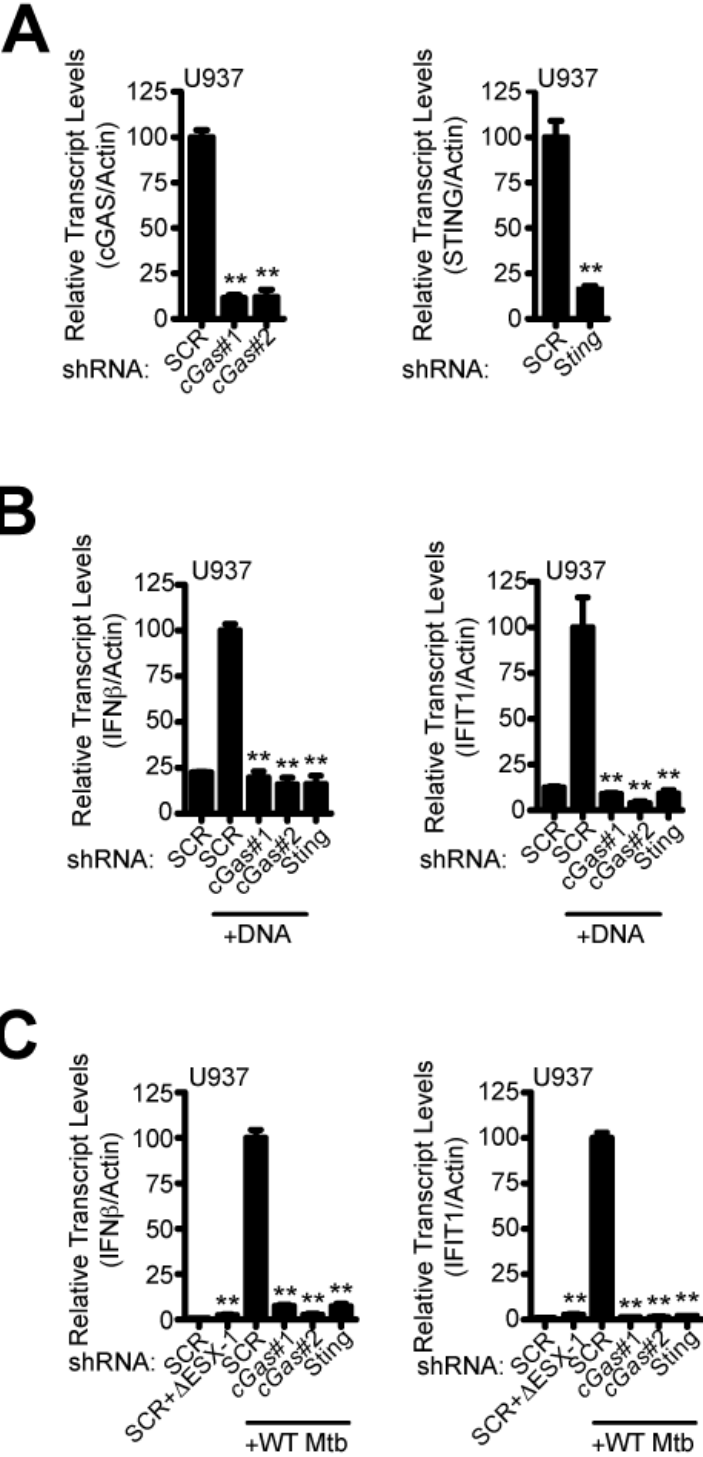
(A) Murine macrophage-like cell line RAW 264.7 was transduced with lentivrial constructs expressing scrambled shRNA (SCR) or shRNAs targeting *cGas* or *Sting*, and mRNA levels were measured by RT-qPCR. mRNA levels are expressed as a percentage relative to SCR-expressing cells.

(B) RAW 264.7 cells stably expressing scramble-shRNA (SCR), shRNA-*cGas*, or shRNA-*Sting* constructs were transfected with ISD for 4 h, and IFN-β and IFIT1 transcript levels were measured. mRNA levels are expressed as percentages relative to transfected SCR-expressing cells.

(C) RAW 264.7 cells stably expressing scramble-shRNA (SCR), shRNA-*cGas*, or shRNA-*Sting* constructs were infected with WT or ΔESX-1 *M. tuberculosis* for 4 h, and IFN-β and IFIT1 transcript levels were measured. mRNA levels are expressed as percentage relative to infected SCR-expressing cells. **$p < 0.005$ by two-tailed t-test.

Figure 2.4

Figure 2.4. cGAS is essential for induction of the cytosolic surveillance pathway in a human macrophage-like cell line.

(A) Human monocyte cell line U937 was transduced with lentivrial constructs expressing scrambled shRNA (SCR) or shRNAs targeting *cGas* or *Sting*, and mRNA levels were measured by RT-qPCR. mRNA levels are expressed as a percentage relative to SCR-expressing cells.

(B) U937 cells stably expressing scramble-shRNA (SCR), shRNA-*cGas*, or shRNA-*Sting* constructs were transfected with ISD for 4 h, and IFN-β and IFIT1 transcript levels were measured. mRNA levels are expressed as percentages relative to transfected SCR-expressing cells.

(C) U937 cells stably expressing scramble-shRNA (SCR), shRNA-*cGas*, or shRNA-*Sting* constructs were infected with WT or ΔESX-1 *M. tuberculosis* for 4 h, and IFN-β and IFIT1 transcript levels were measured. mRNA levels are expressed as percentage relative to infected SCR-expressing cells. **$p < 0.005$ by two-tailed t-test.

Figure 2.5
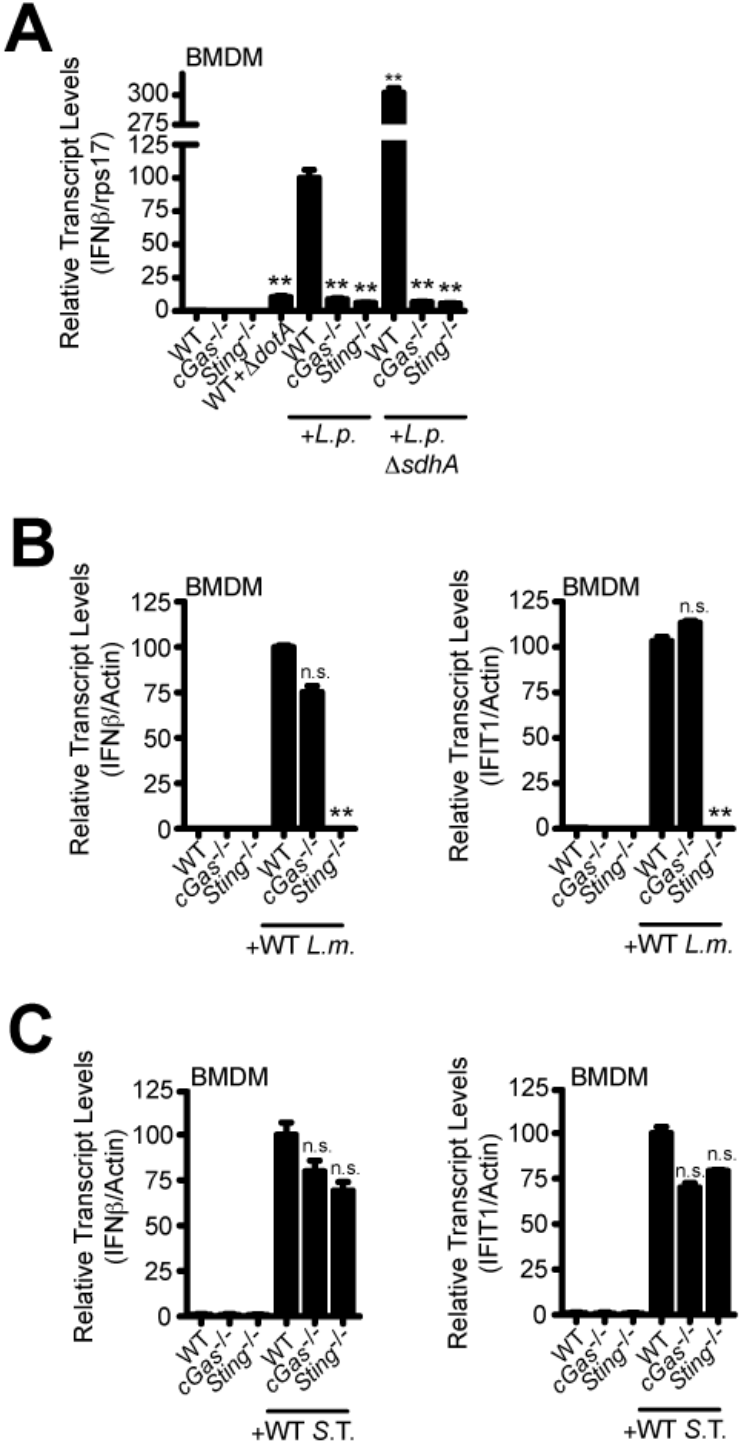
Figure 2.5. cGAS is essential for induction of the cytosolic surveillance pathway in response to some other intracellular bacterial infections.

(A) BMDMs were infected for 4 h with *Legionella pneumophila ΔflaA* (*L.p.*) or *ΔflaAΔsdhA* (*L.p.ΔsdhA*) and transcript levels were measured by RT-qPCR,

(B) Same as (A) but BMDMs were infected with *Listeria monocytogenes* (*L.m.*).

(C) Same as (A) but BMDMs were infected with *Salmonella enterica* serovar Typhimurium (*S. T.*). n.s., not significant, **$p < 0.005$ by two-tailed t-test.

Figure 2.6
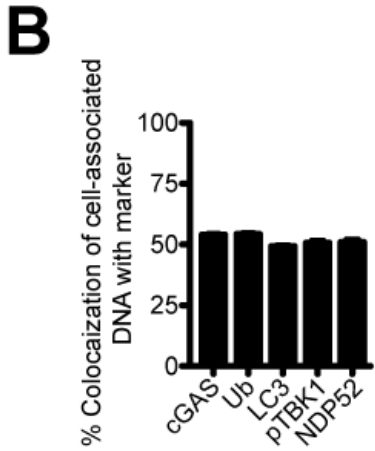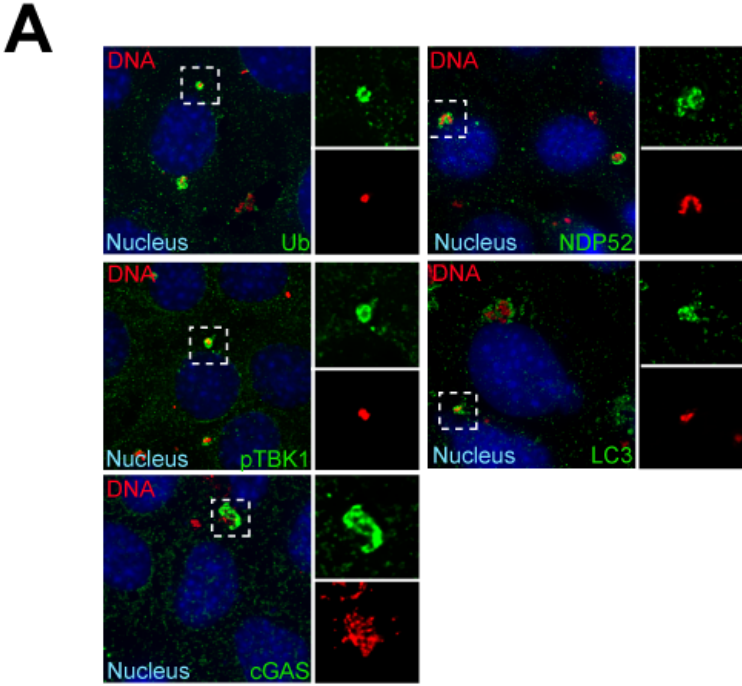
Figure 2.6. cGAS, like selective autophagy markers, is recruited to cytosolic DNA.

(A) Mouse embryonic fibroblasts (MEFs) expressing FLAG-cGAS were transfected with Cy3-labelled plasmid DNA for 4 h and immunostained for 3xFLAG or indicated selective autophagy markers.

(B) Quantification of cGAS+ or selective autophagy marker positive Cy3-DNA from (A).

Figure 2.7
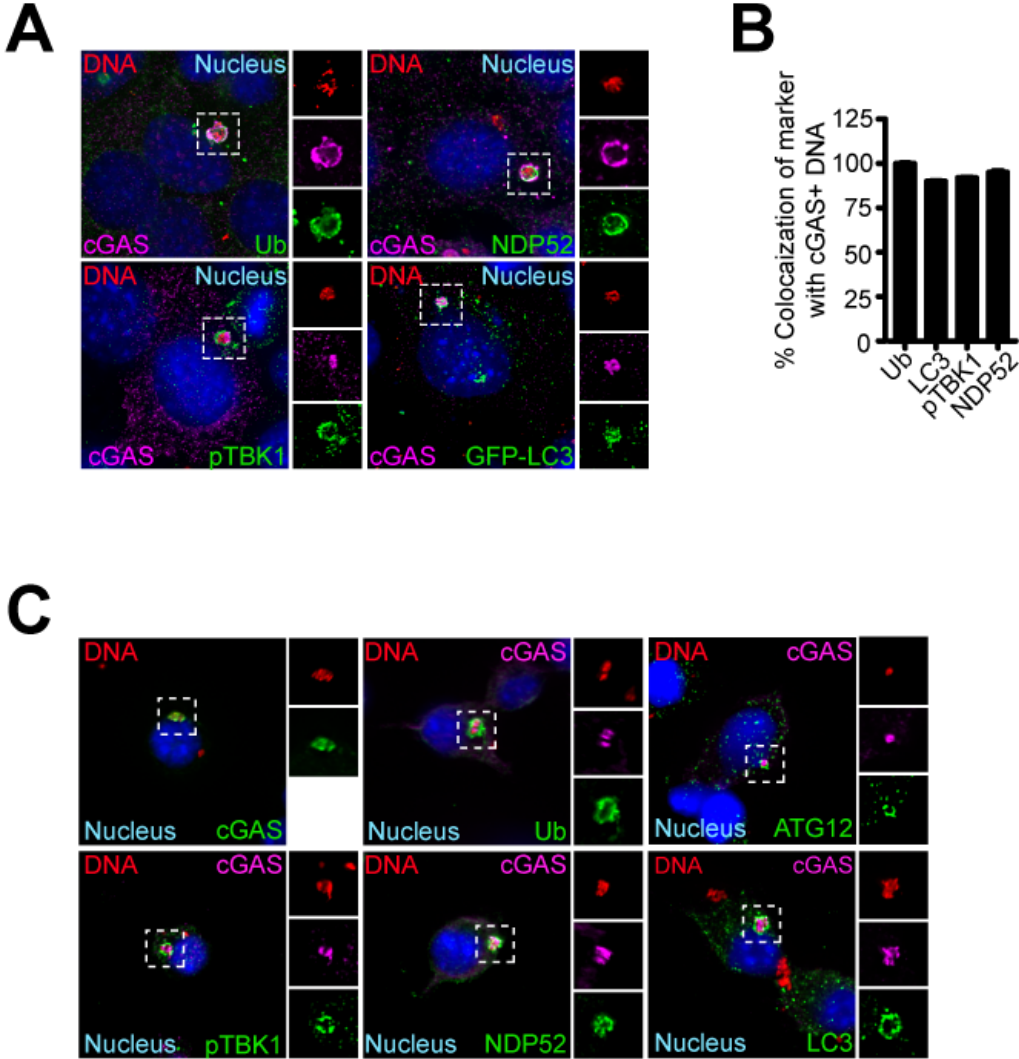
Figure 2.7. cGAS and selective autophagy markers are recruited to the same cytosolic DNA population.

(A) Mouse embryonic fibroblasts (MEFs) expressing 3xFLAG-tagged mouse cGAS were transfected with Cy3-labeled plasmid DNA for 4 h and immunostained for 3xFLAG or selective autophagy markers.

(B) Quantification of cGAS+ Cy3-DNA co-stained with indicated marker from (A). Differences are not statistically significant.

(C) RAW 264.7 cells stably expressing FLAG-cGAS were transfected with Cy3-DNA for 4 h and immunostained for 3xFLAG and indicated selective autophagy markers.

Figure 2.8
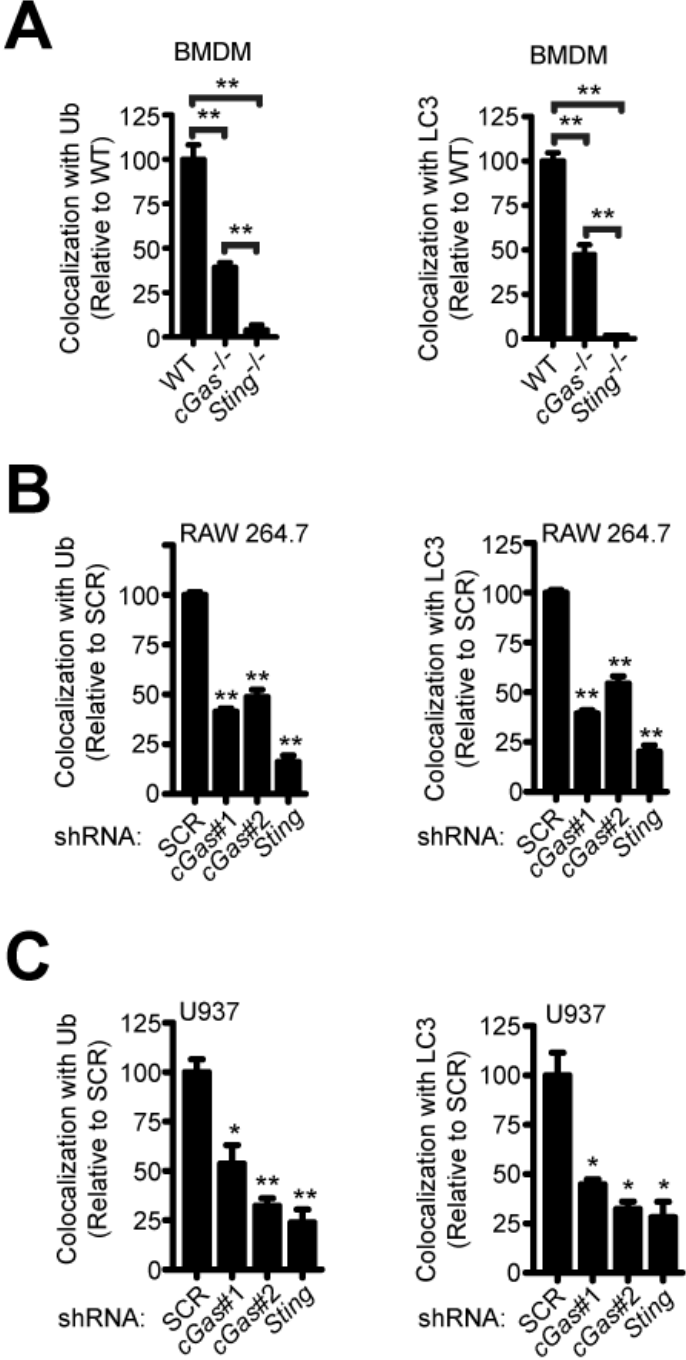
Figure 2.8. cGAS is required for targeting cytosolic DNA to the ubiquitin-mediated selective autophagy pathway.

(A) Quantification of ubiquitin and LC3 colocalization with Cy3-DNA 4 h post-transfection in WT, *cGas*^{-/-}, or *Sting*^{-/-} BMDMs.

(B) Same as (A) but in RAW 264.7 knockdown cell lines.

(C) Same as (A) but in U937 knockdown cell lines. $*p < 0.05$, $**p < 0.005$ by two-tailed t-test.

Figure 2.9
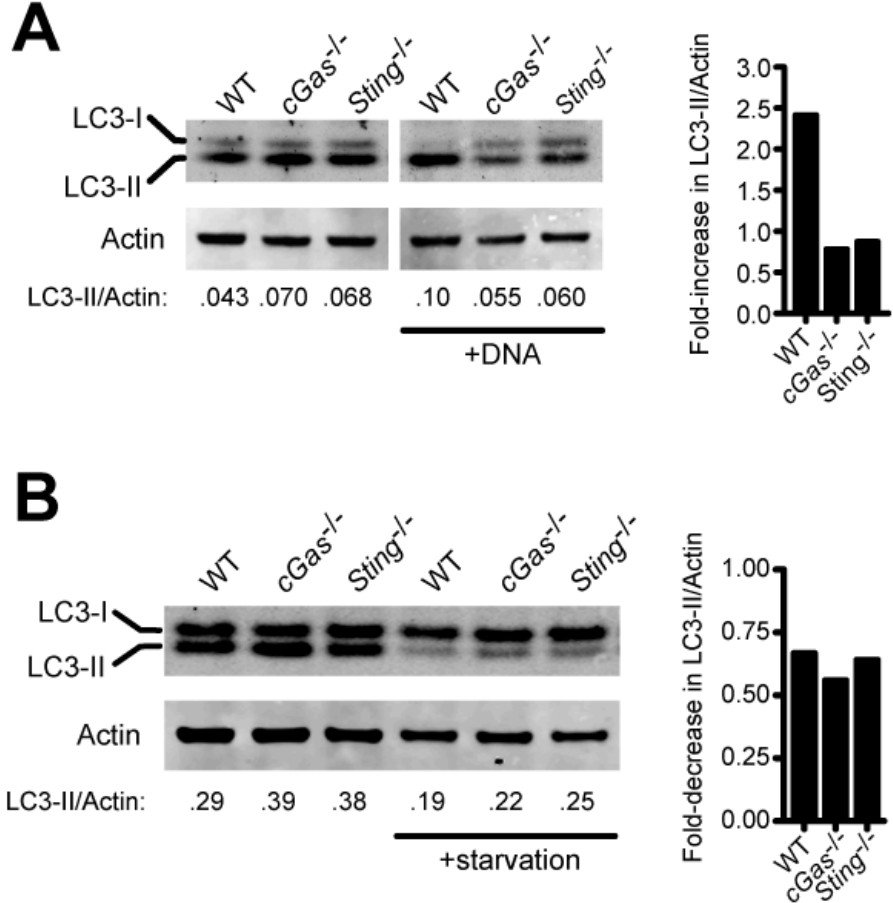
Figure 2.9. cGAS is required for LC3 conversion in response to DNA transfection but not starvation.

(A) WT, *cGas*^{-/-} or *Sting*^{-/-} BMDMs were transfected with ISD for 2 h, and LC3-II conversion was analyzed by quantitative Western blot and expressed as a ratio of LC3-II/Actin (left) and as a fold-increase of this ratio (right).

(B) WT, *cGas*^{-/-} and *Sting*^{-/-} BMDMs were starved for 30 min and LC3-II conversion was analyzed by quantitative Western blot and expressed as a ratio of LC3-II/Actin (left) and as a fold-increase of this ratio (right). Results shown are representative of at least three independent experiments.

Figure 2.10
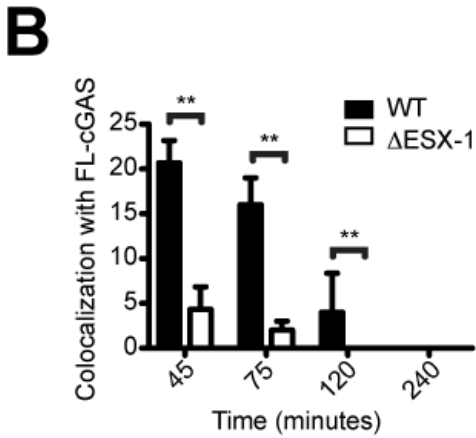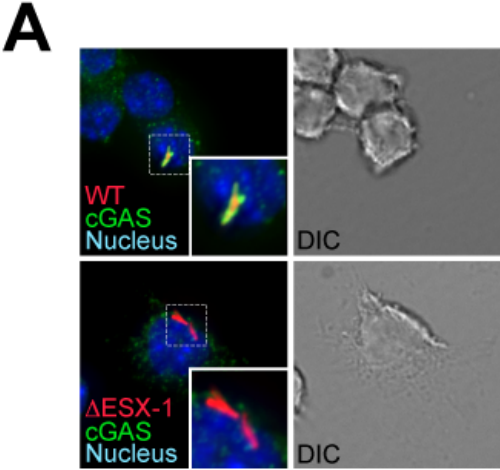
Figure 2.10. cGAS colocalizaes with *M. tuberculosis* in an ESX-1-dependent manner during infection.

(A) RAW 264.7 cells stably expressing FLAG-cGAS were infected with mCherry WT or ΔESX-1 *M. tuberculosis* for 45 min and immunostained for 3xFLAG.

(B) Quantification of cGAS+ *M. tuberculosis* during infection.

Figure 2.11

Figure 2.11. cGAS and selective autophagy markers are recruited to similar *M. tuberculosis* populations during infection.

(A) RAW 264.7 cells stably expressing FLAG-cGAS were infected with mCherry WT or ΔESX-1 *M. tuberculosis* for 45 min and immunostained for 3xFLAG and indicated markers.

(B) Quantification of cGAS+ bacteria co-stained with pTBK1 or LC3 from (A).

(C) Quantification of bacteria colocalized with pTBK1 and LC3 during infection.

Figure 2.12
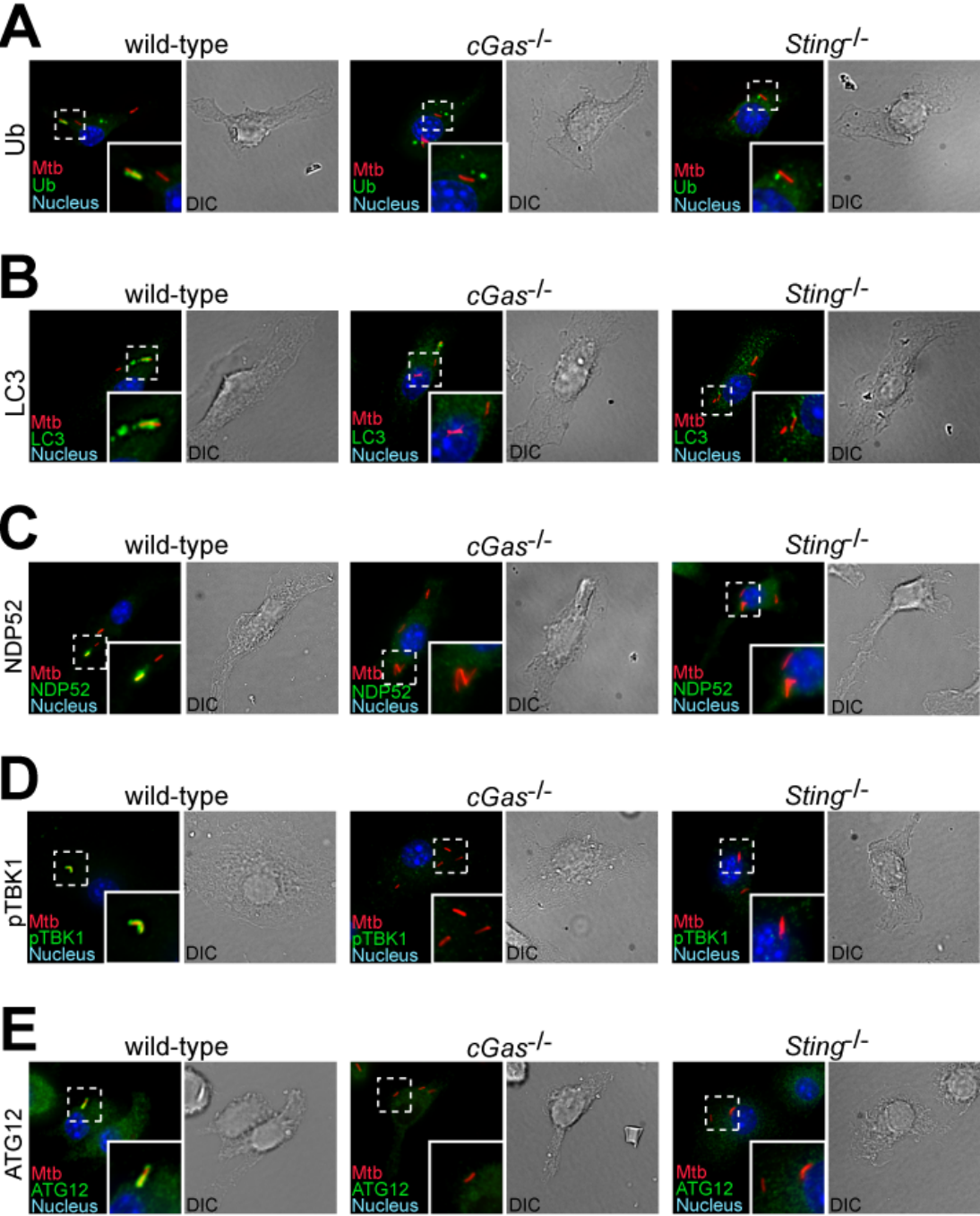
Figure 2.12. cGAS is required for efficient recruitment of selective autophagy markers to

***M. tuberculosis*.**

(A) WT, *cGas^{-/-}*, and *Sting^{-/-}* BMDMs were infected with mCherry WT *M. tuberculosis* and immunostained for ubiquitin 4 h post-infection.

(B) Same as (A) but immunostained for LC3.

(C) Same as (A) but immunostained for NDP52.

(D) Same as (A) but immunostained for pTBK1.

(E) Same as (A) but immunostained for ATG12.

Figure 2.13
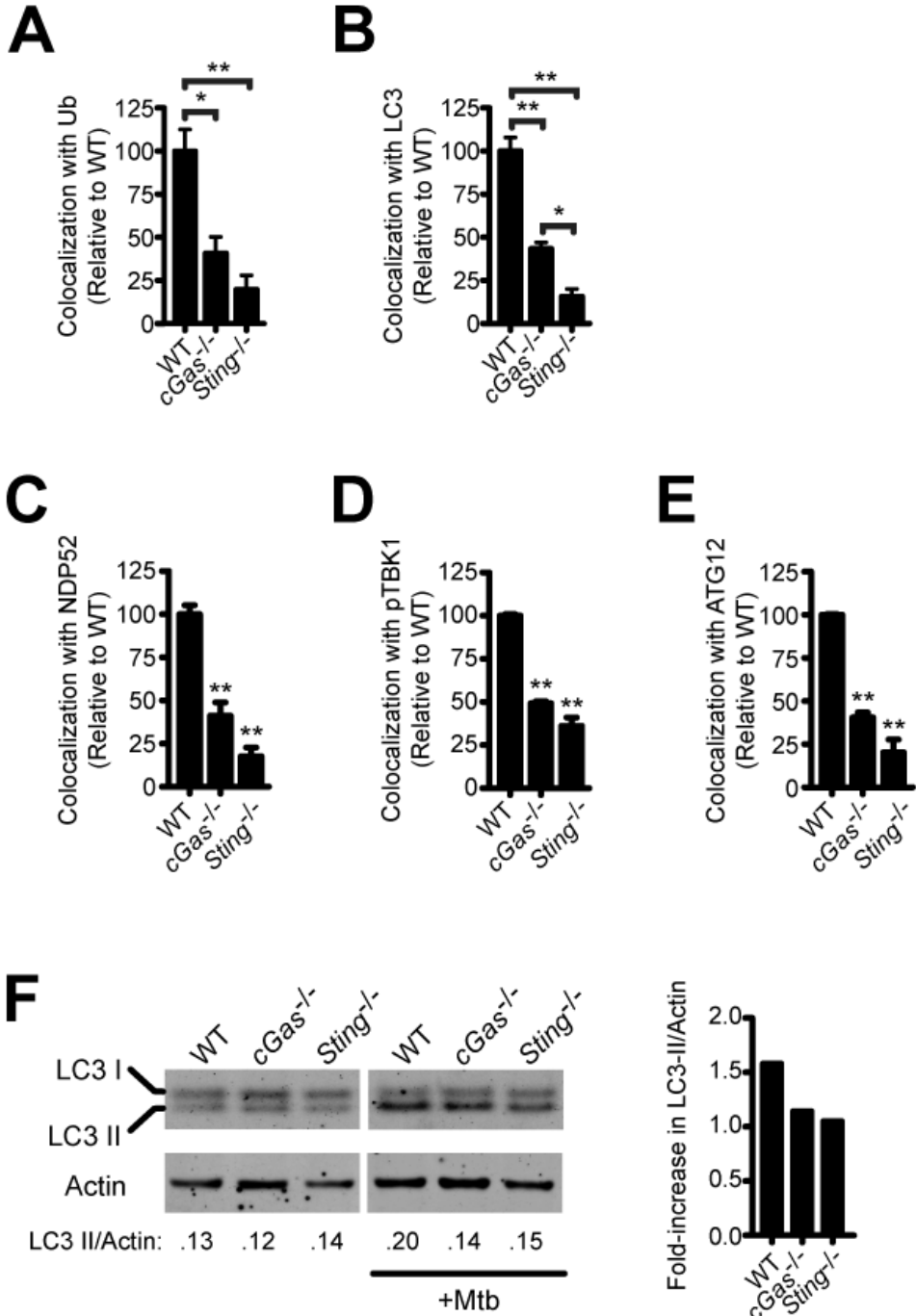
Figure 2.13. cGAS is required to efficiently target *M. tuberculosis* to the ubiquitin-mediated selective autophagy pathway.

(A) Quantification of ubiquitin-positive mCherry *M. tuberculosis* after 4 h infection in WT, *cGas*^{-/-}, or *Sting*^{-/-} BMDMs.

(B) Same as (A) but quantification of LC3-positive bacteria.

(C) Same as (A) but quantification of NDP52-positive bacteria.

(D) Same as (A) but quantification of pTBK1-positive bacteria.

(E) Same as (A) but quantification of ATG12-positive bacteria.

(F) WT, *cGas*^{-/-} or *Sting*^{-/-} BMDMs were transfected with ISD for 2 h, and LC3-II conversion was analyzed by quantitative Western blot and expressed as a ratio of LC3-II/Actin (left) and as a fold-increase of this ratio (right). Results shown are representative of at least three independent experiments. *$p < 0.05$, **$p < 0.005$ by two-tailed t-test.

Figure 2.14
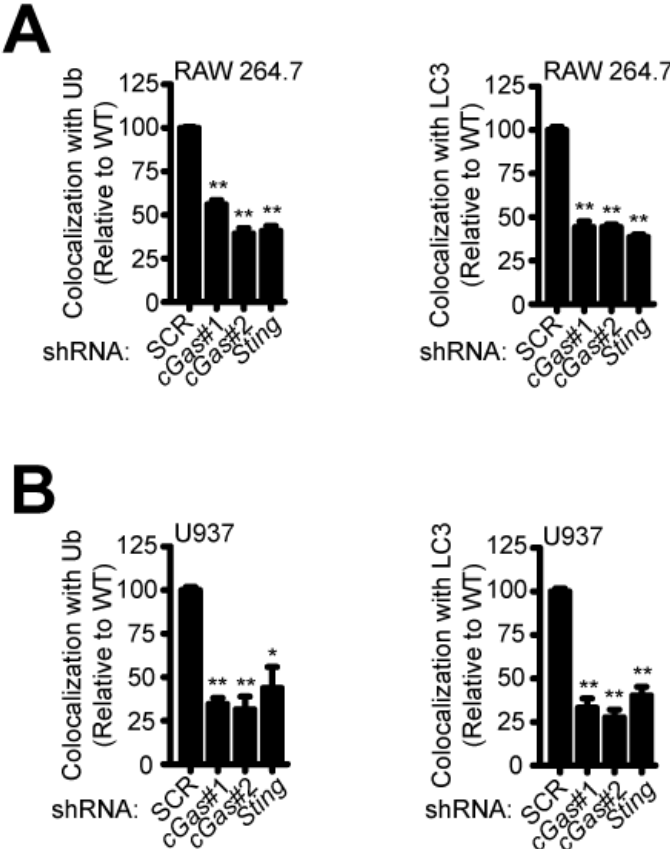
Figure 2.14. cGAS is required to target *M. tuberculosis* to the ubiquitin-mediated selective autophagy pathway in macrophage-like cell lines.

(A) Quantification of ubiquitin- and LC3-positive *M. tuberculosis* in RAW 264.7 knockdown cell lines.

(B) Same as (A) but with U937 knockdown cell lines. $*p < 0.05$, $**p < 0.005$ by two-tailed t-test.
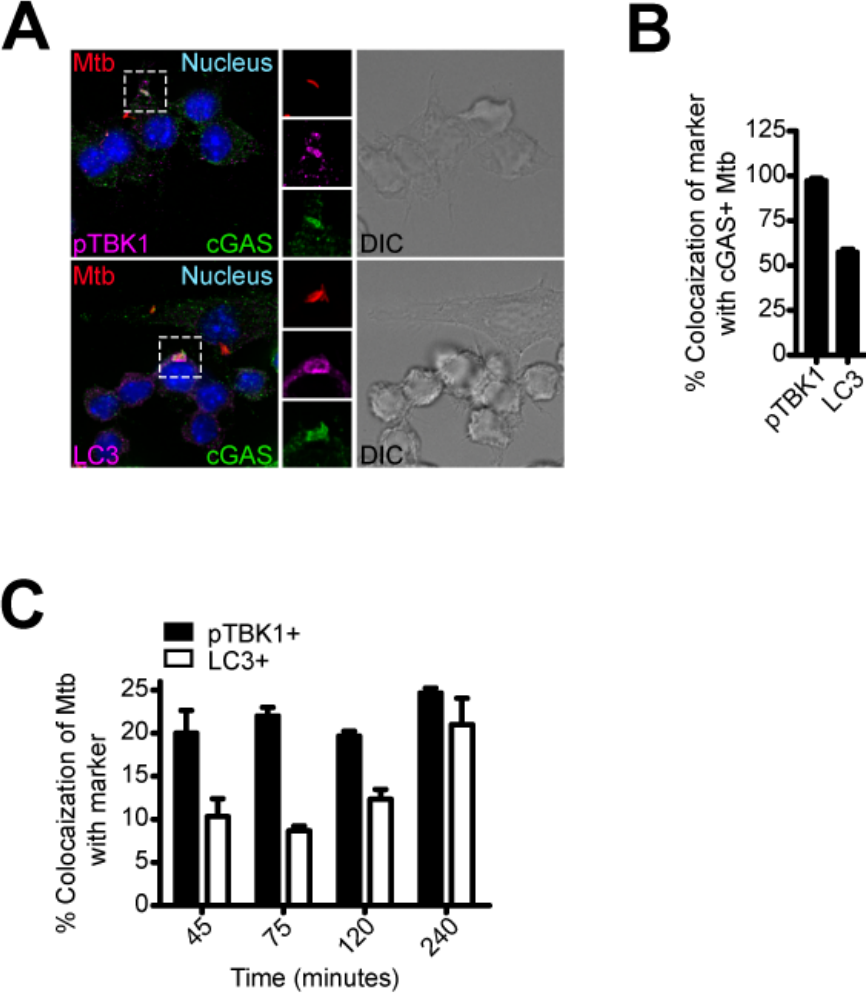
Figure 2.15
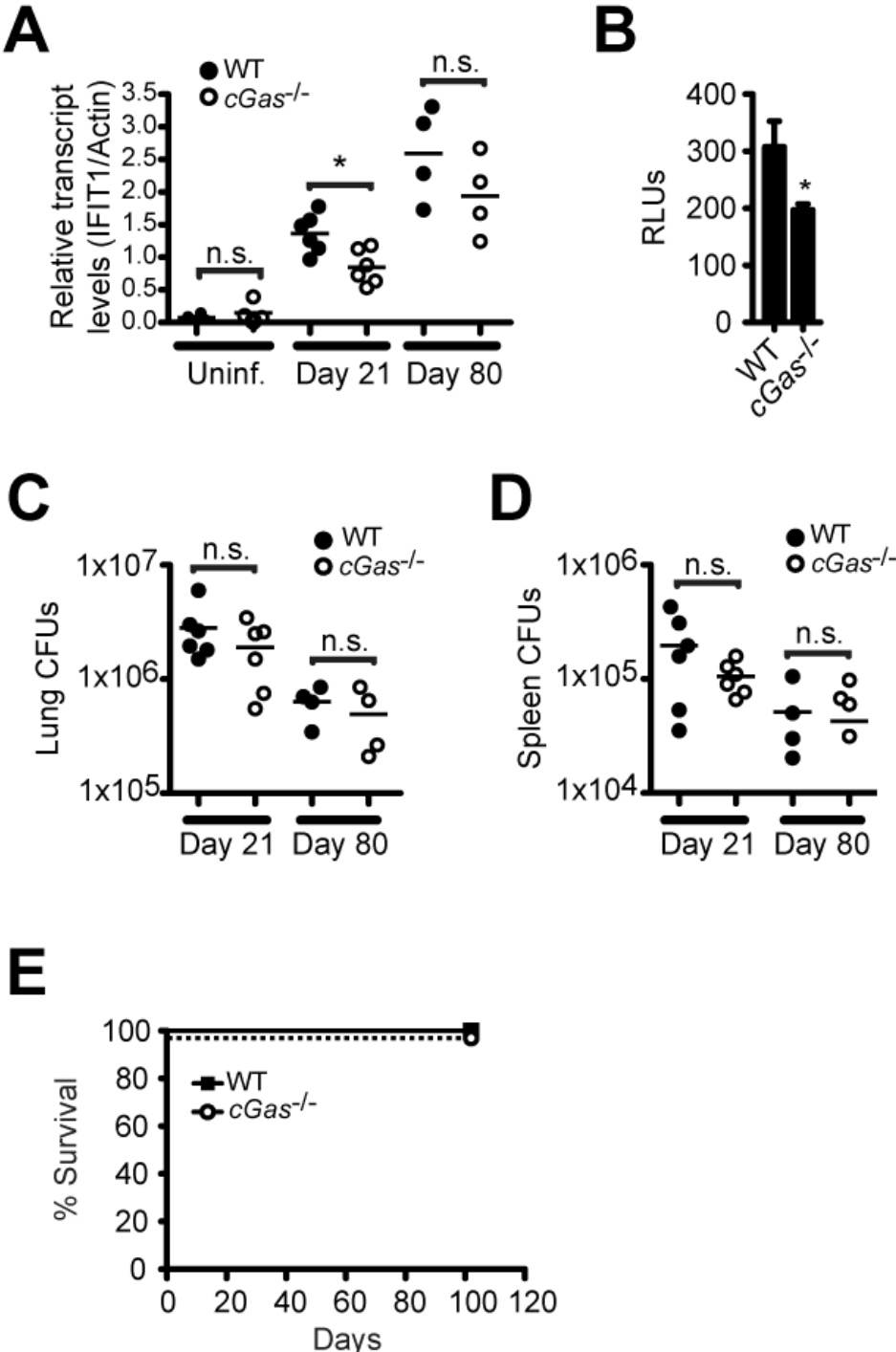
2.15. cGAS is not critical for host responses to *M. tuberculosis* infection *in vivo*.

(A-E) WT and *cGas*-/- mice were infected with ~100 aerosolized *M. tuberculosis* colony forming units (CFUs) (n = 4 or 6 per group).

(A) IFIT1 transcript levels in lungs of uninfected and infected WT and *cGas*-/- mice.

(B) IFN-β serum levels in WT and *cGas*-/- mice 21 days after infection as measured by ISRE-luciferase reporter cells.

(C) *M. tuberculosis* CFUs in lungs 21 and 80 days after infection.

(D) Same as (C) but in spleens.

(P) Survival of infected WT and *cGas*-/- mice monitored for 102 days (n = 6 wild-type and 3 *cGas*-/-). n.s., not significant, *$p < 0.05$ by two-tailed t-test.

Figure 2.16
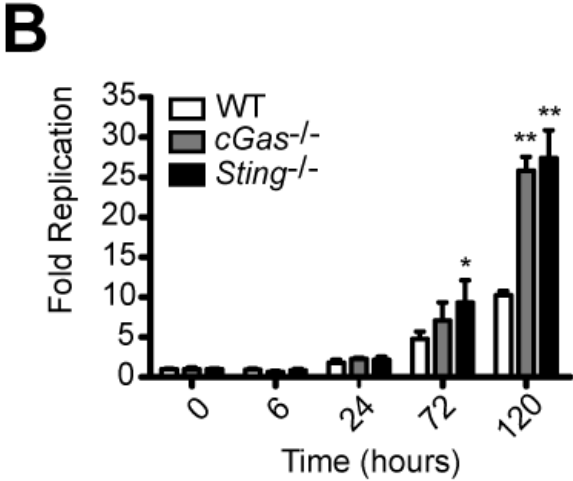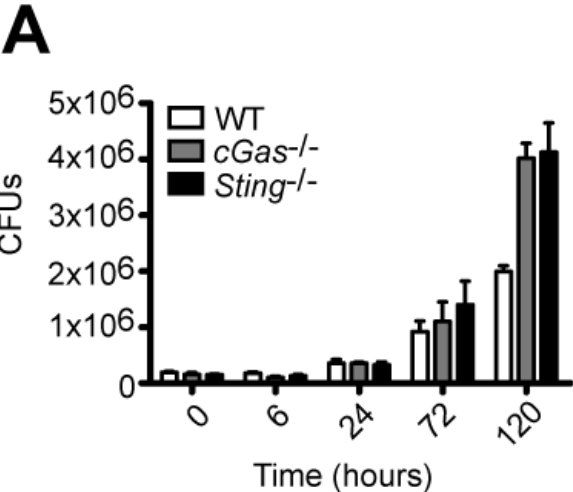
Figure 2.16. cGAS is required to control intracellular replication of *M. tuberculosis* in macrophages.

(A) CFUs from WT, *cGas*^{-/-}, and *Sting*^{-/-} BMDMs infected with *M. tuberculosis* at 6, 24, 72, and 120 h.

(B) CFUs from (A) normalized to CFUs at 0 h. $*p < 0.05$, $**p < 0.005$ by two-tailed t-test.

Figure 2.17
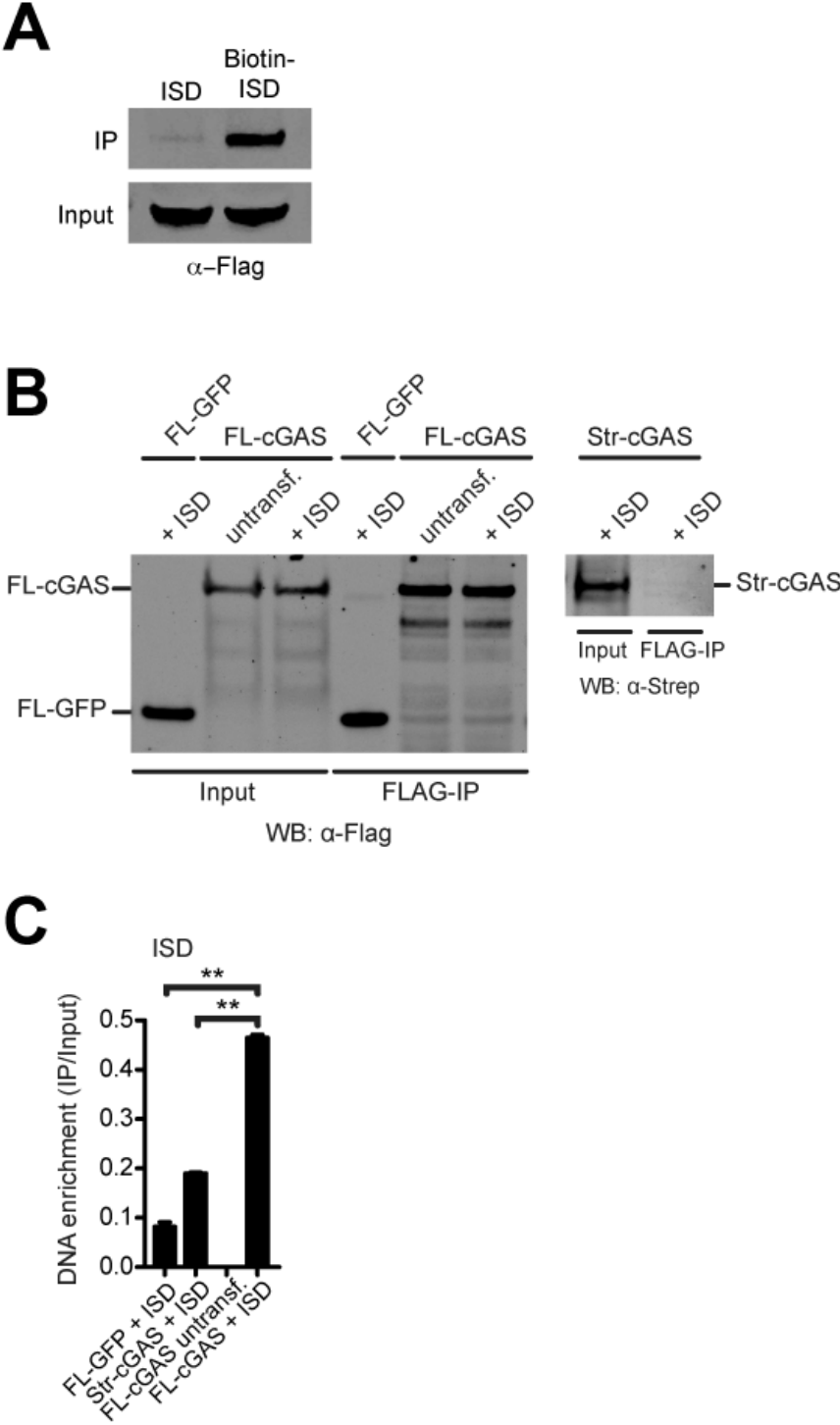
Figure 2.17. cGAS binds to cytosolic DNA.

(A) Western blot of FLAG-cGAS after streptavidin pulldown of cell lysates from FLAG-cGAS-expressing RAW 264.7 cells transfected with interferon-stimulatory DNA (ISD) or biotinylated-ISD.

(B) Western blot of inputs and FLAG immunoprecipitates from untransfected or interferon stimulatory DNA- (ISD-) transfected RAW 264.7 cells stably expressing FLAG-GFP or FLAG-cGAS (left panel), or Strep-cGAS as a negative control (right panel). Whole cell lysates (Input) or IPs (Flag-IP) were visualized by Western blot using anti-FLAG (left) or anti-Strep (right) antibodies.

(C) qPCR analysis of the abundance of ISD from DNA isolated from immunoprecipitated samples in (B) using primers specific to ISD. Amounts were normalized to abundance of ISD in inputs. Results are representative of at least three independent biological experiments. **$p <$ 0.005 by two-tailed t-test.

Figure 2.18
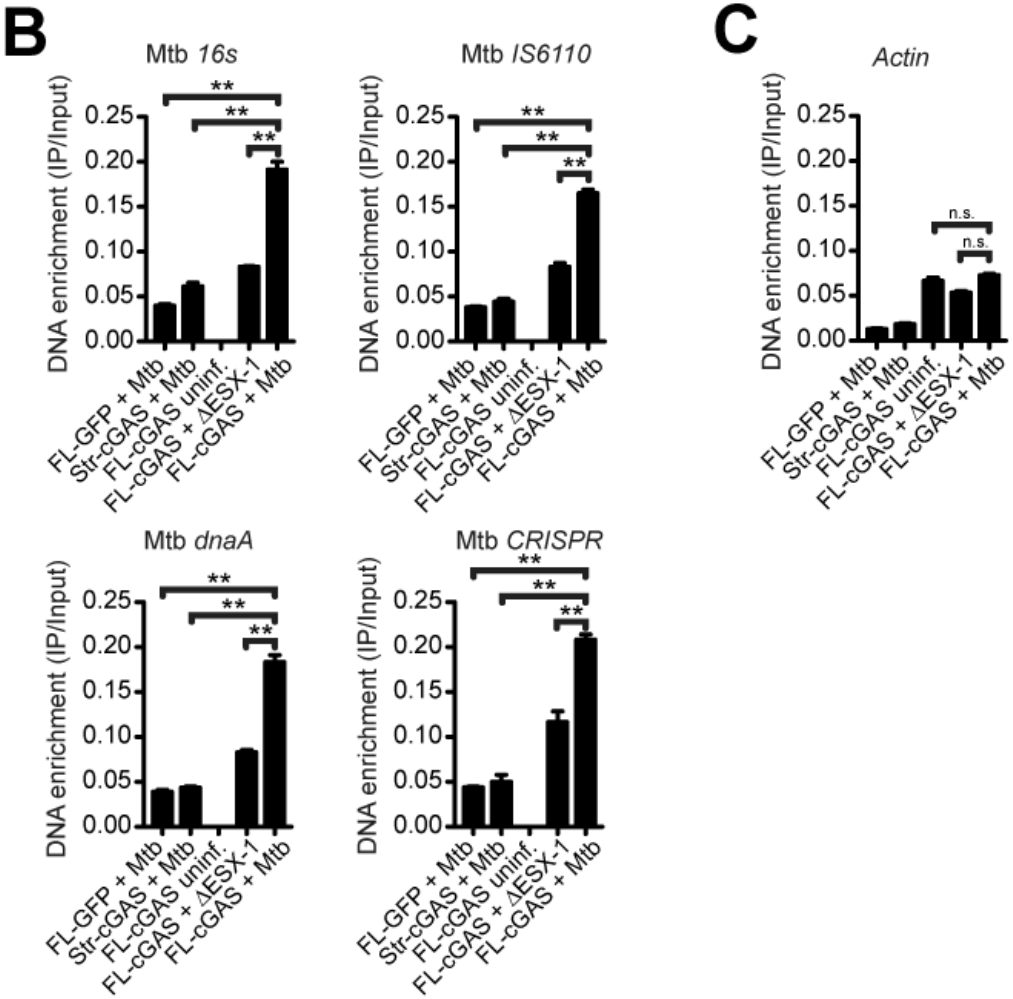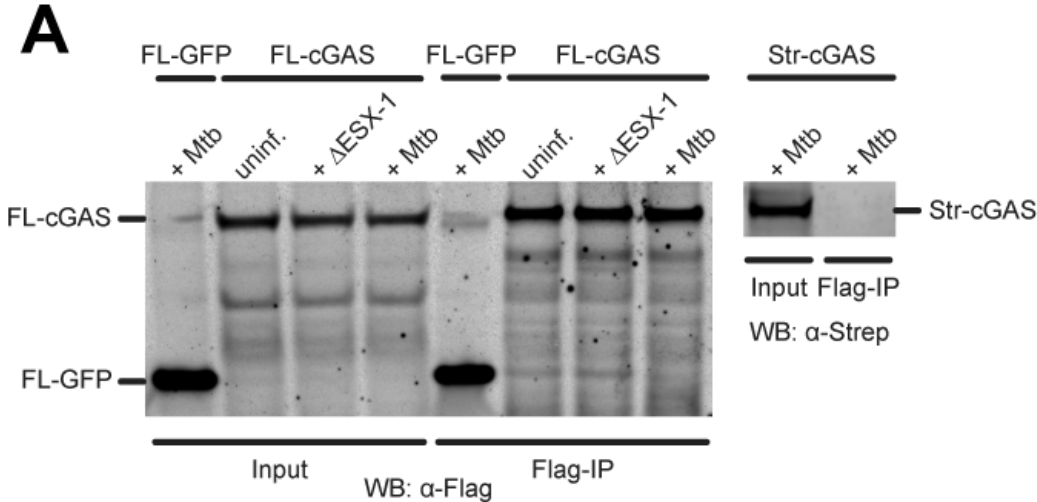
Figure 2.18. cGAS binds to *M. tuberculosis* DNA during infection.

(A) Western blot of inputs and FLAG immunoprecipitates from WT or ΔESX-1 *M. tuberculosis* infected RAW 264.7 cells stably expressing FLAG-GFP or FLAG-cGAS (left panel), or Strep-cGAS as a negative control (right panel). Whole cell lysates (Input) or IPs (Flag-IP) were visualized by Western blot using anti-FLAG (left) or anti-Strep (right) antibodies.

(B) qPCR of *M. tuberculosis*-derived sequences from DNA isolated from IPs in (A). Quantities were normalized to inputs.

(C) Same as (B) but mouse *Actin*. n.s., not significant, **$p < 0.005$ by two-tailed t-test.

Figure 2.19
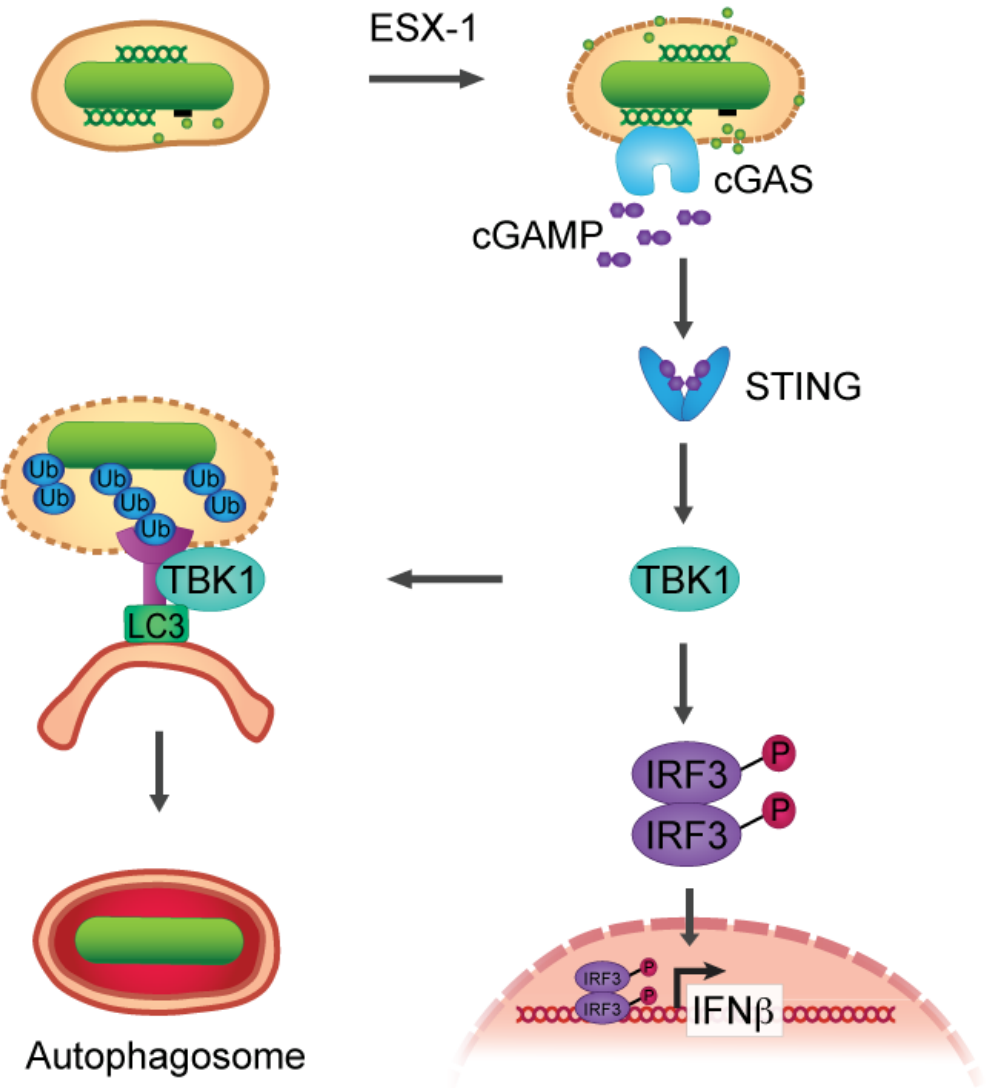
Figure 2.19. Model of cGAS sensing cytosolic DNA during *M. tuberculosis* infection.

Upon phagocytosis of *M. tuberculosis* by a macrophage, the ESX-1 secretion system mediates phagosome permeabilization. This exposes bacterial DNA to the cytosol where cGAS binds it and produces cGAMP. cGAMP binds to and activates STING, leading to activation of the downstream kinase TBK1. TBK1 phosphorylates IRF3, causing its dimerization, translocation into the nucleus, and increased expression of IRF3 targets. Simultaneously, upon binding cytosolic DNA, cGAS activates STING and TBK1, resulting in the recruitment of activated phospho-TBK1 to exposed bacteria. This leads to the tagging of *M. tuberculosis*-containing phagosomes with ubiquitin and the recruitment of selective autophagy proteins, including NDP52 and LC3. The resulting autophagosomes fuse with lysosomes, which efficiently destroy bacteria.

Chapter 3: Characterizing the function and role of the *Mycobacterium tuberculosis* CRISPR-Cas system

Introduction

Most bacteria and archaea exist in complex communities where they must protect themselves from predatory bacteriophages and conjugative plasmids. Clustered, regularly interspaced, short palindromic repeats (CRISPRs), are common genomic loci in bacteria and archaea that provide immunity to previously encountered threats (Sorek et al., 2013). CRISPR loci are comprised of direct repeats separated by unique spacer sequences that are homologous to sequences in these previously encountered bacteriophages or plasmids (Barrangou et al., 2007; Bolotin et al., 2005; Mojica et al., 2000; 2005; Pourcel et al., 2005). Adjacent to this locus is a group of CRISPR-associated (Cas) genes that encode a variety of helicases, nucleases, and RNA-binding proteins responsible for mediating the immune functions of the CRISPR locus (Haft et al., 2005; Jansen et al., 2002; Lillestøl et al., 2006; Makarova et al., 2006). While the identified bacterial and archaeal CRISPR-Cas systems are extremely diverse, the general steps to achieve immunity against foreign nucleic acids are conserved (Figure 3.1)(Sorek et al., 2013). First, when a bacterium encounters a bacteriophage or plasmid, Cas1 and Cas2 incorporate sequences (known as protospacers) from these sources to create new spacers in the CRISPR locus (Heler et al., 2014). Next, the CRISPR locus is transcribed as a full-length RNA transcript and then processed into small CRISPR RNAs (crRNAs), each of which contains a single spacer sequence flanked by several nucleotides of the repeat on both the 5' and 3' ends (Charpentier et al., 2015). Often, the ends of the crRNA are further processed to generate the mature effector crRNA (Charpentier et al., 2015). Finally, other Cas genes,

which form complexes specific to the type of CRISPR-Cas system, utilize the crRNA to scan the cytoplasm, identify targets homologous to the crRNA, and degrade the invading nucleic acid (Plagens et al., 2015).

Although most CRISPR-Cas systems target exogenous DNAs for degradation, there is increasing evidence that these systems may have additional or alternative functions. The CRISPR-Cas system found in the archaea, *Pyrococcus furiosus*, is capable of degrading single-stranded RNAs *in vitro* (Hale et al., 2012; 2008). Interestingly, in a variety of species, some spacers share significant sequence homology with the chromosome (Bolotin et al., 2005; Mojica et al., 2005), suggesting that some CRISPR-Cas systems may be capable of targeting self-RNAs with possible roles in gene regulation. Indeed, CRISPR-Cas systems in *Thermus thermophilus* and *Streptococcus thermophilus* have been shown to degrade single stranded RNA and mRNA transcripts (Staals et al., 2014; Tamulaitis et al., 2014). Reports have also indicated that CRISPR-Cas systems can regulate physiologic states. In *Pseudomonas aeruginosa*, the CRISPR-Cas system regulates biofilm formation, in *Myxococcus xanthus*, the CRISPR-Cas system regulates fruiting body formation, and in *Legionella pneumophila*, Cas2 promotes infectivity (Cady and O'Toole, 2011; Gunderson et al., 2015; Viswanathan et al., 2007).

Intriguingly, bioinformatic analysis of CRISPR loci from multiple bacteria, including *Salmonella enterica* and *Escherichia coli*, showed that the spacers in these bacteria seem to evolve neither quickly nor in response to different environments with varying bacteriophage and plasmid compositions; this pattern of evolution is the opposite of what one would expect from a functional adaptive immune system (Shariat et al., 2015; Touchon et al., 2011). Additionally, in many bacteria with CRISPR loci, the spacers do not match any known plasmid or bacteriophage sequences, and the CRISPR-Cas complexes do not appear to function as canonical immunity

complexes. Together, this provides strong evidence that CRISPR-Cas systems function in additional biological roles beyond immunity against exogenous nucleic acids. Despite the heavy research focus on CRISPR-Cas systems as a biotechnology tool in recent years (Boettcher and McManus, 2015; Mali et al., 2013), there is likely much exciting CRISPR-Cas biology yet to be discovered.

Unlike most bacteria, *Mycobacterium tuberculosis* does not live in a complex bacterial community. Instead, this bacterium exists primarily alone in the sterile tissues of the host, most importantly in the lungs (Kaufmann, 2001). After reaching the lower lung in aerosolized droplets, *M. tuberculosis* is quickly phagocytosed by alveolar macrophages (Russell, 2001). In later stages of infection, the bacteria are contained in granulomas surrounded by immune cells (Kaufmann, 2001; Russell, 2001). Because of its solitary lifecycle in a sterile environment, it is not immediately obvious why *M. tuberculosis* might maintain a large and often unstable restriction system such as the CRISPR-Cas system. Further complicating this question is the observation that the spacers in the *M. tuberculosis* CRISPR locus do no match any known sequences, especially those of known mycobacteriophages. Even so, various laboratory and clinical strains of *M. tuberculosis* contain differing unique spacer sequences, suggesting the system is capable of incorporating new sequences and therefore at least partially functional (Shariat and Dudley, 2014; van Embden et al., 2000). However, while nearly every environmental mycobacterial species (such as *M. smegmatis*) does not contain CRISPR-Cas loci, the presence of a CRISPR-Cas system in only pathogenic mycobacteria (*M. tuberculosis*, *M. bovis*, *M. canettii*) strongly suggests a novel role for the CRISPR-Cas system in virulence or pathogenesis (Rousseau et al., 2009). However, how the CRISPR-Cas system may contribute to these traits is largely unknown.

Here I show that while the *M. tuberculsosis* CRISPR-Cas system is expressed and generates crRNAs, it does not function in restricting plasmid DNA. While it may affect key transcript levels, including those of cryptic prophages, it does not seem to be required for growth either *in vitro* or *in vivo*. Despite this, the widespread maintenance of a large complex genomic locus across pathogenic mycobacterial species strongly indicates it may play a novel role in a yet to be indentified biological process. I provide a discussion as to what functions the *M. tuberculosis* CRISPR-Cas system may serve and ideas for future experiments and directions.

Results

The *M. tuberculosis* CRISPR-Cas system is expressed and processes crRNAs

To begin to assess the functionality of the *M. tuberculosis* CRISPR-Cas system, I performed Northern blot analysis on small RNAs isolated from *M. tuberculosis* grown in liquid culture. Using two different probes that spanned different spacer and repeat regions, I detected small RNAs the expected size of crRNAs (Figure 3.2A). Importantly, in small RNAs from a *Δcas6* mutant strain that is incapable of processing crRNAs, I did not detect any mature crRNAs (Figure 3.2A). I also performed Northern blot analysis on *M. smegmatis*, which is an environmental species of mycobacteria that does not contain a CRISPR-Cas system, and, as expected, I observed no crRNAs (Figure 3.2B). However, when I transformed *M. smegmatis* with a cosmid containing a piece of the *M. tuberculosis* genome containing the CRISPR-Cas system, I detected mature crRNAs (Figure 3.2B). In RT-PCR experiments, I saw expression of all *Cas* genes (except for Csm5 and Csm6, see Discussion) both in *M. tuberculosis* and in *M. smegmatis* with the CRISPR-Cas cosmid (data not shown). Furthermore, recent work suggests that crRNAs alone are very instable and can frequently only be detected when they are in complex with Cas proteins (Brendel et al., 2014), so the detection of crRNAs by Northern blot

additionally supports the notion that Cas complexes are efficiently assembled. Taken together, this demonstrates that the *M. tuberculosis* CRISPR-Cas system is able to process mature crRNAs and assemble Cas complexes.

The *M. tuberculosis* CRISPR-Cas system does not degrade plasmid DNA

Next, I tested the ability of the *M. tuberculosis* CRISPR-Cas system to target double-stranded plasmid DNA for degradation, which is a well-established function of other closely-related CRISPR-Cas systems (Marraffini and Sontheimer, 2008). I generated several plasmids, each containing a different protospacer that matched the CRISPR locus. As a negative control, I generated a plasmid with the non-targeted repeat sequence. I transformed wild-type *M. tuberculosis* Erdman strain with these plasmids and measured transformation efficiency using an internal transformation control of a second plasmid with an alternate antibiotic resistance marker. I observed no difference in transformation efficiency between an empty plasmid, a repeat-containing plasmid, and a spacer-containing plasmid (Figure 3.3). I performed this transformation assay with additional plasmids containing different protospacer sequences (data not shown), as well as with different *M. tuberculosis* strains (CDC1551, H37Rv) and consistently saw no difference in transformation efficiency, regardless of the sequence inserted into the plasmid.

In order to determine if the plasmids I generated were engineered properly for targeting by the CRISPR-Cas system, I generated many more versions of these plasmids and assayed transformation efficiency using the more tractable *M. smegmatis* either with or without the *M. tuberculosis* CRISPR-Cas system. First, I measured the transformation efficiency of the series of plasmids previously assayed in *M. tuberculosis* above, which had sequences inserted upstream of the plasmid's promoter (a strong, constitutive mycobacterial promoter) to prevent

interference between the CRISPR-Cas system and the transcriptional machinery. There was no difference in the transformation efficiency of these plasmids, regardless of the inserted sequence (Figure 3.4A). I next measured the transformation efficiency of a series of plasmids in which the protospacers were inserted downstream of the promoter, with the intention of utilizing the transcriptional machinery to open the DNA helix to allow the CRISPR-Cas system to access the protospacer for targeting (Samai et al., 2015). Again, there was no difference in transformation efficiency of these plasmids (Figure 3.4B). Finally, I generated another series of plasmids that again contained sequences downstream of the promoter, but on the opposite DNA strand to permit the CRISPR-Cas complex access to the DNA strand not occupied by the transcriptional machinery (Samai et al., 2015). Here, too, there was no difference in transformation efficiency (Figure 3.4C). Together, this provides strong evidence that the *M. tuberculosis* CRISPR-Cas system does not target double-stranded plasmid DNA for degradation.

The *M. tuberculosis* CRISPR-Cas system may have alternative biological roles

Because the *M. tuberculosis* CRISPR-Cas system does not seem to target DNA, I attempted to test the ability of the system to target RNA. I performed RNA-seq on wild-type and *Δcas6 M. tuberculosis* grown in liquid culture, but did not observe any overt changes in gene expression (data not shown). This could be because the CRISPR-Cas system modulates gene expression in small increments that were not detected by my analysis or because the CRISPR-Cas system is not maximally functional under these growth conditions.

In additional to a global approach, I also looked specifically at candidate transcripts to assess the ability of the CRISPR-Cas system to regulate gene expression. I measured the transcript levels of several cryptic prophage genes in the phiRv1 region of the *M. tuberculoisis*

genome (Bibb and Hatfull, 2002). If the CRISPR-Cas system did regulate gene transcription, we would predict that prophage gene expression might be controlled by this system. Interestingly, compared to wild-type *M. tuberculosis*, I saw increased prophage gene expression in the *Δcas6* mutant lacking a functional CRISPR-Cas system. While I only performed this experiment once, it provides promising evidence supporting the hypothesis that the *M. tuberculosis* CRISPR-Cas system targets and degrades single-stranded prophage RNAs. Importantly, the CRISPR-Cas systems in *T. thermophilus* and *S. thermophlius* have been shown to target and degrade RNAs, and they have the same Type III-A CRISPR-Cas systems found in *M. tuberculosis* with significant homology and similar gene structures (Staals et al., 2014; Tamulaitis et al., 2014).

In addition to probing the role of the *M. tuberculosis* CRISPR-Cas system in degrading RNAs, I tested its functionality in many other biological processes. I observed no overt defects in the *Δcas6* mutant compared to wild-type in numerous assays: biofilm formation, hypoxia survival, DNA damage survival, and bacteriophage induction.

The CRISPR-Cas system in *M. tuberculosis* does not provide a competitive advantage *in vivo* or *in vitro*

To directly test whether the CRISPR-Cas system is important for *M. tuberculosis* virulence and pathogenesis, I performed competitive infections using a 1:1 mix of wild-type:*Δcas6*. I could easily distinguish the mutant from wild-type using the antibiotic resistance marker that replaced the *cas6* gene in the mutant. Neither strain had a growth advantage in liquid culture (Figure 3.6A), in unactivated or interferon-γ activated macrophages (Figure 3.6B), or in the lungs (Figure 3.6C) or spleens (data not shown) of infected mice. While these results could be due to human-specific virulence effects or complementation of the mutant with wild-

type in a competition experiment, it seems that under these conditions, the CRISPR-Cas system does not contribute to *M. tuberculosis* virulence.

Discussion

The CRISPR-Cas system in *M. tuberculosis* is at least partially functional. The Cas genes are expressed, crRNAs are generated, and Cas complexes are assembled. However, the CRISPR-Cas system does not target plasmid DNA for degradation, and I have only tenuous data so far to indicate that the CRISPR-Cas system can instead target RNA for degradation. Furthermore, my data suggests that the system may not be required for virulence in several of our infection models. However, a vast majority of my data was collected using the Erdman strain as the wild-type strain and as the strain background for my Δ*cas6* mutant. Problematically, the Erdman strain contains a natural mutation in the Cas genes, as it has a common insertion sequence (*IS6110*) replacing genes *Csm5* and *Csm6*. While it is unclear what precise functions these genes have, the lack of a complete set of Cas genes must be taken into account in interpreting my data presented here. It is difficult to determine if my negative results are due to a truly nonfunctional mycobacterial CRISPR-Cas system or simply due to a mutation in this specific isolate of *M. tuberculosis*. Before publishing these results, the transformation experiments and infections should be repeated using strains H37Rv and/or CDC1551, both of which have all of the Cas genes and very similar CRISPR loci compared to each other and Erdman. Because it is difficult to know if my RNA-seq results were due to a mutated set of Cas genes, these and the directed RT-qPCR results should also be repeated in CDC1551 or H37Rv to determine if the CRISPR-Cas system targets RNAs. Additionally, experiments measuring other biological processes, such as DNA damage survival (induced by prophage excision and/or antibiotics), hypoxia survival, and biofilm formation should also be repeated in these alternate

67

strains with *Δcas6* mutants generated in the corresponding background. As an alternative to using *M. tuberculosis* for some of these readouts, I have recently generated plasmids containing *Cas6-Csm6* or *Csm1-6* and a single repeat-spacer-repeat CRISPR locus for testing CRISPR-Cas functionality in *M. smegmatis*.

I performed some transformation efficiency experiments in these alternative *M. tuberculosis* strains (H37Rv and CDC1551), but I observed no protospacer-dependent plasmid restriction. This could be due to targeting of RNA rather than DNA by the *M. tuberculosis* CRISPR-Cas system. Future experiments should focus on measuring the transformation efficiency of plasmids with the alternate orientations of protospacer sequences to test transcription-dependent DNA targeting (Samai et al., 2015) and to measure the transcript levels from these plasmids (Staals et al., 2014; Tamulaitis et al., 2014). Alternatively, mCherry constructs containing protospacer sequences could be generated in order to measure expression levels by either RT-qPCR or fluorescence when the CRISPR-Cas system is present. The CRISPR-Cas system could also block translation of mRNAs by binding them without cleaving them, which would explain the lack of significant differences my RNA-seq data. To test this possibility, we should measure protein levels in addition to transcript levels of a protospacer-containing reporter like mCherry.

Another possible explanation for the apparent lack of function for the *M. tuberculosis* CRISPR-Cas system could be the function of anti-CRISPRs (Bondy-Denomy et al., 2013). Recent work has demonstrated that bacteriophages have a diverse array of proteins that can inhibit bacterial CRISPR-Cas systems in a wide variety of ways (Bondy-Denomy et al., 2013). Therefore, even if the CRISPR-Cas system in these alternative strains seems nonfunctional, the presence of anti-CRISPRs should be explored. To do this, mass spec analysis of the CRISPR-Cas complexes would reveal any regulators of the complex bound directly to it. I have already

generated N-terminal 3xFlag-tagged constructs of each Cas gene under a strong constitutive mycobacterial promoter for this purpose. Alternatively, a transposon mutagenesis screen could identify genes involved in inhibiting the CRISPR-Cas system; in a mutagenized population, any colonies that survive a high multiplicity phage infection could have mutations in anti-CRISPR genes, which allowed the system to protect that bacterium from phage infection. Deleting these anti-CRISPRs would allow for easier characterization of the CRISPR-Cas system in *M. tuberculosis* and likely provide new insight into anti-CRISPR biology.

In many bacterial species, the biological function of CRISPR-Cas systems can be inferred by the sequences of spacers in the CRISPR locus; if the system degrades bacteriophage DNA or RNA, the spacers match segments in bacteriophage genomes almost exactly. In the case of *M. tuberculosis*, none of the CRISPR spacers match known bacteriophage genomes or genomes from any other organism. One obstacle in using bioinformatics to identify targets of this CRISPR-Cas system is our lack of data addressing how much sequence homology is required for targeting in this type of CRISPR-Cas system (Semenova et al., 2011). While experiments addressing this question would first require a functional readout of target degradation, they would provide valuable information to allow us to more efficiently search deep sequencing data sets for matches. For example, it would be immensely helpful to know how many consecutive basepair matches are required for recognition, and where in the crRNA:target complex those basepair matches are most important. Using these search parameters to identify a reliable list of likely targets would help us better hypothesize what the *M. tuberculosis* CRISPR-Cas system may be targeting and therefore how it might be functioning *in vivo*.

While my experiments indicated no role for the CRISPR-Cas system in virulence, this could be due to multiple factors. Aside from the question of CRISPR-Cas functionality, the target

of the system may be specific to human infection. For example, the CRISPR-Cas system may target bacteriophages in the human upper respiratory tract, allowing *M. tuberculsosis* to survive and establish infection in the host (Barr et al., 2013). In our mouse model of infection, *M. tuberculosis*-specific bacteriophages might not be present and would not preferentially infect the *Δcas6* mutant. Some research suggests there may indeed be *M. tuberculosis*-specific bacteriophages in the sputum of both healthy patients and tuberculosis patients, but most known mycobacteriophages were identified using *M. smegmatis* as a host (Hatfull, 2010; Mankiewicz, 1961; Mankiewicz and Liivak, 1967). Indeed, many of these mycobacteriophages are unable to infect *M. tuberculosis*, so it is not surprising that spacers do not match these bacteriophage genomes (Jacobs-Sera et al., 2012). Therefore, the CRISPR-Cas system in *M. tuberculosis* may in fact function as a canonical phage restriction system, but our current knowledge of *M. tuberculosis* bacteriophages is simply too limited. Hunting for new bacteriophages using human sputum and *M. tuberculosis* may enable us to extend our knowledge of the bacteriophages that infect *M. tuberculosis in vivo*. Additionally, with the availability of new deep sequencing data sets profiling the human "phageome" (Yolken et al., 2015), we might find new matches to *M. tuberculosis* spacers, providing a strong link between the CRISPR-Cas system and bacteriophage restriction in *M. tuberculosis*.

Rather than targeting human-specific bacteriophages, the CRISPR-Cas system may restrict human-specific transcripts. Because *M. tuberculosis* accesses the cytosol during infection (see Chapter 2)(Manzanillo et al., 2012; Watson et al., 2012; 2015), it is possible that the CRISPR-Cas system could target host mRNAs, especially if we find that the CRISPR-Cas system does in fact cleave RNA. While the complex is likely too large to be secreted (Staals et al., 2014; Tamulaitis et al., 2014), and the individual subunits do not have secretion signals, if any bacteria lyse during infection inside macrophages, these complexes could be released into

the host cytosol to target mRNAs. Indeed, we observe bacterial genomic DNA in the cytosol during infection (see Chapter 2 Discussion)(Manzanillo et al., 2012; Watson et al., 2012; 2015), so it is not impossible to envision the release of other bacterial components like the CRISPR-Cas system as well. To begin to test this model, we could perform RNA-seq on human macrophages infected with wild-type or *Δcas6 M. tuberculosis* and determine if there are any changes in host mRNA transcript levels when a functional CRISPR-Cas system is present. If any differentially expressed genes even partially match any spacer in the *M. tuberculosis* CRISPR locus, it would provide strong evidence in support of this novel model of host mRNA targeting by a pathogen's CRISPR-Cas system.

Figure 3.1

New spacers incorporated from exogenous DNA

Cas2

Cas1

Cas genes

CRISPR locus: array of direct repeats and unique spacers

pre-crRNA transcribed

Cas6

pre-crRNA processed into mature crRNAs

Effector complex utilizes crRNA to identify and degrade exogenous DNA
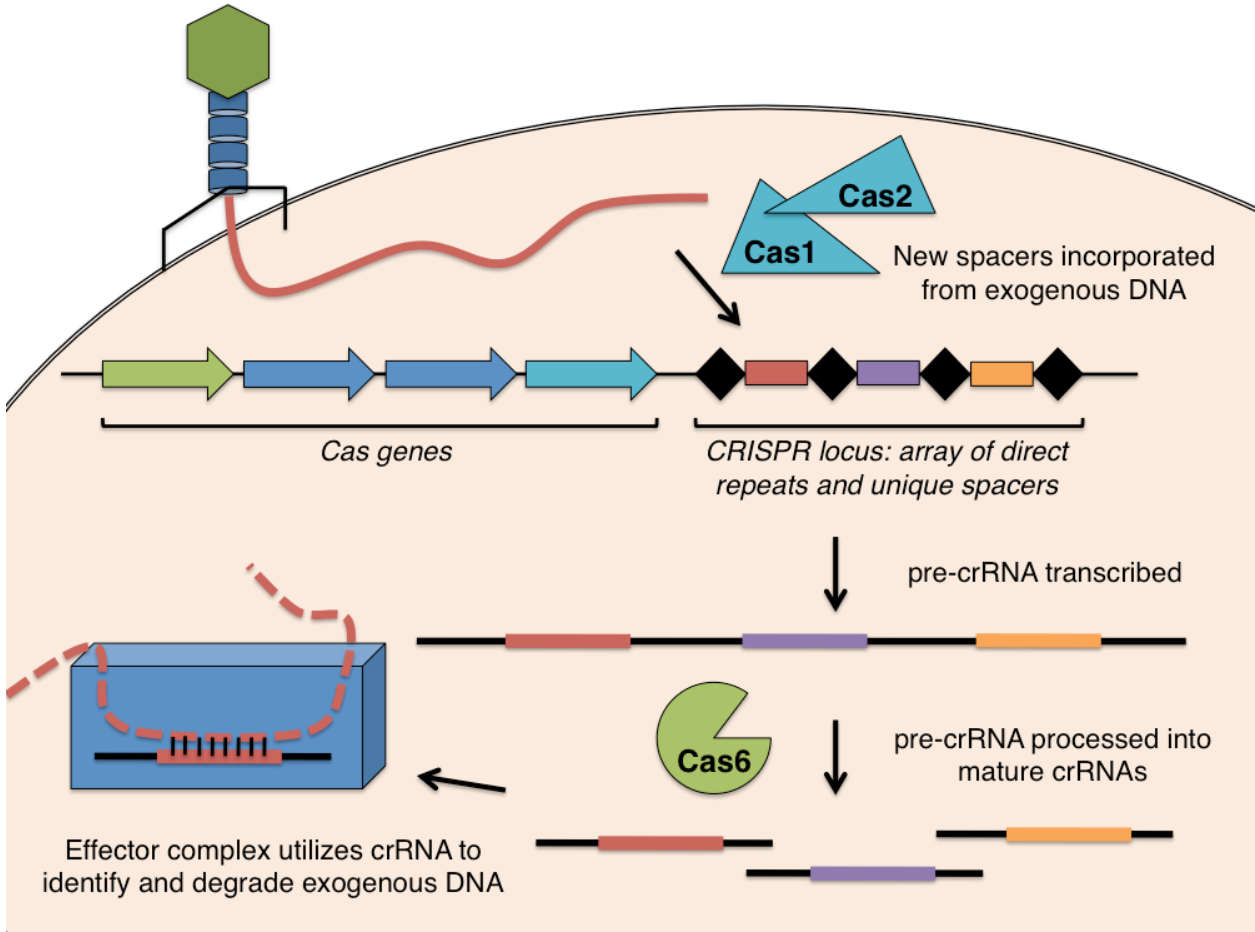
Figure 3.1. Model of a CRISPR-Cas system as an adaptive bacterial immune system.

After exposure to exogenous DNA such as bacteriophages or plasmids, Cas1 and Cas2 incorportate new spacers into the CRISPR locus. Cas6 processes pre-crRNAs, cleaving them into mature crRNAs. The remaining Cas genes, Csm1-6 in *M. tuberculosis,* form a complex to find and degrade exogenous DNA that is complimentary to their bound crRNA.

Figure 3.2
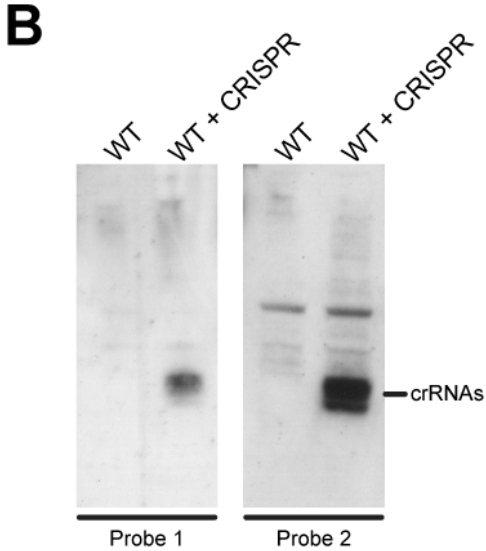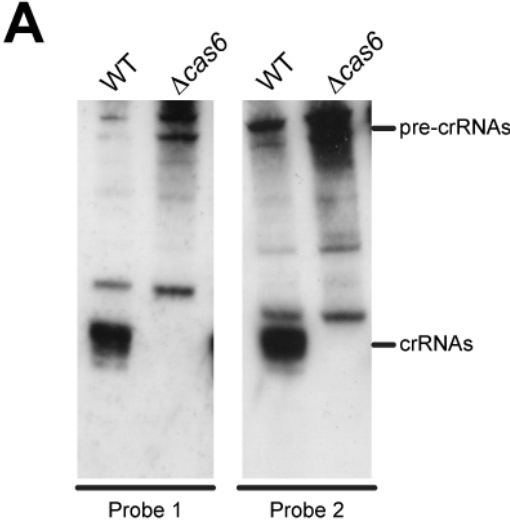
Figure 3.2. The *M. tuberculosis* CRISPR-Cas system generates mature crRNAs.

(A) Northern blot analysis of small RNAs isolated from wild-type or *Δcas6 M. tuberculosis* grown in liquid culture. Probe #1 spans CRISPR spacers #1-4, and probe #2 spans spacers #15-18 (spacer numbers relative to leader position).

(B) Same as (A) but small RNAs were isolated from strains with a non-CRISPR-Cas-containing cosmid (WT) or a cosmid containing *the M. tuberculosis* CRISPR-Cas locus (WT + CRISPR).

Figure 3.3
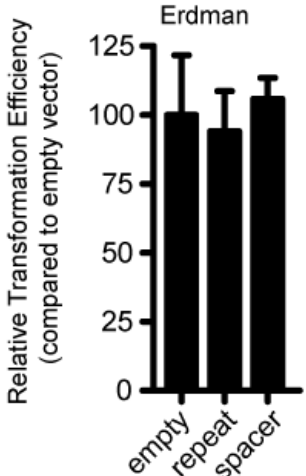
Figure 3.3. The CRISPR-Cas system in *M. tuberculosis* does not restrict plasmid transformation.

M. tuberculosis (Erdman strain) was transformed with plasmids containing either no insert, the CRISPR repeat sequence, or a CRISPR protospacer sequence (spacer #1 relative to leader sequence). Transformation efficiency was determined using a different plasmid with a different antibiotic resistance gene and is presented as relative to the plasmid with no insert.

Figure 3.4
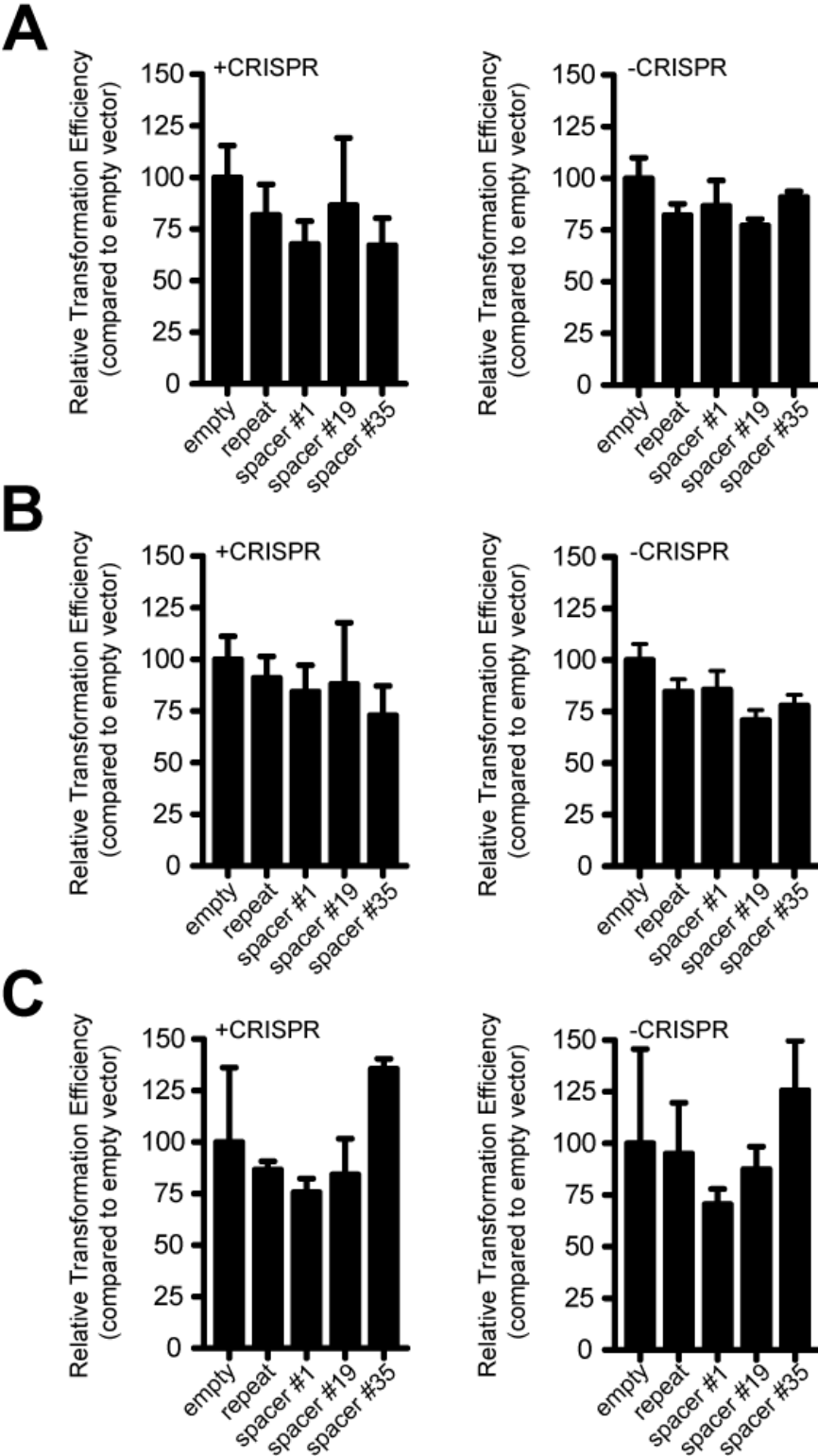
Figure 3.4. The CRISPR-Cas system from *M. tuberculosis* does not restrict plasmid transformation in *M. smegmatis*.

(A*) M. smegmatis* with (left, "+CRISPR") or without (right, "-CRISPR") the *M. tuberculosis* CRISPR-Cas system was transformed with plasmids containing either no insert, the CRISPR-Cas repeat sequence, or one of the CRISPR-Cas spacer sequences (spacers #1, #19, or #35 relative to the leader sequence). Transformation efficiency was determined using a second plasmid with a different antibiotic resistance gene and is presented as relative to the plasmid with no insert.

(B) Same as (A), but repeat and protospacer sequences were inserted downstream of a strong mycobacterial promoter.

(C) Same as (B), but repeat and protospacer sequences were inserted in the reverse complement orientation downstream from the promoter.

Figure 3.5
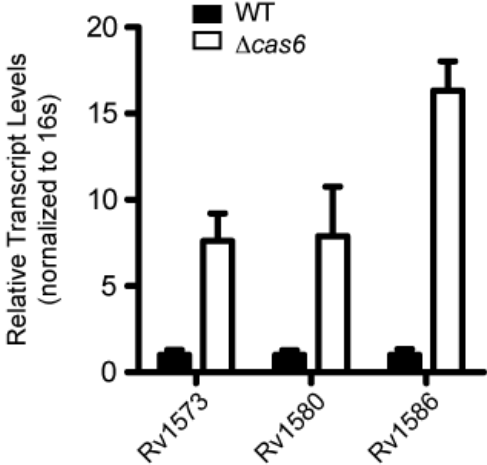
Figure 3.5. The *M. tuberculosis* CRISPR-Cas system controls cryptic prophage gene expression.

RT-qPCR of cryptic prophage phiRv1 transcripts from wild-type and *Δcas6 M. tuberculosis* grown in liquid culture.
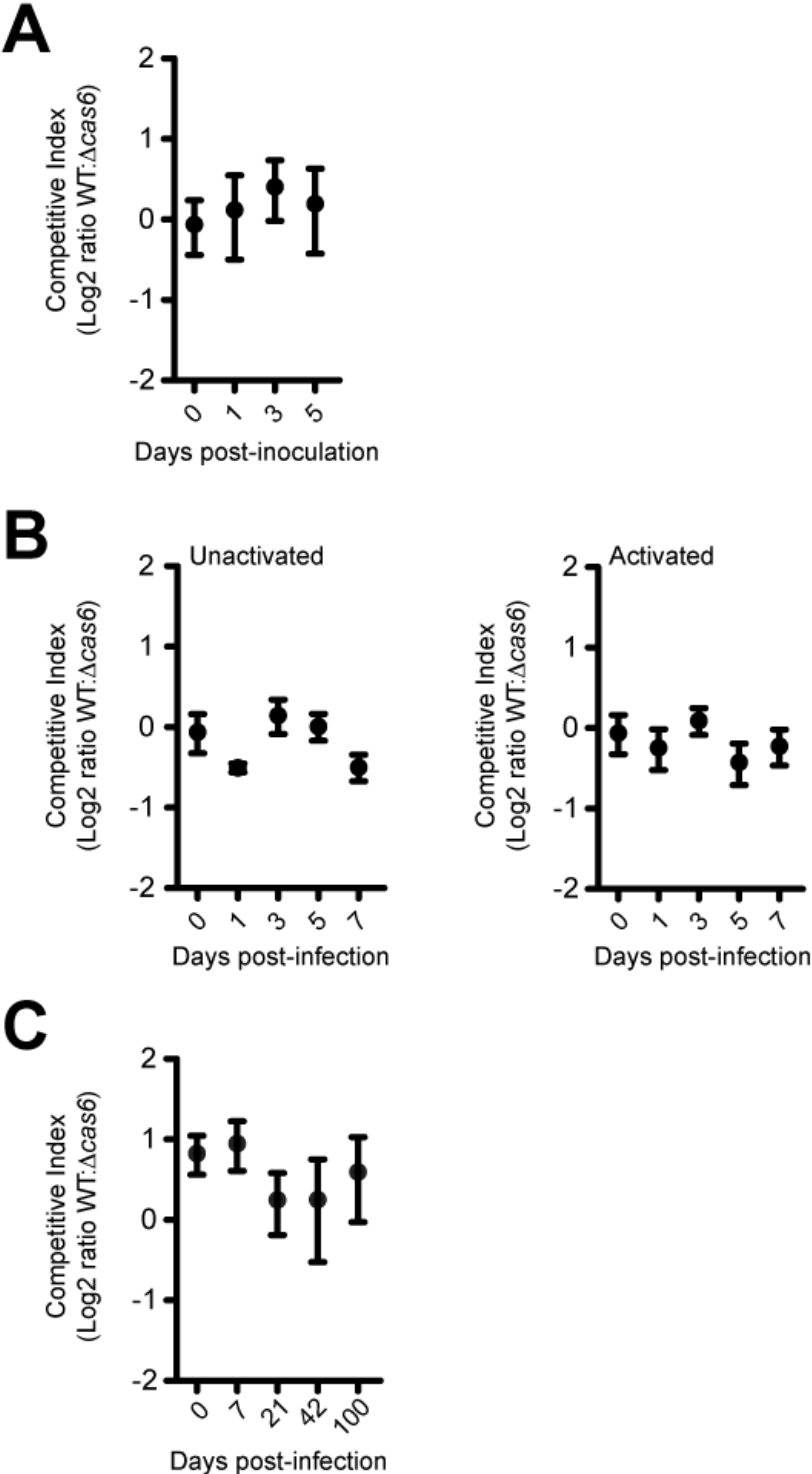
Figure 3.6

Figure 3.6. *Δcas6* mutant *M. tuberculosis* grows normally *in vitro* and *in vivo*.

(A) Wild-type and *Δcas6 M. tuberculosis* were grown in liquid 7H9 broth. Cultures were inoculated with a starting ratio of 1:1 at an OD_{600} of approximately 0.01 and grown until the culture reached $OD_{600} = 1$. Competitive indexes are represented as a log_2 ratio of wild-type to Δcas6.

(B) Unactivated (left) or activated (right) murine bone marrow-derived macrophages were infected with a 1:1 mix of wild-type and *Δcas6 M. tuberculosis*, and competitive indexes were determined at indicated times.

(C) Wild-type BALB/c mice were infected with 1:1 mix of wild-type and *Δcas6 M. tuberculosis* by aerosol exposure of approximately 200 CFUs. At indicated time points, lungs from infected mice were dissected and homogenized to determine competitive indexes.

Chapter 4: Conclusions

In this dissertation, I have described two projects studying diverse aspects of *M. tuberculosis* pathogenesis. In the first, we identified the host sensor responsible for producing type I IFNs and activating selective autophagy in response to cytosolic bacterial DNA in *M. tuberculosis*-infected macrophages. In the second, I tested how the *M. tuberculosis* CRISPR-Cas system functions, either canonically or non-canonically, and if it might contribute to virulence during infection. Each project addresses important questions that will deepen our knowledge of *M. tuberculosis* biology and allow us to develop new generations of antimicrobials, vaccines, or host-directed therapies to better treat tuberculosis and other infectious dieases.

Establishing a role for the CRISPR-Cas system in bacterial virulence and pathogenesis would be a novel discovery and provide precedent for studying other pathogens, such as *Salmonella* species, that also have seemingly nonfunctional systems (Shariat et al., 2015). Importantly, it would be an appealing target for antimicrobials. It is a system only found in archaea and bacteria, so one would expect minimal toxicity in the host from off target effects. Furthermore, because of the diverse nature of CRISPR-Cas systems even between species with highly related systems, very specific inhibitors could likely be developed. As a result, the detrimental effects commonly observed on the host microbiome during broad-spectrum antibiotic treatment could be minimized. Finally, although vaccine strains of *M. tuberculosis* are notoriously unreliable for preventing disease (Kaufmann, 2001), generating CRISPR-Cas mutant strains of other dangerous pathogens could create new possibilities for vaccine strategies.

The selective autophagy and cytosolic surveillance pathways are also attractive targets for developing new therapeutics, specifically host-directed therapies. Viral infections may be

treated successfully with a cGAS or STING agonist like ISD or cGAMP, respectively, because increases in both autophagy and type I IFNs can better control these infections (Jordan and Randall, 2012; Schoggins et al., 2014). However, based on our studies, we know the situation is more complicated during bacterial infections where these two pathways have opposing effects (Watson et al., 2015). Further work is required to identify factors involved specifically in the type I IFN arm, which could be inhibited to dampen the pro-bacterial response without creating an immunocompromised host, or involved specifically in the selective autophagy arm, which could be activated to improve destruction of intracellular bacteria. Because *M. tuberculosis* is becoming increasingly difficult to treat successfully with antimicrobials, adding these types of host-directed therapies to traditional antibiotics may be the key to developing better anti-tuberculosis treatments in the future.

Methods

Cell lines and cell culture.

RAW 264.7 cells (ATCC TIB-71) and mouse embryonic fibroblasts (MEFs, generated from wild-type C57BL/6 mice by F. Mar) were cultured in DMEM with high glucose + 10% FBS + 20 mM HEPES + 2 mM L-glutamine. For selection, RAW 264.7 cells were grown with 5 µg/ml puromycin (Invivogen) or 150 µg/ml hygromycin (Life Technologies). U937 (ATCC CRL-1593.2) cells were cultured in suspension in RPMI + 10% FBS + 20 mM HEPES. For selection, 250 µg/ml hygromycin was added to the media. Before infection, U937 cells were plated on dishes coated with 0.1% gelatin (Sigma) and cultured with 10 ng/ml phorbol 12-myristate 13-acetate (PMA) (Sigma) for 48 h to induce differentiation. Bone marrow derived macrophages (BMDMs) were generated from wild-type C57BL/6 (The Jackson Laboratory), $cGas^{-/-}$ (Schoggins et al., 2014) (or (Li et al., 2013) for experiments with *L. pneumophila*), and $Sting^{gt/gt}$ (referred to as $Sting^{-/-}$)(Sauer et al., 2011) mice that were 8-12 weeks old. $cGas^{-/-}$ mice have a clean deletion of exon 2, which includes the catalytic domain of cGAS, and the knockout targeting cassette was removed, and the mice were fully backcrossed to the C57BL/6 background. All mice were bred and maintained in barrier facilities at Washington University in St. Louis or at the University of California, San Francisco and were handled in accordance with institutional and federal guidelines. Isolated BMDMs were cultured in DMEM + 20% FBS + 2 mM glutamine + 0.11 mg/ml sodium pyruvate + 10% M-CSF (bone marrow media).

Bacterial strains.

The wild-type *Mycobacterium tuberculosis* strain used in these studies was the Erdman strain except when CDC1551 was used as described in the text. The ΔESX-1 mutant has been described previously (Stanley et al., 2003). Wild-type and ΔESX-1 mCherry-expressing strains are also previously described (Watson et al., 2012). All M. *tuberculosis* strains were cultured at 37°C in Middlebrook 7H9 broth or on 7H10 agar plates (BD Biosciences) supplemented with 10% OADC, 0.5% glycerol, and 0.1% Tween-80.

The 10403S strain of *Listeria monocytogenes* was the wild type strain used in these studies. Cultures were grown at 37°C in brain heart infusion broth or agar plates. *Salmonella typhimurium* serovar Typhimurium experiments used the SL1344 strain as the wild type strain. These cultures were grown at 37°C in LB broth or agar plates. The LPO2 *ΔflaA* strain of *L. pneumonphila* is previously described (Monroe et al., 2009) and was used as the wild type strain in order to prevent activation of the host inflammasome during infection. The *ΔsdhA* mutant is also described previously (Monroe et al., 2009). *L. pneumophila* cultures were grown at 37°C on BYCE plates or BYE media with thymidine, cysteine, and ferric nitrate.

Overexpression and knockdown cell lines.

Tagged cGAS constructs were cloned using cGAS-specific primers (forward 5'- GAA GAT CCG CGT AGA AGG ACG -3'; reverse 5'- T GGG TTT CCA ATT TTT GAC AAG CTT TGA-3') and cDNA from mouse BMDMs. PCR products were cloned into Gateway pENTR1a vectors (Life Technologies) containing the indicated N-terminal tags. Constructs were Gateway cloned using LR clonase (Life Technologies) into a pLenti vector with a CMV promoter and puromycin selection marker (Campeau et al., 2009). shRNA sequences were designed using DSIR (Designer of Small Interfering RNA)(Vert et al., 2006) and are listed in Table 1. Constructs

were made by phosphorylating and annealing the primers, and ligating them into the pSicoR-GFP vector (Ventura et al., 2004) with a hygromycin selection marker and BFP.

For stably expressing cell lines, lentivirus was produced by transfecting LentiX cells (Clonetech) with expression or knockdown plasmids and the packaging plasmids, pspAX2 and pMD2.G. Cells were transduced with lentivirus and 8 µg/ml Polybrene (Millipore) overnight, allowed to recover for 24 h, and then grown under antibiotic selection for at least seven days. Expression of tagged constructs was tested by Western blot analysis, and knockdown efficiency was measured by qPCR analysis using primer sets listed in Supplemental Table S2. For transient expression of tagged cGAS in MEFs, cells were plated on cover slips in 24-well dishes and transfected the following day with 150 ng of cGAS expression vector. Cells were cultured an additional 16-24 h before use in subsequent experiments.

Bacterial infections.

For RNA and cytokine analysis during *M. tuberculosis* infection, cells were plated in 6-well dishes: BMDMs and U937 cells were plated at 1×10^6 cells/well, and RAW 264.7 cells were plated at 2×10^6 cells/well. *M. tuberculosis* infections were performed as previously described (Ohol et al., 2010). Briefly, *M. tuberculosis* cultures were grown to log phase, and clumps were removed by low-speed centrifugation (500 g). Cultures were washed twice with PBS and then sonicated briefly to further remove clumps. Cells were infected at a multiplicity of infection (MOI) of 10 in DMEM + 10% horse serum with 10 min spinfection (1000 g). Infected cells were then washed twice with PBS and cultured in bone marrow media. Cells were harvested 4 h post-infection for RNA analysis, and culture supernatants were collected 24 h post-infection for cytokine analysis. For CFU assays, BMDMs were plated in 12-well dishes at 3×10^5 cells/well and infected with *M. tuberculosis* as above at an MOI of 1. At the indicated time points, cells

were washed twice with PBS and lysed in 0.5 ml 0.5% Triton X-100 (Sigma). Serial dilutions were made in PBS + 0.1% Tween-80 and plated on 7H10 agar plates. Colonies were enumerated 2-3 weeks post-infection to determine CFUs.

For *L. monocytogenes* infections, BMDMs were plated in 6-well dishes at $1x10^6$ cells/well. *L. monocytogenes* cultures were grown overnight at 37°C without shaking to prevent expression of flagellin to avoid activating the host inflammasome during infection. Cultures were diluted 1:10 and grown for 3 h until cultures reached log phase. To infect, bacteria and cells were washed twice with HBSS. Cells were infected in HBSS with 10 min spinfection at an MOI of 10. Infected cells were then washed twice with PBS + 50 μg/ml gentamycin, and cultured in BMDM media + 5 μg/ml gentamycin. Cells were harvested 6 h post-infection. For *S.* Typhimurium infections, BMDMs were plated at $1x10^6$ cells/well in 6-well dishes. *S.* Typhimurium cultures were grown overnight at 37°C and then diluted 1:150 in LB + 0.3M NaCl to induce expression of the type III secretion system. Cultures were grown to log phase and washed twice in warm HBSS. Cells were washed twice in warm HBSS and infected as described for *L. monocytogenes* infections, but at an MOI of 5. Additionally, cells were pretreated for 1 hr and then subsequently cultured with 100 μM Caspase-1 Inhibitor II (EMD Chemicals) to prevent activation of the host inflammasome during infection. For *L. pneumophila* infections, BMDMs were plated at $1x10^6$ cells/well in 6-well dishes. Bacteria were patched on BYCE with thymidine, cysteine and ferric nitrate and then resuspended and grown overnight at 37°C with shaking. Cells and bacteria were washed with PBS and infected as described for *L. monocytogenes* at an MOI of 1. Cells were harvested 4 h post-infection.

DNA transfections.

For RNA analysis, cells were plated as described above in 6-well dishes. Cells were transfected with 2 µg of annealed ISD oligos (5'- TAC AGA TCT ACT AGT GAT CTA TGA CTG ATC TGT ACA TGA TCT ACA -3') using either Lipofectamine 2000 (Invitrogen) or PolyJet (SignaGen) as per manufacturer's instructions. ISD oligos were annealed in 5 mM Tris + 25 mM NaCl at 50 uM of each oligo by heating to 98°C for 5 min and then cooling to 25°C over 1 h. For cGAMP transfections, 2'-3' cyclic dinucleotide was purified as previously described (Diner et al., 2013) and transfected into cells using Lipofectamine 2000 (Invitrogen). Cells were harvested at 4 h post-transfection.

RNA isolation and qPCR analysis.

For RNA analysis, cells were harvested in 1 ml Trizol. RNA was isolated using the PureLink RNA Mini Kit (Invitrogen), and samples were DNase treated on-column with PureLink DNase (Invitrogen). cDNA was synthesized using 0.5-1 ug total RNA and the iScript cDNA Synthesis Kit (Bio-Rad). qPCR analysis was performed using Taq DNA Polymerase (NEB) and SYBR Green I (Sigma) as a label. qPCR primers are listed in Table 2, and values reported were in the linear range and normalized to *actin* or *rps17* mRNA levels as indicated. Both the averages and the standard deviations of the raw values were normalized to the average of the treated (infected or transfected) wild-type sample, which was set at 100%.

Mouse infections.

All procedures involving animals were conducted by following the National Institutes of Health guidelines for housing and care of laboratory animals and were performed in accordance with institutional regulations after protocol review and approval by the Institutional Animal Care

and Use Committee of The Washington University in St. Louis School of Medicine. The *cGas*^{-/-} mice used in these experiments were originally described by Schoggins et al. (Schoggins et al., 2014). Embryos derived from parental ES cells (line JM8.N4, Mb21d1[tm1a(EUCOMM)Hmgu]) were received from ECOMM in the C57BL/6N background. The gene trap cassette was removed by crossing this mouse to FLP-deleter and Cre-deleter mice (both C57BL/6J), generating a knockout of exon 2, which contains the catalytic site of cGAS (Schoggins et al., 2014). The resulting mice were further backcrossed to C57BL/6J to remove the FLP and Cre transgenes. Using speed congenics, we verified that the *cGas*^{-/-} mice were 99% C57BL/6 and a mix of B6N and B6J. Mice heterozygous for the mutant *cGas* allele were bred, and wild-type and knockout littermates were used for infection.

The *M. tuberculosis* inoculum was prepared as described for macrophage infections. Age- and sex-matched wild-type and *cGas*^{-/-} mice (male and female littermates, approximately 8-10 weeks old) were infected with approximately 100 *M. tuberculosis* using an inhalation exposure system (Glas-Col). At the indicated times, homogenized lungs and spleens were plated in serial dilutions on 7H10 agar plates to enumerate CFUs in infected mice. RNA from lungs were collected in RLT buffer + β-mercaptoethanol (Qiagen RNeasy Kit), bead beaten, and frozen at -80°C. RNA was isolated using the RNeasy Kit (Qiagen), and DNA was removed with the TURBO DNA-free Kit (Ambion). Blood was collected and serum isolated after organs were dissected. For time-to-death experiments, mice were infected as above and weighed regularly to monitor disease progression. Mouse survival was assessed until day 102 by monitoring body weight of infected mice. Previous work has demonstrated that the number of mice used in this study is sufficient to give accurate and reproducible results.

Cytokine measurements.

Cell culture supernatant IFN-β levels were measured using VeriKine-HS Mouse IFN Beta Serum ELISA Kit (PBL Assay Science) according to the manufacture's instructions. IFN-β levels in mouse serum and cell culture supernatants were measured using L929 ISRE-luciferase reporter cells as previously described (Woodward et al., 2010). Briefly, reporter cells were plated in a 96-well dish and incubated with serum or supernatants for 6-8 h. Cells were washed and reporter activity was measured using the Luciferase Reporter Assay (Promega) according to the manufacturer's instructions.

Antibodies.

The following primary antibodies were used for microscopy studies: mouse monocolonal antibodies against ubiquitinylated proteins (Millipore, clone FK2), Calcoco2 (NDP52, accession number NM_001271018) (Abnova, No. H00010241_B01P), and 3xFLAG (Sigma, clone M2); and rabbit polyclonal antibodies against 3xFLAG (GenScript, No. A00170), phospho-TBK1 (Cell Signaling, D52C2 #5483S), Atg12 (Cell Signaling, #2011S), and LC3B (Life Technologies, No. L10382). Secondary antibodies used were: Alexa 488- and 647-conjugated goat anti-rabbit and Alexa 488- and 647-conjugated goat anti-mouse IgG antisera (Molecular Probes). The following primary antibodies for Western blot analysis: mouse monoclonal antibodies against actin (Sigma, clone AC-40) and 3xFLAG (Sigma, clone M2); and rabbit polyclonal antibodies against phospho-IRF3 (Cell Signaling, 404G #4947S), LC3B (Abcam, No. ab48394), and strep-tag (GenScript, No. A00626). Secondary antibodies used in Western blot analysis included IRDye680 and IRDye800 goat anti-mouse and IRDye680 and IRDye goat anti-rabbit IgG antisera (Li-Cor).

Microscopy.

Cells were plated on cover slips in 24-well dishes and either transfected with 100 ng Cy3-DNA (Mirus Label IT Plasmid Delivery Control Cy3) or infected with mCherry *M. tuberculosis* as described above at an MOI of 1. At the designated time points, cells were fixed in 4% paraformaldehyde for 10 min at room temperature. The fixed cells were washed three times in PBS and permeabilized by incubating them in PBS containing 5% non-fat milk and 0.05% saponin (Calbiochem) (PBS-MS). Cover slips were incubated in primary antibody diluted in PBS-MS for 1-3 h. The cover slips were then washed three times in PBS and incubated in secondary antibody for 1 h. After two washes in PBS and two washes in deionized water, the cover slips were mounted onto glass slides using Prolong Gold Antifade Reagent (Molecular Probes). Images were acquired on a Nikon Ti-E microscope fitted with a Coolsnap HQ2 CCD camera (Photometrics) controlled by NIS-Elements 4.20 (Build 982) software (Nikon Instruments) and then deconvolulted with Huygens Deconvolution software (Scientific Volume Imaging).

Colocalization of markers with *M. tuberculosis* and cytosolic DNA.

To quantify the percentage of *Mycobacterium*-containing phagosomes or cytosolic DNA puncta colocalized with different cellular markers, infected cells were visualized directly by fluorescence microscopy. A series of images were captured including internalized bacteria or cell associated DNA and the cellular marker. Overlayed fluorescent images were analyzed to enumerate the number of Mycobacterium-containing phagosomes or cell-associated DNA that co-localized with the corresponding marker. Bacteria or cytosolic DNA were considered positive for the presence of a marker when they contained detectable amounts of the antibody/fluorescence signal. A minimum of one hundred bacteria or DNA puncta were analyzed

per cover slip for each treatment and designated post-infection time. Each experiment was completed in triplicate cover slips, and data is expressed as a percentage relative to wild-type. For triple labeling experiments, one hundred marker-positive bacteria or DNA puncta were assessed for colocalization with the second marker. For example, one hundred cGAS+ bacteria were assessed for pTBK1 colocalization. In experiments with knockout or knockdown cells, genotypes were blinded throughout experimentation, processing, and quantification.

LC3 conversion assays

BMDMs were plated at 3×10^5 cells/well in 12-well dishes. For DNA treatment, cells were transfected with 1.5 µg ISD and harvested 2 h post-transfection. For starvation, cells were washed twice with HBSS, incubated in HBSS to induce starvation, and harvested 30 min post-starvation. For *M. tuberculosis* infections, cells were infected at an MOI of 20 and harvested 2 h post-infection. To harvest, cells were resuspended and directly lysed in 2x NuPage LDS Sample Buffer (Invitrogen) and then sonicated. Samples were run on 4-12% Bis-Tris gels in MES running buffer (Invitrogen). The same Westerns blots were split and probed with rabbit anti-LC3 antibody (Abcam) and mouse anti-actin (Sigma) as an internal loading control. Blots were imaged using IRDye secondary antibodies (Licor) and the Odyssey infrared imaging system. The ratio of LC3-II/Actin was calculated using the fluorescent intensity of each band (LC3-II and Actin) for every sample. The fold-change of this ratio was calculated by comparing the treated and untreated samples.

Biotin-DNA pulldowns.

5'-biotinylated ISD oligos (Elim Biopharm, Hayward, CA) were annealed as described above. $2x10^8$ RAW 264.7 cells expressing FL-cGAS were transfected with 40 µg of biotinylated or non-biotinylated ISD. 2 h post-transfection, cells were harvested and lysed by sonication in 50 mM Tris pH 7.4 + 150 mM NaCl + 0.075% NP-40. Cleared cell lysates were incubated with streptavidin agarose (Invitrogen) for 2 h, and beads were washed five times with lysis buffer. Proteins were eluted by resuspending the agarose in 2x NuPage LDS Sample Buffer (Invitrogen) and boiling, and precipitated proteins were visualized by Western blot analysis with anti-3xFlag antibody (Abcam).

cGAS immunoprecipitation and DNA analysis.

RAW 267.4 cells were plated at $5x10^7$ cells/15 cm plate. Cells were infected at an MOI of 20 or transfected with 25 µg of annealed ISD using PolyJet (SignaGen). At 45 min post-infection or post-transfection, cells were washed twice with cold PBS and harvested. Cells were fixed for 5 min in 4% PFA and quenched with 1 M Tris pH 7.4 for 5 min. Cells were washed with PBS and frozen at -80°C until processing. Fixed cells were lysed in 50 mM Tris pH 7.4, 150 mM NaCl, 1 mM EDTA, 0.1% NP-40, and 1.25% Triton X-100 with 30 min total sonication in BioRuptor water bath sonicator. Tagged constructs were immunoprecipated using M2 FLAG Magnetic Beads (Sigma) at 4°C overnight. Immunoprecipitates were washed twice with 50 mM Tris, 150 mM NaCl, 1 mM EDTA, and 0.05% NP-40 (Wash Buffer); once with Wash Buffer + 500 mM NaCl; and twice more with Wash Buffer. Immunoprecipitated proteins were eluted with FLAG peptide (synthesized by Bioneer, Inc., Alameda, CA). IP efficiency was confirmed by boiling samples to reverse crosslinks and performing SDS-PAGE and Western blot analysis with anti-3xFLAG (Sigma) and anti-2xStrep (GenScript) antibodies. Samples for DNA analysis were diluted in 10 mM Tris + 1 mM EDTA + 0.65% SDS and incubated for 16 h at 65°C to reverse

crosslinks. Samples were treated with 0.2 mg/ml proteinase K (Sigma) for 2 h at 37°C and nucleic acids were extracted with phenol:chloroform:isoamyl alcohol and precipitated with ethanol. DNA pellets were resuspended in 10 mM Tris, and an equal percentage of the immunoprecipitated material was used in qPCR analysis to measure the abundance of specific DNA sequences. Primers designed to amplify ~100 bp fragments from the *M. tuberculosis* and mouse genome (listed in Table 3) were used in qPCR analysis.

Statistics.

Statistical analysis of data was performed using GraphPad Prism software (Graphpad, San Diego, CA). Two-tailed unpaired Student's t-tests were used for analysis of gene expression, microscopy images, and in vitro CFU assays. Unless otherwise noted, all results are representative of at least two independent biological experiments and are reported as the mean ± SD (n = 3 per group). The sample sizes used in this study were sufficient to detect differences as small as 10-20% using the statistical methods described.

CRISPR-Cas bacterial strains.

The *M. tuberculosis Δcas6* strain was generated using phage recombineering (van Kessel and Hatfull, 2007), replacing the cas6 genes with the hygromycin resistance gene. The strain was selected with 50 μg/ml hygromycin, and successful knockout was confirmed by PCR and RT-qPCR. The *M. smegmatis* "+CRISPR" strain was transformed with a cosmid containing basepairs 3,100,300 through 3,135,800 of the *M. tuberculosis* genome, which includes the Cas genes, Rv2816c-2824c, and the entire CRISPR spacer and repeat locus. The "–CRISPR" strain

was transformed with a different cosmid containing basepairs 2,246,500 through 2,282,000 of the *M. tuberculosis* genome.

Northern blot analysis.

M. tuberculosis or *M. smegmatis* cultures were grown in 7H9 broth at 37°C until reaching approximately $OD_{600} = 1$, and 20 mls of culture were pelleted and harvested in 1 ml Trizol. Small RNAs were isolated and enriched using bead beating and the mirVana Small RNA Isolation Kit (Ambion). 1 ug of RNA was mixed with 2x TBE-Urea sample buffer (Roche), heated to 70°C for 10 min, and run on 15% TBE-Urea gels (Invitrogen) beside DIG-labeled ladder (Roche). Gels were transferred onto nylon membranes (GE Healthcare Amersham). Membranes were dried and crosslinked (Stratalinker). Northern blots were probed using non-radioactive DIG-labeled probes. Probe sequence was cloned into the TOPO blunt vector, which contains a forward SP6 promoter and a reverse T7 promoter. DIG-labeled probes were made by in vitro transcription (Roche DIG-labeling kit). Probes were hybridized to blots using the Easy Hyb system (Roche) according to manufacturer's instructions and imaged using anti-DIG-AP (Roche) and CDP-Star (Roche) on film.

Transformation efficiency assays.

Repeat- and spacer-containing plasmids were cloned by annealing oligonucleotides with repeat or spacer sequences (listed in Table 4) and ligating these pieces into pMV261-Zeo[R] digested with either DraI (to insert upstream of promoter) or BamHI and EcoRI (to insert downstream of promoter). Competent *M. tuberculosis* or *M. smegmatis* cells were prepared by growing cultures to approximately $OD_{600} = 1.0$, washed three times with ice cold 10% glycerol,

and concentrated 100x in 10% glycerol. 100 µl aliquots of competent cells were transformed with 150 ng of Zeo^R plasmid (empty or containing repeat or spacer sequences) and 150 ng of empty pMV261-Kan^R (as an internal control for transformation efficiency and electrocompetency of cells). After 3 or 18 hours of recovery at 37°C in 1 ml 7H9 media, 100 µl of the transformation was plated on 7H10 agar with 20 µg/ml kanamycin, and 100 µl was plated on 7H10 with 50 µg/ml zeocin. When colonies were visible, CFUs were enumerated, and transformation efficiency was calculated by dividing the number of CFUs on zeocin plates by the number of CFUs on kanamycin plates.

Competitive indexes.

For competitive index assays, individual wild-type and $\Delta cas6$ cultures were grown to approximately $OD_{600} = 1$. Based on culture density, strains were mixed 1:1 and used to inoculate cultures at approximately $OD_{600} = 0.01$, to infect macrophages at an MOI of 1, or to infect mice with an inoculum of 200 bacteria. At each time point, samples were collected, and serial dilutions in PBS + 0.05% Tween-80 were plated on plain 7H10 agar and 7H10 agar with 50 µg/ml hygromycin. Mutant CFUs were enumerated by counting colonies on hygromycin plates, and wild-type CFUs were calculated by subtracting the mutant CFUs from the total CFUs on plain 7H10 plates (wild-type and mutant). Competitive index was calculated by dividing wild-type CFUs by mutant CFUs.

Tables

Table 1. shRNA target sequences

Gene	Species	Target Sequence (5' – 3')
SCR	Mouse	CCTAAGGTTAAGTCGCCCT
cGas #1	Mouse	GGTGAATAAAGTTGTGGAA
cGas #2	Mouse	GAATTTGATGTTATGTTTA
Sting	Mouse	GAATGTTCAATCAGCTACA
SCR	Human	GGTTAAGTCGCCCTCGCTC
cGas #1	Human	GCTTCTAAGATGCTGTCAA
cGas #2	Human	GAATTTGATGTCATGTTTA
Sting	Human	GGGTTTACAGCAACAGCAT

Table 2. RT-qPCR oligonucleotides

Gene	Species	Forward (5' – 3')	Reverse (5' – 3')
Ifn-β	Mouse	TCCGAGCAGAGATCTTCAGGAA	TGCAACCACCACTCATTCTGAG
Ifit1	Mouse	CGTAGCCTATCGCCAAGATTTA	AGCTTTAGGGCAAGGAGAAC
Tnf-α	Mouse	ATGGCCTCCCTCTCATCAGT	GTTTGCTACGACGTGGGCTA
Actin	Mouse	GGTGTGATGGTGGGAATGG	GCCCTCGTCACCCACATAGGA
cGas	Mouse	CCACTGAGCTCACCAAAGAT	CAGGCGTTCCACAACTTTATTC
Sting	Mouse	TGGCCTTCTGGTCCTCTATAA	CTCGTAGACGCTGTTGGAATAA
Ifn-β	Human	CTTCTCCACTACAGCTCTTTCC	GCCAGGAGGTTCTCAACAATA
Ifit1	Human	CCAGAAATAGACTGTGAGGAAGG	CCCTATCTGGTGATGCAGTAAG
Actin	Human	GACCACCTTCAACTCCATCAT	CCTGCTTGCTAATCCACATCT
cGas	Human	GCCCTGCTGTAACACTTCTTAT	GGATAGCCGCCATGTTTCTT
Sting	Human	GCTGCTGTCCATCTATTTCTACT	GCCGCAGATATCCGATGTAATA
Rv1573c	Mtb	CACACCAGCACGTTTCAACCACTT	AGTCCGAGTTGCCGGTTGAT
Rv1580c	Mtb	ACGAATCGCCGACATGGCTTTCAA	TCACTGGTCGACCTCTATGGTGT
Rv1586c	Mtb	ATCGAGCTGGAAGCCTTCATGTCA	TTTCGACAGCGTTGTAGTCGTCCA

Table 3. Oligonucleotides for DNA analysis of cGAS pulldowns

Gene	Species	Forward (5' – 3')	Reverse (5' – 3')
16s	Mtb	CCGGAATTACTGGGCGTAAA	AGTACTCTAGTCTGCCCGTATC
dnaA	Mtb	CGACAACGACGAGATTGATGA	CGGTAGCGGAATCGGTATTG
IS6110	Mtb	CCCGTCTACTTGGTGTTGG	CTTCAGCTCAGCGGATTCTT
CRISPR	Mtb	GTCGTCAGACCCAAAAC	GTTTCCGTCCCCTCTC
ISD	n/a	TACAGATCTACTAGTGATCTATGAC	TGTAGATCATGTACAGATCAGT
Actin	Mouse	CTGAGTCTCCCTTGGATCTTTG	CCACAGCACTGTAGGGTTTA

Table 4. CRISPR repeat and spacer sequences

Region	Species	Sequence (5' – 3')
Repeat	Mtb	GTCGTCAGACCCAAAACCCCGAGAGGGGACGGAAAC
Spacer #1	Mtb	TTAAAACCGTGTTGCACTGCAACCCGGAATTCTTGCAC
Spacer #19	Mtb	TGGATTGCGCTAACTGGCTTGGCGCTGATCCTGGTG
Spacer #35	Mtb	CTGACGGCACGGAGCTTTCCGGCTTCTATCAGGTA

References

Alimuddin, Z., Mario, R., Richard, H., and Reyn, von, C.F. (2013). Tuberculosis (N Engl J Med).

Auerbuch, V., Brockstedt, D.G., Meyer-Morse, N., O'Riordan, M., and Portnoy, D.A. (2004). Mice Lacking the Type I Interferon Receptor Are Resistant to Listeria monocytogenes. J Exp Med *200*, 527–533.

Barr, J.J., Auro, R., Furlan, M., Whiteson, K.L., Erb, M.L., Pogliano, J., Stotland, A., Wolkowicz, R., Cutting, A.S., Doran, K.S., et al. (2013). Bacteriophage adhering to mucus provide a non-host-derived immunity. Proc. Natl. Acad. Sci. U.S.a. *110*, 10771–10776.

Barrangou, R., Fremaux, C., Deveau, H., Richards, M., Boyaval, P., Moineau, S., Romero, D.A., and Horvath, P. (2007). CRISPR provides acquired resistance against viruses in prokaryotes. Science *315*, 1709–1712.

Berry, M.P.R., Graham, C.M., McNab, F.W., Xu, Z., Bloch, S.A.A., Oni, T., Wilkinson, K.A., Banchereau, R., Skinner, J., Wilkinson, R.J., et al. (2010). An interferon-inducible neutrophil-driven blood transcriptional signature in human tuberculosis. Nature *466*, 973–977.

Bhat, N., and Fitzgerald, K.A. (2014). Recognition of cytosolic DNA by cGAS and other STING-dependent sensors. European Journal of Immunology *44*, 634–640.

Bibb, L.A., and Hatfull, G.F. (2002). Integration and excision of the Mycobacterium tuberculosis prophage-like element, phiRv1. Molecular Microbiology *45*, 1515–1526.

Birmingham, C.L., Smith, A.C., Bakowski, M.A., Yoshimori, T., and Brumell, J.H. (2006). Autophagy controls Salmonella infection in response to damage to the Salmonella-

containing vacuole. J. Biol. Chem. *281*, 11374–11383.

Boettcher, M., and McManus, M.T. (2015). Choosing the Right Tool for the Job: RNAi, TALEN, or CRISPR. Molecular Cell *58*, 575–585.

Bolotin, A., Quinquis, B., Sorokin, A., and Ehrlich, S.D. (2005). Clustered regularly interspaced short palindrome repeats (CRISPRs) have spacers of extrachromosomal origin. Microbiology *151*, 2551–2561.

Bondy-Denomy, J., Pawluk, A., Maxwell, K.L., and Davidson, A.R. (2013). Bacteriophage genes that inactivate the CRISPR/Cas bacterial immune system. Nature *493*, 429–432.

Brehm, M.A., Wiles, M.V., Greiner, D.L., and Shultz, L.D. (2014). Generation of improved humanized mouse models for human infectious diseases. J. Immunol. Methods *410*, 3–17.

Brendel, J., Stoll, B., Lange, S.J., Sharma, K., Lenz, C., Stachler, A.-E., Maier, L.-K., Richter, H., Nickel, L., Schmitz, R.A., et al. (2014). A complex of Cas proteins 5, 6, and 7 is required for the biogenesis and stability of clustered regularly interspaced short palindromic repeats (crispr)-derived rnas (crrnas) in Haloferax volcanii. J. Biol. Chem. *289*, 7164–7177.

Burdette, D.L., and Vance, R.E. (2013). STING and the innate immune response to nucleic acids in the cytosol. Nature Immunology *14*, 19–26.

Burdette, D.L., Monroe, K.M., Sotelo-Troha, K., Iwig, J.S., Eckert, B., Hyodo, M., Hayakawa, Y., and Vance, R.E. (2011). STING is a direct innate immune sensor of cyclic di-GMP. Nature *478*, 515–518.

Cady, K.C., and O'Toole, G.A. (2011). Non-identity-mediated CRISPR-bacteriophage interaction mediated via the Csy and Cas3 proteins. J. Bacteriol. *193*, 3433–3445.

Campeau, E., Ruhl, V.E., Rodier, F., and Smith, C.L. (2009). A versatile viral system for expression and depletion of proteins in mammalian cells. PloS One.

Carrero, J.A., Calderon, B., and Unanue, E.R. (2004). Type I interferon sensitizes lymphocytes to apoptosis and reduces resistance to Listeria infection. The Journal of Experimental ….

Charpentier, E., Richter, H., van der Oost, J., and White, M.F. (2015). Biogenesis pathways of RNA guides in archaeal and bacterial CRISPR-Cas adaptive immunity. FEMS Microbiol. Rev. *39*, 428–441.

Choi, J., Park, S., Biering, S.B., Selleck, E., Liu, C.Y., Zhang, X., Fujita, N., Saitoh, T., Akira, S., Yoshimori, T., et al. (2014). The Parasitophorous Vacuole Membrane of Toxoplasma gondii Is Targeted for Disruption by Ubiquitin-like Conjugation Systems of Autophagy. Immunity *40*, 924–935.

Choy, A., Dancourt, J., Mugo, B., O'Connor, T.J., Isberg, R.R., Melia, T.J., and Roy, C.R. (2012). The Legionella effector RavZ inhibits host autophagy through irreversible Atg8 deconjugation. Science *338*, 1072–1076.

Clemens, D.L., Lee, B.-Y., and Horwitz, M.A. (2000). Deviant Expression of Rab5 on Phagosomes Containing the Intracellular Pathogens Mycobacterium tuberculosis andLegionella pneumophila Is Associated with Altered Phagosomal Fate. Infect. Immun. *68*, 2671–2684.

Clemens, D.L., Lee, B.-Y., and Horwitz, M.A. (2002). The Mycobacterium tuberculosis phagosome in human macrophages is isolated from the host cell cytoplasm. Infect. Immun. *70*, 5800–5807.

Collins, A.C., Cai, H., Li, T., Franco, L.H., Li, X.-D., Nair, V.R., Scharn, C.R., Stamm, C.E., Levine, B., Chen, Z.J., et al. (2015). Cyclic GMP-AMP Synthase Is an Innate Immune

DNA Sensor for Mycobacterium tuberculosis. Cell Host & Microbe.

Creasey, E.A., and Isberg, R.R. (2012). The protein SdhA maintains the integrity of the Legionella-containing vacuole. Proc. Natl. Acad. Sci. U.S.a. *109*, 3481–3486.

Darwin, K.H., Ehrt, S., Gutierrez-Ramos, J.-C., Weich, N., and Nathan, C.F. (2003). The proteasome of Mycobacterium tuberculosis is required for resistance to nitric oxide. Science *302*, 1963–1966.

de Jonge, M.I., Pehau-Arnaudet, G., Fretz, M.M., Romain, F., Bottai, D., Brodin, P., Honoré, N., Marchal, G., Jiskoot, W., England, P., et al. (2007). ESAT-6 from Mycobacterium tuberculosis dissociates from its putative chaperone CFP-10 under acidic conditions and exhibits membrane-lysing activity. J. Bacteriol. *189*, 6028–6034.

Deretic, V., and Levine, B. (2009). Autophagy, immunity, and microbial adaptations. Cell Host & Microbe *5*, 527–549.

Deretic, V., Saitoh, T., and Akira, S. (2013). Autophagy in infection, inflammation and immunity. Nature Reviews Immunology *13*, 722–737.

Dey, B., Dey, R.J., Cheung, L.S., Pokkali, S., Guo, H., Lee, J.-H., and Bishai, W.R. (2015). A bacterial cyclic dinucleotide activates the cytosolic surveillance pathway and mediates innate resistance to tuberculosis. Nature Medicine *21*, 401–406.

Di Paolo, N.C., Doronin, K., Baldwin, L.K., Papayannopoulou, T., and Shayakhmetov, D.M. (2013). The Transcription Factor IRF3 Triggers "Defensive Suicide" Necrosis in Response to Viral and Bacterial Pathogens. Cell Reports *3*, 1840–1846.

Gao, D., Wu, J., Wu, Y.-T., Du, F., Aroh, C., Yan, N., Sun, L., and Chen, Z.J. (2013). Cyclic GMP-AMP synthase is an innate immune sensor of HIV and other retroviruses. Science *341*, 903–906.

Gunderson, F.F., Mallama, C.A., Fairbairn, S.G., and Cianciotto, N.P. (2015). Nuclease activity of Legionella pneumophila Cas2 promotes intracellular infection of amoebal host cells. Infect. Immun. *83*, 1008–1018.

Gutierrez, M.G., Master, S.S., Singh, S.B., Taylor, G.A., Colombo, M.I., and Deretic, V. (2004). Autophagy Is a Defense Mechanism Inhibiting BCG and Mycobacterium tuberculosis Survival in Infected Macrophages. Cell *119*, 753–766.

Haft, D.H., Selengut, J., Mongodin, E.F., and Nelson, K.E. (2005). A guild of 45 CRISPR-associated (Cas) protein families and multiple CRISPR/Cas subtypes exist in prokaryotic genomes. PLoS Comput Biol.

Hale, C.R., Majumdar, S., Elmore, J., Pfister, N., Compton, M., Olson, S., Resch, A.M., Glover, C.V.C., III, Graveley, B.R., Terns, R.M., et al. (2012). Essential Features and Rational Design of CRISPR RNAs that Function with the Cas RAMP Module Complex to Cleave RNAs. Molecular Cell *45*, 292–302.

Hale, C., Kleppe, K., Terns, R.M., and Terns, M.P. (2008). Prokaryotic silencing (psi)RNAs in Pyrococcus furiosus. Rna *14*, 2572–2579.

Hatfull, G.F. (2010). Mycobacteriophages: genes and genomes. Annu. Rev. Microbiol. *64*, 331–356.

Heler, R., Marraffini, L.A., and Bikard, D. (2014). Adapting to new threats: the generation of memory by CRISPR-Cas immune systems. Molecular Microbiology *93*, 1–9.

Jacobs-Sera, D., Marinelli, L.J., Bowman, C., Broussard, G.W., Guerrero Bustamante, C., Boyle, M.M., Petrova, Z.O., Dedrick, R.M., Pope, W.H., Science Education Alliance Phage Hunters Advancing Genomics And Evolutionary Science Sea-Phages Program, et al. (2012). On the nature of mycobacteriophage diversity and host preference. Virology

434, 187–201.

Jansen, R., Embden, J.D.A.V., Gaastra, W., and Schouls, L.M. (2002). Identification of genes that are associated with DNA repeats in prokaryotes. Molecular Microbiology *43*, 1565–1575.

Jordan, T.X., and Randall, G. (2012). Manipulation or capitulation: virus interactions with autophagy. Microbes Infect. *14*, 126–139.

Kaufmann, S.H.E. (2001). How can immunology contribute to the control of tuberculosis? Nature Reviews Immunology *1*, 20–30.

Kawai, T., and Akira, S. (2010). The role of pattern-recognition receptors in innate immunity: update on Toll-like receptors. Nature Immunology *11*, 373–384.

Lamkanfi, M., and Dixit, V.M. (2011). Modulation of inflammasome pathways by bacterial and viral pathogens. J Immunol *187*, 597–602.

Leber, J.H., Crimmins, G.T., Raghavan, S., Meyer-Morse, N.P., Cox, J.S., and Portnoy, D.A. (2008). Distinct TLR- and NLR-Mediated Transcriptional Responses to an Intracellular Pathogen. PLOS Pathog *4*, e6.

Lee, J., Remold, H.G., Ieong, M.H., and Kornfeld, H. (2006). Macrophage apoptosis in response to high intracellular burden of Mycobacterium tuberculosis is mediated by a novel caspase-independent pathway. J Immunol *176*, 4267–4274.

Li, X.-D., Wu, J., Gao, D., Wang, H., Sun, L., and Chen, Z.J. (2013). Pivotal roles of cGAS-cGAMP signaling in antiviral defense and immune adjuvant effects. Science *341*, 1390–1394.

Liang, Q., Seo, G.J., Choi, Y.J., Kwak, M.-J., Ge, J., Rodgers, M.A., Shi, M., Leslie, B.J.,

Hopfner, K.-P., Ha, T., et al. (2014). Crosstalk between the cGAS DNA Sensor and Beclin-1 Autophagy Protein Shapes Innate Antimicrobial Immune Responses. Cell Host & Microbe *15*, 228–238.

Lillestøl, R., Redder, P., Garrett, R.A., and Brügger, K. (2006). A putative viral defence mechanism in archaeal cells. Archaea *2*, 59–72.

Lippmann, J., Müller, H.C., Naujoks, J., Tabeling, C., Shin, S., Witzenrath, M., Hellwig, K., Kirschning, C.J., Taylor, G.A., Barchet, W., et al. (2011). Dissection of a type I interferon pathway in controlling bacterial intracellular infection in mice. Cellular Microbiology *13*, 1668–1682.

Lippmann, J., Rothenburg, S., Deigendesch, N., Eitel, J., Meixenberger, K., Van Laak, V., Slevogt, H., N'Guessan, P.D., Hippenstiel, S., Chakraborty, T., et al. (2008). IFNβ responses induced by intracellular bacteria or cytosolic DNA in different human cells do not require ZBP1 (DLM-1/DAI). Cellular Microbiology *10*, 2579–2588.

Liu, L., Yang, M., Kang, R., Dai, Y., Yu, Y., Gao, F., Wang, H., Sun, X., Li, X., Li, J., et al. (2014). HMGB1–DNA complex-induced autophagy limits AIM2 inflammasome activation through RAGE. Biochemical and Biophysical Research Communications *450*, 851–856.

MacMicking, J.D., North, R.J., LaCourse, R., Mudgett, J.S., Shah, S.K., and Nathan, C.F. (1997). Identification of nitric oxide synthase as a protective locus against tuberculosis. Pnas *94*, 5243–5248.

Makarova, K.S., Grishin, N.V., Shabalina, S.A., Wolf, Y.I., and Koonin, E.V. (2006). A putative RNA-interference-based immune system in prokaryotes: computational analysis of the predicted enzymatic machinery, functional analogies with eukaryotic RNAi, and hypothetical mechanisms of action. Biology Direct *1*, 7.

Mali, P., Esvelt, K.M., and Church, G.M. (2013). Cas9 as a versatile tool for engineering biology. Nat. Methods *10*, 957–963.

Manca, C., Tsenova, L., Bergtold, A., Freeman, S., Tovey, M., Musser, J.M., Barry, C.E., Freedman, V.H., and Kaplan, G. (2001). Virulence of a Mycobacterium tuberculosis clinical isolate in mice is determined by failure to induce Th1 type immunity and is associated with induction of IFN-alpha /beta. Pnas *98*, 5752–5757.

Mankiewicz, E. (1961). Mycobacteriophages isolated from Persons with Tuberculous and Non-tuberculous Conditions. , Published Online: 30 September 1961; | Doi:10.1038/1911416b0 *191*, 1416–1417.

Mankiewicz, E., and Liivak, M. (1967). Mycobacteriophages isolated from Human Sources. Nature *216*, 485–486.

Manzanillo, P.S., Shiloh, M.U., Portnoy, D.A., and Cox, J.S. (2012). Mycobacterium Tuberculosis Activates the DNA-Dependent Cytosolic Surveillance Pathway within Macrophages. Cell Host & Microbe *11*, 469–480.

Marraffini, L.A., and Sontheimer, E.J. (2008). CRISPR interference limits horizontal gene transfer in staphylococci by targeting DNA. Science *322*, 1843–1845.

Mayer-Barber, K.D., Andrade, B.B., Barber, D.L., Hieny, S., Feng, C.G., Caspar, P., Oland, S., Gordon, S., and Sher, A. (2011). Innate and Adaptive Interferons Suppress IL-1α and IL-1β Production by Distinct Pulmonary Myeloid Subsets during Mycobacterium tuberculosis Infection. Immunity *35*, 1023–1034.

McDonald, K.L., Szyk, A., and LaRonde-LeBlanc, N. (2008). Evidence for pore formation in host cell membranes by ESX-1-secreted ESAT-6 and its role in Mycobacterium marinum escape from the vacuole. Infection and ….

Mojica, F.J.M., Díez Villaseñor, C., Soria, E., and Juez, G. (2000). Biological significance of a family of regularly spaced repeats in the genomes of Archaea, Bacteria and mitochondria. Molecular Microbiology *36*, 244–246.

Mojica, F.J.M., Díez-Villaseñor, C.S., García-Martínez, J., and Soria, E. (2005). Intervening Sequences of Regularly Spaced Prokaryotic Repeats Derive from Foreign Genetic Elements. J Mol Evol *60*, 174–182.

Monroe, K.M., McWhirter, S.M., and Vance, R.E. (2009). Identification of Host Cytosolic Sensors and Bacterial Factors Regulating the Type I Interferon Response to Legionella pneumophila. PLOS Pathog *5*, e1000665.

Ng, V.H., Cox, J.S., Sousa, A.O., MacMicking, J.D., and McKinney, J.D. (2004). Role of KatG catalase-peroxidase in mycobacterial pathogenesis: countering the phagocyte oxidative burst. Molecular Microbiology *52*, 1291–1302.

Nguyen, K.T., Piastro, K., Gray, T.A., and Derbyshire, K.M. (2010). Mycobacterial biofilms facilitate horizontal DNA transfer between strains of Mycobacterium smegmatis. J. Bacteriol. *192*, 5134–5142.

O'Connell, R.M., Saha, S.K., Vaidya, S.A., Bruhn, K.W., Miranda, G.A., Zarnegar, B., Perry, A.K., Nguyen, B.O., Lane, T.F., Taniguchi, T., et al. (2004). Type I interferon production enhances susceptibility to Listeria monocytogenes infection. J Exp Med *200*, 437–445.

O'Riordan, M., Yi, C.H., Gonzales, R., Lee, K.-D., and Portnoy, D.A. (2002). Innate recognition of bacteria by a macrophage cytosolic surveillance pathway. Pnas *99*, 13861–13866.

Ohol, Y.M., Goetz, D.H., Chan, K., Shiloh, M.U., Craik, C.S., and Cox, J.S. (2010). Mycobacterium tuberculosis MycP1 Protease Plays a Dual Role in Regulation of ESX-1 Secretion and Virulence. Cell Host & Microbe *7*, 210–220.

Ojha, A.K., Baughn, A.D., Sambandan, D., Hsu, T., Trivelli, X., Guerardel, Y., Alahari, A., Kremer, L., Jacobs, W.R., and Hatfull, G.F. (2008). Growth of Mycobacterium tuberculosis biofilms containing free mycolic acids and harbouring drug-tolerant bacteria. Molecular Microbiology *69*, 164–174.

Opitz, B., Vinzing, M., Van Laak, V., Schmeck, B., Heine, G., Günther, S., Preissner, R., Slevogt, H., N'Guessan, P.D., Eitel, J., et al. (2006). Legionella pneumophila induces IFNbeta in lung epithelial cells via IPS-1 and IRF3, which also control bacterial replication. J. Biol. Chem. *281*, 36173–36179.

Ouellet, H., Ouellet, Y., Richard, C., Labarre, M., Wittenberg, B., Wittenberg, J., and Guertin, M. (2002). Truncated hemoglobin HbN protects Mycobacterium bovis from nitric oxide. Pnas *99*, 5902–5907.

Parrish, N.M., Dick, J.D., and Bishai, W.R. (1998). Mechanisms of latency in Mycobacterium tuberculosis. Trends in Microbiology *6*, 107–112.

Pieters, J. (2008). Mycobacterium tuberculosis and the Macrophage: Maintaining a Balance. Cell Host & Microbe *3*, 399–407.

Plagens, A., Richter, H., Charpentier, E., and Randau, L. (2015). DNA and RNA interference mechanisms by CRISPR-Cas surveillance complexes. FEMS Microbiol. Rev. *39*, 442–463.

Pourcel, C., Salvignol, G., and Vergnaud, G. (2005). CRISPR elements in Yersinia pestis acquire new repeats by preferential uptake of bacteriophage DNA, and provide additional tools for evolutionary studies. Microbiology *151*, 653–663.

Riley, R.L., Mills, C.C., Nyka, W., Weinstock, N., Storey, P.B., Sultan, L.U., Riley, M.C., and Wells, W.F. (1995). Aerial dissemination of pulmonary tuberculosis. A two-year study of

contagion in a tuberculosis ward. 1959.

Rongvaux, A., Jackson, R., Harman, C.C.D., Li, T., West, A.P., de Zoete, M.R., Wu, Y., Yordy, B., Lakhani, S.A., Kuan, C.-Y., et al. (2014). Apoptotic caspases prevent the induction of type I interferons by mitochondrial DNA. Cell *159*, 1563–1577.

Rousseau, C., Gonnet, M., Le Romancer, M., and Nicolas, J. (2009). CRISPI: a CRISPR interactive database. Bioinformatics *25*, 3317–3318.

Russell, D.G. (2001). Mycobacterium tuberculosis: here today, and here tomorrow. Nature Reviews Molecular Cell Biology *2*, 569–586.

Samai, P., Pyenson, N., Jiang, W., Goldberg, G.W., Hatoum-Aslan, A., and Marraffini, L.A. (2015). Co-transcriptional DNA and RNA Cleavage during Type III CRISPR-Cas Immunity. Cell *161*, 1164–1174.

Sauer, J.-D., Sotelo-Troha, K., Moltke, von, J., Monroe, K.M., Rae, C.S., Brubaker, S.W., Hyodo, M., Hayakawa, Y., Woodward, J.J., Portnoy, D.A., et al. (2011). The N-ethyl-N-nitrosourea-induced Goldenticket mouse mutant reveals an essential function of Sting in the in vivo interferon response to Listeria monocytogenes and cyclic dinucleotides. Infect. Immun. *79*, 688–694.

Schoggins, J.W., MacDuff, D.A., Imanaka, N., Gainey, M.D., Shrestha, B., Eitson, J.L., Mar, K.B., Richardson, R.B., Ratushny, A.V., Litvak, V., et al. (2014). Pan-viral specificity of IFN-induced genes reveals new roles for cGAS in innate immunity. Nature *505*, 691–695.

Semenova, E., Jore, M.M., Datsenko, K.A., Semenova, A., Westra, E.R., Wanner, B., van der Oost, J., Brouns, S.J.J., and Severinov, K. (2011). Interference by clustered regularly interspaced short palindromic repeat (CRISPR) RNA is governed by a seed sequence.

Proc. Natl. Acad. Sci. U.S.a. *108*, 10098–10103.

Shariat, N., and Dudley, E.G. (2014). CRISPRs: molecular signatures used for pathogen subtyping. Appl. Environ. Microbiol. *80*, 430–439.

Shariat, N., Timme, R.E., Pettengill, J.B., Barrangou, R., and Dudley, E.G. (2015). Characterization and evolution of Salmonella CRISPR-Cas systems. Microbiology (Reading, Engl.) *161*, 374–386.

Sorek, R., Lawrence, C.M., and Wiedenheft, B. (2013). CRISPR-mediated adaptive immune systems in bacteria and archaea. Annu. Rev. Biochem. *82*, 237–266.

Staals, R.H.J., Zhu, Y., Taylor, D.W., Kornfeld, J.E., Sharma, K., Barendregt, A., Koehorst, J.J., Vlot, M., Neupane, N., Varossieau, K., et al. (2014). RNA targeting by the type III-A CRISPR-Cas Csm complex of Thermus thermophilus. Molecular Cell *56*, 518–530.

Stanley, S.A., Johndrow, J.E., Manzanillo, P., and Cox, J.S. (2007). The Type I IFN response to infection with Mycobacterium tuberculosis requires ESX-1-mediated secretion and contributes to pathogenesis. J Immunol *178*, 3143–3152.

Stanley, S.A., Raghavan, S., Hwang, W.W., and Cox, J.S. (2003). Acute infection and macrophage subversion by Mycobacterium tuberculosis require a specialized secretion system. Pnas *100*, 13001–13006.

Stetson, D.B., and Medzhitov, R. (2006). Recognition of Cytosolic DNA Activates an IRF3-Dependent Innate Immune Response. Immunity *24*, 93–103.

Storek, K.M., Gertsvolf, N.A., Ohlson, M.B., and Monack, D.M. (2015). cGAS and Ifi204 cooperate to produce type I IFNs in response to Francisella infection. J Immunol *194*, 3236–3245.

Sturgill-Koszycki, S., Schlesinger, P.H., Chakraborty, P., Haddix, P.L., Collins, H.L., Fok, A.K., Allen, R.D., Gluck, S.L., Heuser, J., and Russell, D.G. (1994). Lack of acidification in Mycobacterium phagosomes produced by exclusion of the vesicular proton-ATPase. Science *263*, 678–681.

Sun, L., Wu, J., Du, F., Chen, X., and Chen, Z.J. (2013). Cyclic GMP-AMP synthase is a cytosolic DNA sensor that activates the type I interferon pathway. Science *339*, 786–791.

Tamulaitis, G., Kazlauskiene, M., Manakova, E., Venclovas, Č., Nwokeoji, A.O., Dickman, M.J., Horvath, P., and Siksnys, V. (2014). Programmable RNA shredding by the type III-A CRISPR-Cas system of Streptococcus thermophilus. Molecular Cell *56*, 506–517.

Tattoli, I., Sorbara, M.T., Yang, C., Tooze, S.A., Philpott, D.J., and Girardin, S.E. (2013). Listeria phospholipases subvert host autophagic defenses by stalling pre-autophagosomal structures. The EMBO Journal *32*, 3066–3078.

Teles, R.M.B., Graeber, T.G., Krutzik, S.R., Montoya, D., Schenk, M., Lee, D.J., Komisopoulou, E., Kelly-Scumpia, K., Chun, R., Iyer, S.S., et al. (2013). Type I interferon suppresses type II interferon-triggered human anti-mycobacterial responses. Science *339*, 1448–1453.

Thurston, T.L.M., Wandel, M.P., Muhlinen, von, N., Foeglein, Á., and Randow, F. (2012). Galectin 8 targets damaged vesicles for autophagy to defend cells against bacterial invasion. Nature *482*, 414–418.

Touchon, M., Charpentier, S., and Clermont, O. (2011). CRISPR distribution within the Escherichia coli species is not suggestive of immunity-associated diversifying selection. … Of Bacteriology.

Unterholzner, L. (2013). The interferon response to intracellular DNA: why so many receptors? Immunobiology *218*, 1312–1321.

van der Wel, N., Hava, D., Houben, D., Fluitsma, D., van Zon, M., Pierson, J., Brenner, M., and Peters, P.J. (2007). M. tuberculosis and M. leprae translocate from the phagolysosome to the cytosol in myeloid cells. Cell *129*, 1287–1298.

van Embden, J.D., van Gorkom, T., Kremer, K., Jansen, R., van Der Zeijst, B.A., and Schouls, L.M. (2000). Genetic variation and evolutionary origin of the direct repeat locus of Mycobacterium tuberculosis complex bacteria. J. Bacteriol. *182*, 2393–2401.

van Kessel, J.C., and Hatfull, G.F. (2007). Recombineering in Mycobacterium tuberculosis. Nat. Methods *4*, 147–152.

Vance, R.E., Isberg, R.R., and Portnoy, D.A. (2009). Patterns of Pathogenesis: Discrimination of Pathogenic and Nonpathogenic Microbes by the Innate Immune System. Cell Host & Microbe *6*, 10–21.

Ventura, A., Meissner, A., Dillon, C.P., McManus, M., Sharp, P.A., Van Parijs, L., Jaenisch, R., and Jacks, T. (2004). Cre-lox-regulated conditional RNA interference from transgenes. Pnas *101*, 10380–10385.

Vergne, I., Chua, J., and Deretic, V. (2003). Tuberculosis toxin blocking phagosome maturation inhibits a novel Ca2+/calmodulin-PI3K hVPS34 cascade. J Exp Med *198*, 653–659.

Vergne, I., Chua, J., Lee, H.-H., Lucas, M., Belisle, J., and Deretic, V. (2005). Mechanism of phagolysosome biogenesis block by viable Mycobacterium tuberculosis. Pnas *102*, 4033–4038.

Vert, J.-P., Foveau, N., Lajaunie, C., and Vandenbrouck, Y. (2006). An accurate and interpretable model for siRNA efficacy prediction. BMC Bioinformatics *7*, 520.

Viswanathan, P., Murphy, K., Julien, B., Garza, A.G., and Kroos, L. (2007). Regulation of dev, an operon that includes genes essential for Myxococcus xanthus development and CRISPR-associated genes and repeats. J. Bacteriol. *189*, 3738–3750.

Watson, R.O., Bell, S.L., MacDuff, D.A., Kimmey, J.M., Diner, E.J., Olivas, J., Vance, R.E., Stallings, C.L., Virgin, H.W., and Cox, J.S. (2015). The Cytosolic Sensor cGAS Detects Mycobacterium tuberculosis DNA to Induce Type I Interferons and Activate Autophagy. Cell Host & Microbe.

Watson, R.O., Manzanillo, P.S., and Cox, J.S. (2012). Extracellular M. tuberculosis DNA Targets Bacteria for Autophagy by Activating the Host DNA-Sensing Pathway. Cell *150*, 803–815.

Welin, A., and Lerm, M. (2012). Inside or outside the phagosome? The controversy of the intracellular localization of Mycobacterium tuberculosis. Tuberculosis (Edinb) *92*, 113–120.

West, A.P., Khoury-Hanold, W., Staron, M., Tal, M.C., Pineda, C.M., Lang, S.M., Bestwick, M., Duguay, B.A., Raimundo, N., MacDuff, D.A., et al. (2015). Mitochondrial DNA stress primes the antiviral innate immune response. Nature *520*, 553–557.

White, M.J., McArthur, K., Metcalf, D., Lane, R.M., Cambier, J.C., Herold, M.J., van Delft, M.F., Bedoui, S., Lessene, G., Ritchie, M.E., et al. (2014). Apoptotic caspases suppress mtDNA-induced STING-mediated type I IFN production. Cell *159*, 1549–1562.

Woodward, J.J., Iavarone, A.T., and Portnoy, D.A. (2010). c-di-AMP secreted by intracellular Listeria monocytogenes activates a host type I interferon response. Science *328*, 1703–1705.

World Health Organization (2012). Global Health Observatory (GHO) data.

World Health Organization (2014). Global tuberculosis report 2014.

Xu, J., Laine, O., Masciocchi, M., Manoranjan, J., Smith, J., Du, S.J., Edwards, N., Zhu, X., Fenselau, C., and Gao, L.-Y. (2007). A unique Mycobacterium ESX-1 protein co-secretes with CFP-10/ESAT-6 and is necessary for inhibiting phagosome maturation. Molecular Microbiology *66*, 787–800.

Yolken, R.H., Severance, E.G., Sabunciyan, S., Gressitt, K.L., Chen, O., Stallings, C., Origoni, A., Katsafanas, E., Schweinfurth, L.A.B., Savage, C.L.G., et al. (2015). Metagenomic Sequencing Indicates That the Oropharyngeal Phageome of Individuals With Schizophrenia Differs From That of Controls. Schizophr Bull sbu197.

Zhang, Y., Yeruva, L., Marinov, A., Prantner, D., Wyrick, P.B., Lupashin, V., and Nagarajan, U.M. (2014). The DNA sensor, cyclic GMP-AMP synthase, is essential for induction of IFN-β during Chlamydia trachomatis infection. J Immunol *193*, 2394–2404.

Zhao, Z., Fux, B., Goodwin, M., Dunay, I.R., Strong, D., Miller, B.C., Cadwell, K., Delgado, M.A., Ponpuak, M., Green, K.G., et al. (2008). Autophagosome-Independent Essential Function for the Autophagy Protein Atg5 in Cellular Immunity to Intracellular Pathogens. Cell Host & Microbe *4*, 458–469.
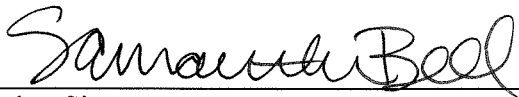
Zughaier, S.M., Zimmer, S.M., Datta, A., Carlson, R.W., and Stephens, D.S. (2005). Differential induction of the toll-like receptor 4-MyD88-dependent and -independent signaling pathways by endotoxins. Infect. Immun. *73*, 2940–2950.
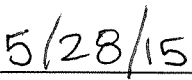
Publishing Agreement

It is the policy of the University to encourage the distribution of all theses, dissertations, and manuscripts. Copies of all UCSF theses, dissertations, and manuscripts will be routed to the library via the Graduate Division. The library will make all theses, dissertations, and manuscripts accessible to the public and will preserve these to the best of their abilities, in perpetuity.

Please sign the following statement:

I hereby grant permission to the Graduate Division of the University of California, San Francisco to release copies of my thesis, dissertation, or manuscript to the Campus Library to provide access and preservation, in whole or in part, in perpetuity.

_____   5/28/15
Author Signature   Date